UNIVERSITA' DEGLI STUDI DI PARMA

DOTTORANDO DI RICERCA IN SCIENZE CHIMICHE

CICLO XXIII

2008-2010

NEW CATALYTIC SYSTEMS BASED ON NANODISPERSED METALS IN INORGANIC MATRICES PREPARED USING THE SOL-GEL TECHNIQUES

COORDINATORE:

PROF. A. GIRLANDO

TUTOR:

PROF. P. MOGGI

DOTTORANDO:

SONA ALFRED NDEME

2011

DEDICATED TO MY MOTHER

BERTHA FULE SONA

TABLE OF CONTENTS

PART ONE

THEORY

INTRODUCTION

This research project began with the wish and trials to optimise an egg shell catalyst used in the Fischer-Tropsch synthesis, and is finishing with a trial to make an optimised egg shell catalyst on a hard core as a support. The formation of an eggshell catalyst was studied by many research groups, using various preparation methods like the vapour phase deposition, precipitation and co-precipitations, impregnations, ultra sound techniques, sol-gel techniques and many other methods for the production of dispersed nanoparticles like the use of clusters as precursors. This project exploited the sol-gel techniques for the impregnation and anchorage of cobalt and iron in the oxidic crystalline state, on inorganic supports like silica gel and alumina gel, which eventually can be promoted with ruthenium oxide.

The decision to pursue this research project was determined by the rapid depletion of fossil crude oil, and the need for new forms of clean energy sources. The increasing scarcity of crude oil and the extremely high growing prizes, joint to the presence of coal in many developing countries like China, India, African nations and other Asian countries, not forgetting the recent progress made in the use of biomass as feedstock for the Fischer-Tropsch synthesis, is making this process to become one of the most convenient ways of producing fuel. A good reason for which large production plants are being constructed all over the world.

Knowing that ruthenium finely dispersed and deposited on MgO with alkalis as promoters, is an optimum catalyst for the ammonia synthesis, this project also started the study of double supports like MgO on alumina, using the same sol-gel techniques. This was done as an attempt to improve the mechanical resistance of the catalyst.

The study of these catalysts proceeded with characterization using methods like the B.E.T. single point method for surface area measurements, the Temperature Programmed Reduction

(T.P.R.), the Temperature Programmed Oxidation (T.P.O.), the Temperature Programmed Desorption (H_2-T.P.D.), the Thermal Gravimetric Analysis (T.G.A.), Infrared spectroscopy (FT-IR) and X-ray Diffraction (X.R.D.). Other methods like the RAMAN spectroscopy, TEM and SEM with EDS, were carried out by our friends and collaborators of the University of Perugia, who are also working on the development of the same type of catalysts using the ultra sound technique as a preparation method, and their catalysts were tested in our laboratory plants for comparison.

The catalysts were also tested in laboratory plants we constructed, using fixed bed reactors to study the percentage of conversions of carbon monoxide and the selectivity of the various hydrocarbons produced in the case of the Fischer-Tropsch synthesis, and the productivity in the case of the ammonia synthesis at low pressure

CHAPTER ONE

1) CATALYSIS

1.1) What Are Catalysts? (1, 2)

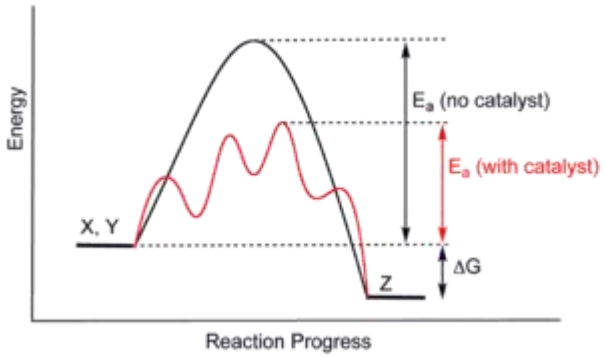

***Graph 1**: An example of a reaction in the presence of, and in the absence of a catalyst.*

$$X + Y \rightarrow Z$$

Catalysts are substances that, although they bring about changes in the velocity or the speed with which equilibrium conditions are obtained in a reaction, they remain unaltered and do not change the free energy of the process involved. They are used in a wide range of chemical reactions which go from the simple conversion of hydrogen from the ortho-position to the para-

position, caused by metals, to the very complex biological reaction catalysed by enzymes. Although the application of these substances runs back to the beginning of the chemical industry, in the early 800, it is still on the wave crest of scientific research, because almost all industrial products need catalytic processes to be economically advantageous. It is enough to take a glance either at the pharmaceutical industry or the petroleum industry. Just to mention a few of these processes: the ammonia synthesis, the Fischer-Tropsch synthesis, the olefin oxidation, both partial and total. In the petroleum industry almost all processes are carried out catalytically.

Nowadays, the catalytic research program is driven towards highly innovative systems, apt at resolving environmental and energy producing problems. In fact, there's the growing necessity for very efficient fuels with the minimum possible quantity of pollutants. The exploration of new processes for energy capturing, like the photo-catalytic breaking of water molecules, and the necessity for more efficient catalysts, for the trapping and destroying of environmental pollutants. In the recent years, the progress made in the nanotechnology and computational chemistry, has provided exciting research prospective, based on making better the existing processes and a look up for innovative catalytic systems. It is also very interesting to see how catalysis could bring about a range of different products, beginning with the same reactants. Like in the case of syngas, where the reactants are CO and H_2, but the range of product varies with the type of metal used as a catalyst.

Nanotechnologies are those technologies involved in the design, characterization, production and application of structures, devices and systems, controlling shape and size on a nanometric scale. On trying to exploit three modern trends of nanotechnologies, i.e.

a) New and improved control of the sizes and manipulation of nano scale building blocks.
b) New and improved characterization of materials on a nano scale (e.g., spatial resolution, chemical sensitivity).
c) New and improved understanding of the relationships between nanostructure and its properties and how these can be engineered.

and combining these techniques with a greater understanding of reaction kinetics has brought about the interest in the study of innovative methods of synthesizing heterogeneous catalysts in the chemical industry. Many research workers are studying new methods of creating mechanically adaptable support systems, others are working on methods of deposition and dispersion on the surfaces and many others are working on the selection of suitable precursors, to be able to have good and resistant catalytic systems. Ultrasonic wave chemistry gives a good example of a deposition method, and the product will be used as a comparing system in this research. Precursors like bimetallic clusters are used, combined with sol-gel techniques to make catalytic systems, and the resulting product will also be used to make out some differences in this research. Lately there is a lot of interest in the sol-gel method, because of the great versatility and variability, in the ways of proceeding, in order to produce the exact forms and structures desired.

Heterogeneous catalysts display a very high complexity, in their texture, structure and chemical activity, all of which have a very strong impact on their performance. This complexity has been the pushing force behind the improvements and modernization of the preparation methods. In this i participated as a Ph.D. research student, using the various methods of experimental characterization, both of structure and activity, of the fresh and used catalyst.

1.2) Thermodynamic And Kinetic Aspects Of Catalysis

In a general reaction which goes to equilibrium,

$$aA + bB + \cdots \leftrightarrow mM + nN + \cdots \qquad [2]$$

where *r* is rate velocity, expressed in moles of transformed reactants per unit time per unit volume (unit mass),and it is the difference between the rate velocity of the forward reaction r_a, and the rate velocity of the reverse reaction r_b.

$$r = r_a - r_b. \qquad [3]$$

The value at equilibrium, of *r* is zero. If the previous expression has to be compatible with thermodynamics, the activities of the various components of the reaction at equilibrium should

be zero. In this case assuming ideal conditions, the same could be said of their concentrations.

$$r = r_a \left[1 - \frac{\prod_i c_i^{\alpha_i}}{K(T)}\right] \qquad [4]$$

Where K(T) is the equilibrium constant

α_i is the stoichiometric coefficient of, component *i,* which can be either positive or negative, depending on the fact that component *i* is either a reactant or a product. From equations [3] and [4], equation [5] is obtained.

$$r_b = \frac{r_a}{K(T)} \prod_i C_i^{\alpha_i} \qquad [5]$$

Therefore from the thermodynamic equilibrium data, it is possible to obtain both velocity rates for the forward and the reverse reaction. With this established, it is useful to recall another equation for rate velocity.

$$r_a = k \prod_i C_i^{v_i} \qquad [6]$$

Where *k* is the velocity constant for the reaction, and has a temperature dependence given by the Arrhenius equation.

$$K(T) = Ae^{-\frac{E_a}{RT}} \qquad [7]$$

Where *A* is the frequency factor and E_a is the activation energy for one mole. This is the energy barrier to be surmounted if reaction has to occur. Theexponents v_i, called reaction order, expresses the sensibility of a system, as concentration changes occur to the reactants. They are determined empirically, elaborating velocity data obtained experimentally.

For instance , considering the catalytic synthesis of ammonia,i.e.

$$N_2 + 3H_2 \leftrightharpoons 2NH_3 \qquad [8]$$

This reaction is carried out at high pressures and in the presence of supported porous Fe as catalyst, promoted by an alkali metal. Experience shows that, the forward reaction could be comfortably represented as follows:

$$r_a = k p_{N_2}^{v_{N_2}} p_{H_2}^{v_{H_2}} p_{NH_3}^{v_{NH_3}}. \qquad [9]$$

Where $v_{N_2} = 1$, $v_{H_2} = 1{,}5$ and $v_{NH_3} = -1$.

Substituting equation $[9]$ in equation $[4]$, the following expression is obtained:-

$$r = A e^{-\frac{E_a}{RT}} \frac{p_{N_2} p_{H_2}^{1.5}}{NH_3} \left(1 - \frac{p_{NH_3}^2}{k p_{N_2} p_{H_2}^3}\right) \qquad [10]$$

This is the global expression used for the velocity rate of this synthesis, and was proposed by Temkin and Pyzhev. It is the one used in projecting most industrial plants. The composition of the mixture can be expressed in degree of progress (λ), which is expressed as the change in the number of moles of a chosen component, divided by its stoichiometric coefficient. If the influence of temperature on the velocity constant and on the equilibrium constant is considered, the surface represented on graph 2 can be considered a good representation of the velocity of reaction.

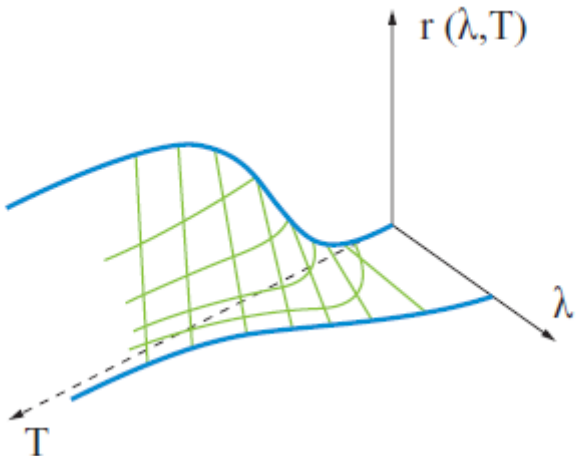

***Graph 2**. The dependence on temperature and the degree of progress, of the velocity of reaction.*

1.3) THE SURFACE REACTION KINETICS.

1.3.1) The Langmuir Model

A heterogeneous catalytic reaction proceeds through a succession of steps and if the ones due to emigration and diffusion of reactants and products are ignored the main steps are, the adsorption of the reactants on the surface, the surface reaction, and the desorption of products from the surface. Every step has a characteristic velocity, which is the same for every step when the stationary state is realized. In this way it becomes extremely difficult to evaluate reaction rates. The reason for the application of the approximation of the rate determining step, intended as the slow step which conditions the reaction velocity. This means, for the other steps, the concentration of the species involved remain equal to those at equilibrium.
According to the Langmuir theory, there's the existence of surface sites, with various degrees of occupation, (θ_ι), (where ι is a generic specie), for all species. Therefore

$$\sum_i \theta_i + \theta_v = 1 \qquad [11]$$

Where $\theta_v$is the fraction of free sites.

Adsorption occurs after a collision between a reacting specie and the site on the surface, in which case, the velocity of adsorption depends on the partial pressure (p_ι) of the specie in the reacting mixture, and the fraction of free sites. This means the velocity of adsorption, which expresses the degree of filling up of the various species on the various sites with respect to time, is given by

$$\frac{d\theta_\iota}{dt} = k_\iota p_\iota (1 - \sum_j \theta_j) - k_{-\iota}\theta_\iota \qquad [12]$$

where $k_{-\iota}$and k_ι are the velocity constants for desorption and adsorption respectively. For a

gas of partial pressure (p_ι), with molecules having mass (m_ι), the kinetic theory for gases gives:-

$$k_\iota = \frac{p_\iota}{\sqrt{2\pi m_\iota K_B T}} e^{-\frac{\varepsilon^*}{K_B T}} \qquad [13]$$

where ε^* is the activation energy for one molecule, and $[K_B]$the Boltzmann constant. At the equilibrium conditions, all the left hand terms of equation $[12]$ becomes zero, and this equation becomes a system of linear equations whose solution gives the degree of coverage of the sites.

$$\theta_\iota = \frac{b_\iota p_\iota}{1+\sum_j b_j p_j} \qquad [14]$$

where $b_\iota = \frac{k_\iota}{k_{-\iota}}$. Equation $[14]$ is the Langmuir isotherm. It is the equation used to describe the kinetics of heterogeneous catalytic reactions.

1.4) Catalysis On Real Surfaces

The situation which has been studied can be considered ideal, since it takes all sites as equal in shape and energy. This situation is nearly obtained only in cases where the surface is mono crystalline obtained through epitaxial deposition. Real surfaces have a lot of defects, which bring about very different morphological and energetic situations at the sites. Reason for which sites behave differently, the one from the other.

If the velocity of a surface reaction, could be expressed as

$$r = k_s f(C) \qquad [15]$$

where k_s is the velocity constant, and f(C) expresses the dependence of the system on the

composition, and on a real heterogeneous surface it is reasonable to suppose that the activation energy (E_a), has different values on different sites, and are distributed according to the following function $\varphi(E_a)$, conveniently normalized, such that $\varphi(E_a)dE_a$ gives that fraction of sites with activation energy between E_a and $E_a + dE_a$,

in this case, the reaction velocity is expressed a medium value, through all sites.

$$r = \int_0^\infty r_s \varphi(E_{as}) dE_{as} = f(C) A_s \int_0^\infty e^{-\frac{E_{as}}{RT}} \varphi(E_{as}) dE_{as} \qquad [16]$$

where r_s is the velocity of the surface reaction, with corresponding activation energy E_s and A_s is the pre- exponential factor of the Arrhenius' equation. From an analysis of superficial energy for heterogeneous solids we have

$$\varphi(E_{as}) = \gamma e^{hE_{as}} \; E_1 < E_s < E_2 \qquad [17]$$

with *h* and γ, constant in this interval, while they become zero outside this interval. Substituting $[17]$ in $[15]$ and integrating, we obtain the following:-

$$r = \pm \frac{A_s \gamma e^{hE_a}}{(h - \frac{1}{RT})} e^{-\frac{E_a}{RT}} f(C) \qquad [18]$$

This equation takes into account the fact that one of the two integration limits, due to the rapid variation of the exponential function, is ignored. The sign to choose depends on the sign of the denominator. There is an interesting resemblance between equation $[18]$ and equation $[15]$ if we do not consider the dependence on the pre-exponential factor, of the activation energy. This reveals that the reaction proceeds on that very small fraction of active sites, which correspond to a minimum of activation energy. Moreover, if the same reaction is carried out on two catalysts prepared with the same composition but having undergone different treatments, a relationship between the pre-exponential factor and the activation energy must be observed. A similar situation is observed if the same reaction is made to be catalysed by the same catalyst,

though reactants are only similar. This is the compensation effect.

1.5) The Kinetics Of Some Heterogeneous Catalytic Reactions

If we consider the C-C bond breaking by hydrogen, with the formation of hydrocarbons with smaller molecular weight. For example,

$$CH_3 - CH_3 + H_2 \longrightarrow 2CH_4 \qquad [19]$$

a reaction which is catalysed by transition metals like Fe, Co and Ni, and is very important in reforming. Experimental results show that, it is a reaction which is strongly inhibited in the presence of hydrogen, almost giving a negative order of reaction. If we assume the first step is the dissociative adsorption of the paraffin, with a partial dehydrogenation and the formation of an unsaturated specie on the surface,

$$CH_3 - CH_3 \leftrightarrows C_2H_x + aH_2 \qquad [20]$$

where $a = \frac{6-x}{2}$, and values like 1,2 and 3 for *a*, correspond to adsorbed species like ethylene, acetylene and the acetylene radical. Successively there's a hydrogen attack on the adsorbed specie, which is the rate determining step

$$C_2H_x + H_2 \longrightarrow CH_y + CH_x \longrightarrow 2CH_4 \qquad [21]$$

with a rate velocity which can be expressed as

$$r = kp_{H_2}\theta \qquad [22]$$

where θ is the fraction of the of the surface covered by C_2H_x, and can be calculated

assuming the adsorption step at equilibrium. In this we obtain the following expression:-

$$r = \frac{k p_{C_2H_6} p_{H_2}^{1-a}}{1 + b p_{C_2H_6} p_{H_2}^{-a}} \approx k b^n p_{C_2H_6}^n p_{H_2}^{1-na} \qquad [23]$$

where b=$\frac{k_1}{k_{-1}}$,is the adsorption equilibrium constant. The last approximation is possible only if pressure changes are not very great and if the values attributed to n vary from 0 to 1. In concluding, an experimental evaluation of the order of reaction with respect to hydrogen and the hydrocarbon makes it possible to give values to the parameter *a*, for different catalysts. For example, for Fe *a* is 2, while for Ni *a* is 3, and for Co *a* is 2. These values reveal how adsorbed hydrocarbon on different metals, in the presence of hydrogen breakdown with different speeds.

If we take the case of ammonia, where kinetically it is assumed that the rate determining step is not the surface reaction, but the dissociative adsorption of N_2 on the surface, $N_2 \longrightarrow 2N - \sigma$. The rate velocity of this reaction is expressed as follows:-

$$r = k p_{N_2} (1 - \theta)^2 \qquad [24]$$

where $\theta_y = (1 - \theta)$ is the quantity of free active sites. The occupied active sites could be calculated considering the global reaction at equilibrium.

$$N - \sigma + \left(\frac{2}{3}\right) H_2 \leftrightarrows NH_3 \qquad [25]$$

Applying the Langmuir model the following expression is obtained:-

$$\theta = \frac{b\left(\frac{p_{NH_3}}{p_{H_2}^{1,5}}\right)}{1 + b\left(\frac{p_{NH_3}}{p_{H_2}^{1,5}}\right)} . \qquad [26]$$

In conclusion, keeping in mind equation $[11]$, the following approximations could be done

$$r = kp_{N_2}(1-\theta)^2$$

$$= kp_{N_2}\left[\frac{1}{1+b\left(\frac{p_{NH_3}}{p_{H_2}^{1.5}}\right)}\right]^2$$

$$= k_s p_{N_2}\left(\frac{p_{NH_3}^{1.5}}{p_{NH_3}}\right)^{2n} \qquad [27]$$

with 0<n<1. Even in this case, the last step is valid only for pressure variations within a limited range. When $n = 0.5$, equation$[25]$ coincides with equation $[10]$.

In a heterogeneous catalytic reaction, at least one of the reactants form an unstable intermediate specie with the site on the surface. This intermediate in turn, releases the catalyst at the end of the reaction. It is therefore reasonable to suppose that if a reaction is conducted on different catalyst, there should be a relationship between the activity of the reaction and the heat of reaction for the formation of this intermediate. In fact increasing the heat of reaction, diminishes the activation energy barrier for the formation of the intermediate, for which reason the rate velocity is less. This is a particular application of the *Brönsted-Evans-Polanyirule,* which expresses the existence of a linear relationship between the activation energy and the heat of reaction in an elementary reaction. If the heat of reaction is very high, the intermediate becomes very stable, and the rate velocity of the whole process, which has as rate determining step the decomposition of the intermediate, becomes less. Therefore it is expected that the velocity of the reaction increases as the heat of reaction for the formation of the intermediate increases, and then decreases after having reached a maximum. This is a typical behaviour which generates a curve, called by *Aleksej Alexandrvič Balandin*, like a “volcano”.

CHAPTER TWO

2) AN INNOVATIVE PREPARATION METHOD IN HETEROGENEOUS CATALYSIS

In this thesis a few preparation methods, directly related to superficial deposition, are being considered. Like the sol gel technique, the ultra-sound deposition and combinations of these methods with other precursor preparations, like cluster formation.

2.1) THE SOL-GEL TECHNIQUE (3)

The sol- gel process, begins with the formation of a sol, which then turns into a gel. A sol is a suspension of solid particles with different dimensions, ranging from 1 nm to 1 μm. These particles which give a colloidal nature to solvents, are obtained through hydrolysis and a partial condensation of a precursor like a metallic alkyl oxide and are maintained in suspension by Brownian motion. Further condensation brings about a three dimensional network in the sol, producing a gel. The gel is a bi-phasic substance, i.e. a solid network trapping liquids. Ageing and drying do eliminate the trapped liquids and solvents and the manner in which this occurs produces a different type of gel. For example, if drying occurs either by evaporation or by supercritical extraction or in cryogenic conditions, the gels obtained are xerogel, aerogel and cryogel. The most important characteristic of the sol-gel method, which makes it a good preparation method for catalysis is the possibility of controlling the results obtained. This gives the following advantages:

- The capacity of obtaining extremely pure products, because the reactants are pure.

- The capacity of modifying physical characteristics like the distribution of the dimension of pores and the pore volume.
- The capacity of obtaining superficial dispersion down to molecular levels, with metal oxides and mixed metal oxides.
- Highly homogeneous systems.
- The possibility of preparing catalytic systems at low temperatures.
- The possibility of introducing numerous components in a single preparation step.

On the contrary, there are some problems which limit the use of this technique in an industrial scale like the high costs of the reagents, and the difficulty in reproducing the preparations, due to extra high sensitivity to environmental conditions like temperature and humidity.

To be able therefore to use the advantages, it is necessary to evaluate the four key steps involved in the sol-gel process, understanding how the various controlling parameters affect each and every step.

- ✓ Step 1; Gel formation;
- ✓ Step 2; Ageing;
- ✓ Step 3; Solvent removal, drying;
- ✓ Step 4; Thermal treatment.

2.1.1) Gel Formation

The precursors most frequently used in the sol-gel processes are the metal alkoxides, because of the ease to find them commercially and of their high purity. The process implies, either a hydrolysis of the alkoxide (hydrolytic sol-gel), the formation of a colloidal suspension and its evolution into a gel through condensation or the condensation of the precursors without the addition of water (non hydrolytic sol-gel)

2.1.1.1) Hydrolytic Sol-Gel

2.1.1.1.a) Hydrolysis

As seen in the reaction equation that follows, metal alkoxides can be hydrolysed either in an acidic environment or in a basic environment. This is due to the nucleophilic attack of water onto the electropositive metal centre.

$$M - OR + H_2O \rightleftharpoons M - OH + R - OH \qquad [1]$$

Hydrolysis reactions are conditioned by the following parameters:

I. Acidity of the solution: The kinetics of a hydrolysis reaction in a neutral environment is too slow. Reason for which they are carried out in either an acidic or a basic environment.
II. The molar ratio relationship between water and the alkoxide: Since water is a reactant, its concentration affects the reaction rate, and the greater the concentration, the faster the reaction.
III. The nature of the groups bonded to the metal: There's the steric effect; Large and cumbersome groups slow down hydrolysis of the metal. Then there's the inductive effect; The substitution of the alkoxide with alkyls, increase the electron density on the metal while a substitution with a hydroxyl group reduces the electron density. Therefore in acidic catalysis the substitution of alkoxidic group with hydroxyl groups diminishes the rate of hydrolysis, and vice versa in basic catalysis.
IV. Solvent nature: Since hydrolysis occurs with either acidic or basic catalysis, the presence of free hydrogen in solution could influence the catalytic effect. Solvents that do not form hydrogen bonds with OH^-, renders the hydroxyl a stronger nucleophile, while protic solvents render the hydrogen ion more electrophile. The capacity of forming

hydrogen bonds with the solvent can also influence the hydrolytic mechanism. For example activating a weak out going group, to realise an SN_2 (bimolecular nucleophilic substitution).

2.1.1.1.a.i) Hydrolysis In Acidic Catalysis

A proton is added to an oxygen of the alkoxidic group in the first step of hydrolysis in an acidic solution. This increases the electrophilic nature of the metal atom, making it more open to attack by water, the nucleophile. The reaction mechanism which is an SN_2, gives the formation of a five bonded metal atom, as intermediate. The reaction rate increases in the presence of substitutes with little steric hindrance, and those with an electron donating capacity.

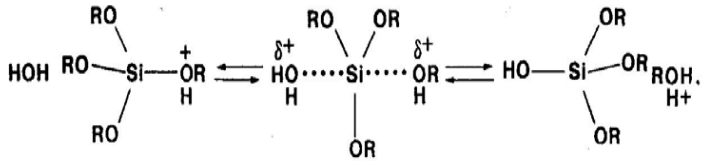

[2]

2.1.1.1.a.ii) Hydrolysis In Basic Catalysis

With equal catalyst concentrations, hydrolysis in a basic environment is slower than that in an acidic environment. The first substitution of the alkoxidic group proceeds slowly, but as substitution increases, the substitution rate also increases.

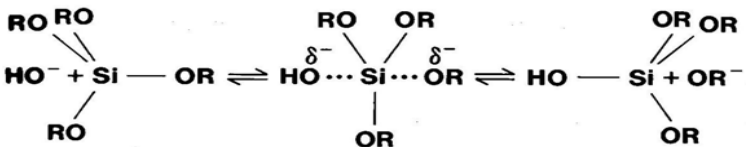

[3]

This hydrolytic reaction is sensible to substituents which, tend to stabilize the negative charge, with their steric hindrance and their inductive effects.

2.1.1.1.b) Condensation

The hydroxyl groups formed during hydrolysis of the alkoxide, tends to polymerize with the formation of groups like M-O-M. The condensation reaction proceeds in two ways. In the first case, the hydroxyl group attacks the metal atom with a subsequent expulsion of a water molecule. While in the other case, the hydroxyl group attacks the metal of another molecule, already hydrolysed partially, with the expulsion of an alcohol.

$$M(OR)_{n-1} + M(OR)_{n-1} \rightleftharpoons (RO)_{n-1}M\text{-}O\text{-}M(OR)_{n-1} + H_2O \quad [4]$$

$$M(OR)_n + M(OR)_{n-1}(OH) \rightleftharpoons (RO)_{n-1}\,M\text{-}O\text{-}M(OR)_{n-1} + ROH \quad [5]$$

Although the network formation of alkoxidic reactions is spontaneous, the sol-gel conditions often require catalyst which accelerate the reaction and in this way bring about the formation of the type of network desired. The catalysts normally used are acids and bases or the fluoride ion. The minimum condensation velocity corresponds to the pH at the iso-electric point. At higher pH's, the -OH groups of the network lose hydrogen (deprotonation), while at lower pH's, they gain hydrogen. The condensation reaction evolves into a gel.

2.1.1.1.b.i) Acid Catalytic Condensation

A condensation reaction in an acidic environment implies an addition of a proton to the hydroxyl group attached to the metal atom, increasing its electrophilic nature, and therefore enhancing the nucleophilic attack. This is a mechanism which implies the formation of a penta-coordinated intermediate. The substitution of the alkoxidic group with other electron attracting groups, destabilizes the positive charge formation in the intermediate transition state, hence slowing the condensation kinetics.

2.1.1.1.b.ii) Basic Catalytic Condensation

$$-M-O^{-} + -M-OH \longrightarrow -M-O-M- + -OH \qquad [6]$$

When a de-protonated hydroxyl attacks a metal having neutral hydroxyls, there's a nucleophilic attack. The acidity of -M-OH depends on the nature of the substituents. If -OR and -OH groups are substituted by -O-M a diminishing electron density is created on the metal, and a consequent increase of acidity on the remaining -OH groups. The lowest reaction rate corresponds to the pH of the iso-electric point.

2.2) Variables That Influence Hydrolysis And Condensation

The relative velocities of hydrolysis and condensation determines the structure and type of gel formed. The following factors play an important role in influencing this structure.

1. **pH Of The Solution**

The basic catalysis brings about the slowest reaction kinetics for hydrolysis, and this rate reaction increases as the substitution of alkoxidic groups with hydroxyl groups increase. The reaction goes to completion and it is non-reversible. Condensation is faster and proceeds with the addition of a monomer to an $-M-O^{-}$ group of the growing cluster, forming a highly ramified network (fig. 1: B).

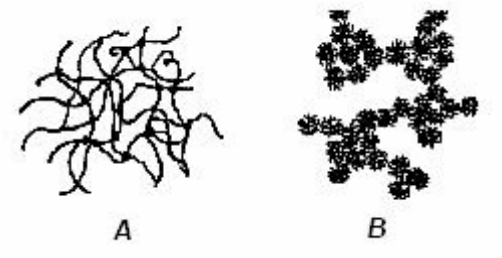

***Fig 1**: Network types obtained from A) acidic catalysis and B) basic catalysis.*

In the acidic catalysis instead, hydrolysis is faster, and the reverse reaction is also favoured (re-esterification reaction). The rate of the condensation reaction diminishes as the degree of substitution increases and goes on through the addition of neutral species to protonated M-OH groups. This brings about the formation of less ramified chains (fig. 1: A). Thus the conclusion, a rapid hydrolysis and a slow condensation (acidic catalysis), favours a linear polymer formation while a slow hydrolysis and a rapid condensation (basic catalysis), favours a ramified polymer formation. These different polymer formation causes great differences in the characteristics of the surface, after drying and calcining.

2. The Effect Of The Ratio Between Water And Alkoxide

The quantity of water used and the velocity with which it is added, influences greatly the gel to be formed. The "hydrolytic ratio", which is given as the number of moles of water with respect to the number of moles of metallic alkoxide, is the of fundamental importance to gelation. There are three interesting regions:

- R<1: The infinite network which is characteristic to gels cannot be formed. Gelation does not proceed without a local excess of water because only very few metal hydroxides are able to do cross-linking. In this condition, the favoured reaction is the condensation between an alkoxide and a hydroxide, with the elimination of an alcohol molecule, and not the desired reaction between two hydroxides.
- 1<R<m: Where m is the stoichiometric molar quantity. In this case there's still a water deficit. Polymers could be formed through hydroxyl reactions, but network formation and ramification becomes difficult. There will be a prevalence of the linear product.
- R>m: Putting an excess of water into the alkoxide, helps the formation of a polymeric gel with chain cross-linking, but this also increases the time of gelation, as the quantity of water increases. Not forgetting that water is a product of condensation between two hydroxides.

3. The Nature Of The Precursors

Hydrolysis and condensation are two nucleophilic substitution reactions, and therefore the reactivity of the metal alkoxides depend on the partial positive charge that is created on the metal atom and on its coordination number. In fact the bigger the alkoxidic group bonded to the metal, the lower its reactivity. Another aspect to take into consideration is the relative velocities of hydrolysis and condensation of the different precursors. For example, putting together different reactants with the same alkoxidic group like, $Al(OEth)_3$ and $Si(OEth)_4$, the resulting product, due to the different hydrolytic velocities caused by the different metal atom, is an auto-condensational polymer and not a hetero- condensational polymer. This characteristic can hinder the capacity to control gel formation and to obtain a desired product (e.g. the dispersion of active metal sites on the surface). The use of different alkoxides could avoid this difficulty, taking note of the increase in reaction velocity as the alkoxidic group goes smaller, or making a pre-hydrolysis of the less reactive precursor before adding the more reacting partner. Another way can be, to slow down the reactivity of the more reactive component using an appropriate ligand. Then, an increase in temperature increases both reaction rates , but the less reactive reaction is increased more. This could be enough to compensate the difference.

4. The Nature Of The Solvent

The exchange of alkylic group between the solvent and the alkoxide could modify the rate velocity of the process. A reason why, it is often necessary to dissolve an alkoxide in a solvent with the same alkylic group. A more influential effect is obtained from a solvent, whether or not it is protic. Protic solvents reduce the reaction velocity of the acid catalyzed hydrolysis, or the base catalyzed hydrolysis, due to their capacity to react with H^+ and $OH^=$. Aprotic solvents favourhydrolysis and condensation because their electrophilic and nucleophilic nature of the reactants are boosted.

5. Temperature Effect

An increase in temperature increases the rate velocity of hydrolysis and condensation, and therefore the entire process of gel formation.

2.3) Gelation

The evolution of the condensation reaction causes growth of the polymer chains, and thereby increasing the viscosity of the colloidal solution. The gelation time can be considered as the time necessary for the transition from a viscous fluid to an elastic solid. That is, the change from sol to gel. The same variables which enhance the condensation rate velocity reduce the time of gelation. The characteristics of the gel keep evolving even after the gel point.

2.4) Non Hydrolytic Sol-Gel

When condensation occurs directly without hydrolysis, there's non hydrolytic sol-gel. This reaction can be of various types.

a. Single component non hydrolytic sol-gel: This is when condensation is between precursors of the same type. For example, TEOS and $SiCL_4$

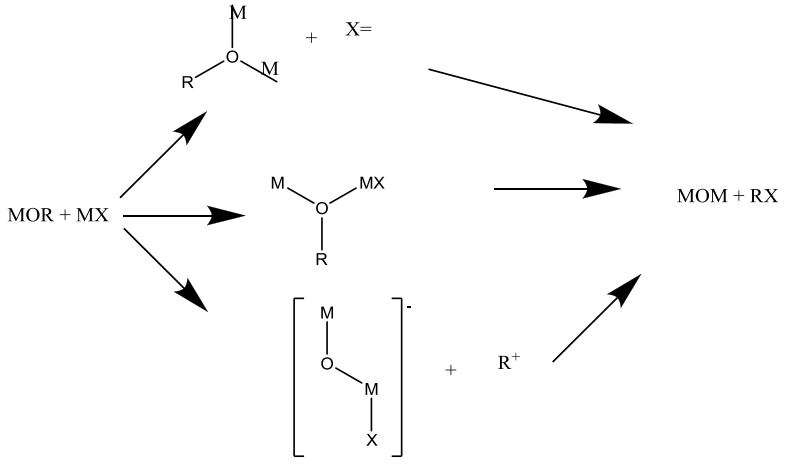

Fig. 2: *A single component condensation*

b. Multiple-component non hydrolytic sol-gel: When there's condensation between precursors of different metals, like $SiCl_4$ and $Al[OCH(CH_3)_2]_3$.

$$MOR + M'X \longrightarrow MOM' + RX \qquad [7]$$

In this case, reaction [7] has to be protected against the other possible reactions like;

$$MOR + M'X \longrightarrow MX + M'OR \qquad [8]$$

$$MOR + MX \longrightarrow MOM + RX \qquad [9]$$

$$M'X + M'OR \longrightarrow M'OM' + RX \qquad [10]$$

2.5) Ageing And Hydro-Thermal Treatment

The working conditions used in this part of the process could make us identify two different processes

- Ageing: This is carried out at low temperatures, atmospheric pressures and consequently very long operating periods.
- Hydro-Thermal treatment: They are fast, and are carried out at higher temperatures and pressures.

Another difference is given by the fact that, the hydro-thermal treatment is a desired process while ageing is casual. Generally the structural and morphological characteristics that can be modified using the one or the other process are the following:

- ❖ A change in the crystal dimension
- ❖ A change in the dimension of the amorphous particles
- ❖ A transition of amorphous particles into crystalline particles
- ❖ Crystalline transitions ($\alpha \rightarrow \beta \rightarrow \gamma$)

- ❖ A change in the porosity.

These are transformations that follow the laws of thermodynamics, so they proceed in the direction where there's a diminution of the free energy. Poly-condensation continues after gelation, increasing the connectivity of the network, by the formation of ulterior cross-links. A process favoured by the presence of hydroxyl groups.

Syneresis is the expulsion of small quantities of liquid from the pores as a consequence of further bonding due to the continuation of the condensation reaction. This continuation of the bonding causes contraction of the gel and the consequence is syneresis. The presence of organic solvents capable of forming hydrogen bonds with the hydroxyl groups of the network, causes a slow down of condensation and syneresis.

Coarsening is the non-reversible diminution of the surface area due to re-precipitation and re-dissolution of the surface particles. The superficial morphology makes it possible, for particles in different zones to have different solubilities. For example, convex surfaces are more soluble than concave surfaces. A gel in a liquid in which it is soluble, tends to re-precipitate the dissolved materials on the regions where the surface has a negative curvature (concave surfaces). This process causes an increase in the medium pore dimension and therefore a decrease in the specific surface area.

2.6) Drying

This is the evaporation of the solvent contained in the pores, a phenomenon governed by various parameters:

- ✓ Temperature
- ✓ Relative humidity
- ✓ Particle size
- ✓ Eventual air flow in the area.

Any rational treatment of drying takes into consideration capillarity. The expression which best expresses the vapour pressure inside a capillary tube is given by the Kelvin equation.

$$\ln \frac{P}{P^{\circ}} = -\frac{V2\gamma cos\theta}{rRT} = -\frac{VP_c}{RT} \qquad [11]$$

P =Vapour pressure;

P° = Saturation vapour pressure;

γ = Surface tension of the liquid;

θ = Contact angle between liquid and solid;

V = Molar volume of the liquid;

R = Pore radius.

P_c = Capillary pressure

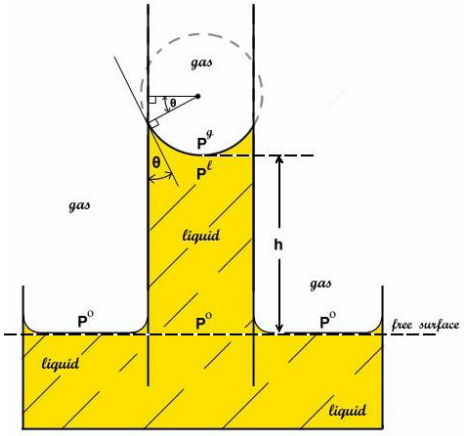

Fig 3: *The various pressure forces involved in capillarity.*

$$P_c = P^g - P^l = \frac{2\gamma cos\theta}{r} \qquad [12]$$

From the Kelvin equation we deduce a slow evaporation from tiny pores because of low vapour pressures. The exact contrary happens to large pores. Now when a solvent is trapped in a pore, the curved surface which separates the liquid from the vapour generates a capillary pressure. This capillary pressure developed in tiny pore can get so high that, they cause the break down the walls of the bigger pores, and a complete collapse of the structure of the gel.

This could be avoided in the following ways:

- ✓ Increase particle dimension through ageing;
- ✓ Low oven temperatures during drying;
- ✓ Increase in the relative humidity;
- ✓ Minimum air flow currents.

From the above description, drying can be divided up into different phases. Initially the gel undergoes a volume decrease which is proportional to the quantity of evaporated liquid, and the liquid vapour interface is on the surface. Here the liquid/vapour meniscus' radius is large with respect to the pore diameter, and the capillary pressure is low. At the arrival of a critical point where the radius of the meniscus is equal to the pore diameter, and the particles are so well packed that no further rearrangement is possible, the evaporating film continues inside the pore and this can bring about fractures on the pore walls. After this critical point, the liquid/vapour meniscus is no more on the surface, but is drawn back to a point where the liquid is isolated. Here evaporation proceeds only by diffusion. There's an increase in capillary pressure, which might provoke structural rearrangements, and make the gel compact. The stress that is generated from contraction is greater in gels prepared with acidic catalysis, because of the minor pore dimensions. Those prepared by the basic catalysis instead, are made of dense clusters separated by large empty spaces, and therefore generate very low superficial tension.

2.7) Thermal Treatment

To be able to give a final catalytically useful form to the gel, it is necessary to undergo specific thermal treatments. This is heating in the presence of various reactive gasses like in the air, oxygen or hydrogen. The heating eliminates all residual organic matter and oxidize or reduce the specimen. The exposure of a gel sample, to high temperatures for a certain period, causes a decrease in the surface area, and might also cause some re-crystallization. Normally the gel undergoes a more severe thermal treatment than the treatment it would encounter in the reactor

CHAPTER THREE

3) APPLICATIONS OF THE PREPARATION METHOD

Using the sol-gel techniques to prepare catalysts for heterogeneous catalysis limits the methodology to a few simple ways of proceeding. These can be divided up into three main groups:- 1) Impregnation; 2) Sol-Gel in Bulk; 3) Grafting (or Anchorage).

3.1) IMPREGNATION

This is the method most extensively used in the preparation of heterogeneous catalysts, and consists of a diffusional transportation of catalytically active species into the pores and on surface of the support. The impregnation is carried out in a way that the deposition of the active species is on the surface. This confers higher activity, limiting the amount of active sites which remain in the bulk of the catalytic system, and in this way avoiding diffusional kinetic problems.

The impregnation method can also be divided up into two sub methods which mostly depend on the nature of the support, and especially on its adsorbing capacity. The adsorbing capacity inorganic matrix support, depends not only on the nature of the support, but also on the pH of the solution where it is found and the iso-electric point of the surface.

a) Total Immersion: This method is used when the support is capable of interaction with the precursor in the solution. Mass transfer in this case is exclusively through diffusion. Here there's a high adsorbing capacity.

b) Incipient Wetness: This method is used instead, when the adsorbing capacity is low. The pore volume is studied and an estimate is made on the amount of solution that can be adsorbed on the support through capillarity. The precursor will then be dissolved in the smallest possible volume of solvent, and then corrected to the calculated volume of solution.

3.2) SOL-GEL IN BULK

In earlier research programs for graduate thesis (1), this preparation method has not been studied much. It was expected to be one of the easiest method of preparation and a method for producing very active catalysts, with respect to other methods like impregnation and anchorage. This method in the case of metal based catalysts supported on matrices produced from alkoxides, can be carried out in two different ways. In the first case, the alkoxide , in an adequate solvent and an acidic environment, undergoes hydrolysis when heated with reflux. After cooling, the solution of the metal precursor is added under vigorous agitation. This mixture is then left to rest, where solvent evaporation brings about gelation . The second method consists of dissolving the metal precursor in an adequate solvent, and while heating and agitating, the alkoxide is then added. The heating and agitation goes on until the solution becomes homogenous. Then water is added to bring about hydrolysis.

3.3) ANCHORAGE

When there is interaction with bond formation between the support surface and the deposited precursor (for example, real covalent bonds), brought about by chemical reactions between functional groups, both on the support surface and on the precursor, there is anchorage. The

preparation of catalysts using this method is done in various stages. Initially the inorganic matrix used as support, is treated thermally to different levels (from normal heating in an oven for drying, to real calcining, to be able to control the types and quantity of functional groups on the surface). Once there is contact between the metal precursor and the functional groups at the surface of the support, there is reaction, which can be either a condensation or an addition. This depends on the group which comes along with the metal. They are as follows: Either

$$Y[\text{sup-OH}] \quad + \quad MX_n \longrightarrow \quad [\text{sup-O}]_yMX_{n-y} \quad + \quad yHX$$

in the case of a condensation, or

$$[\text{sup-OH}] \quad + \quad M_3(CO)_{12} \quad \longrightarrow \quad [\text{sup-O}]M_3H(CO)_{10} \quad + \quad 2CO$$

in the case of an oxidative addition. Then, the part of the precursor not bonded to the surface is washed off. After ageing and drying, the metal precursor undergoes an adequate treatment for activation.

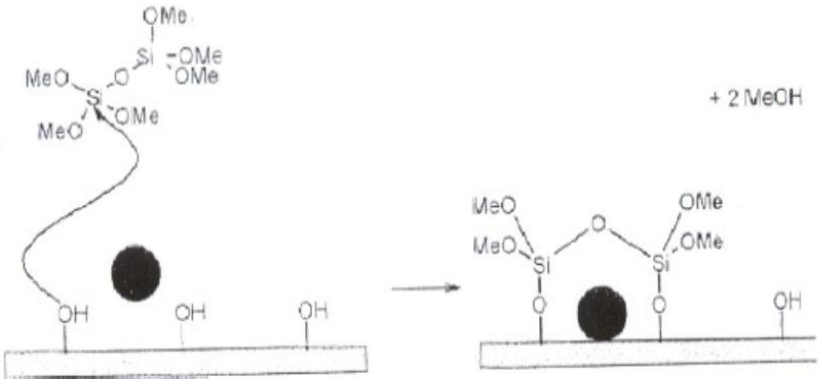

***Fig 4**: An Anchorage Formation Mechanism*

Another method of preparation is the Vapour phase deposition, which has not been exploited in this research.

CHAPTER FOUR

4) OTHER PREPARATION METHODS

4.1) THE ULTRA-SOUND CHEMISTRY (4)

Ultra-sound chemistry is the use of ultrasound to enhance or alter chemical reactions. Ultra-sound chemistry in the true sense of the term occurs when ultrasound waves induce true chemical effects on the reaction system, such as forming free radicals which accelerate the reaction. However, ultrasound may have other mechanical effects on the reaction, such as increasing the surface area between the reactants, accelerating dissolution, and/or renewing the surface of a solid reactant or catalyst.

The chemical effects of ultrasound waves are not derived from a direct coupling of the acoustic fields with chemical species on a molecular level. Ultrasound has frequencies from around 16 kilohertz to tens of megahertz. In liquids, this means wavelengths from centimeters down to microns, which are not molecular dimensions. Instead, when sound passes through a liquid, the formation, growth, and implosive collapse of bubbles can occur, as depicted in Figure 4 this process is called acoustic cavitation.

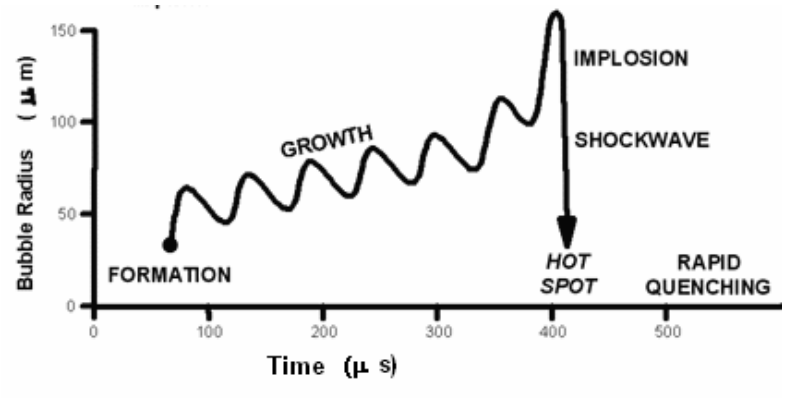

***Figure 4**: Acoustic cavitation*

Ultrasound chemistry and luminescence are effects which come principally from acoustic cavitation: the formation, growth and implosive collapse of bubbles in liquids irradiated with high-intensity ultrasound [5]. Bubble collapse during cavitation serves as an effective means of concentrating the diffuse energy of sound waves (compression of a gas generates heat). When the compression of bubbles occurs during cavitation, heating is more rapid than can be experienced in any form of thermal transportation, creating a short lived localized hot spot. These hot spot have temperatures of about 5000°C, and pressure of about 1000 atm, and heating and cooling rate is above 1010 °K/s [6] There is a nearly universal consensus that this hot spot is the source of homogeneous sound chemical effects.

Ultrasound has proven to be a very useful tool in enhancing the reaction rates in a variety of reacting systems. It has successfully increased the conversion, improved the yield, changed the reaction pathway, and/or initiated the reaction in biological, chemical, and electrochemical systems. This non classical ultrasound chemical method of rate enhancement, is becoming a widely used laboratory technique. However, its use in industry is limited because the process of producing ultrasound waves, is very inefficient and burdened with high operating costs. It is beginning to attract attention because the operating costs can be bypassed by reducing or eliminating other process costs. The use of ultrasound waves enables operations at milder operative conditions (e.g., lower temperatures and pressures), eliminate the need for extra costly solvents, reduce the number of steps for the synthesis while simultaneously increasing end yields, permits the use of lower purity reagents and solvents, and increases the activity of

existing catalysts. For these reasons, use of ultrasound waves appear to be a promising alternative for high-value chemicals and pharmaceuticals. In addition, research is continually underway to make it a feasible option in the on-going effort to intensify large-scale processes. Hoechst and several other companies are working on a project with Germany's Clausthal Technical University (Clausthal-Zellerfeld) which uses a modular reactor to produce up to 4 metric tons of Grignard reagent per year. They found ultrasound waves to increase the conversion by a factor of five and reduce the induction period from 24 h to 50 min (7).

With such high enhancements in rates, it is no wonder that the number of publications in this field has increased significantly in the last 20 years (8). Much of the pioneering work in this field has been done by chemical scientists and physicists who have found that the chemical, and some mechanical, effects of ultrasound are a result of the implosive collapse of cavitation bubbles. The interest of the chemical engineer in capturing and quantifying these beneficial effects is rising, but publications in such crucially applied areas as mass transfer, reaction kinetics, reaction modelling, and reactor design are scarce.

Ultrasonic irradiation differs from traditional energy sources (such as heat, light or ionizing radiation) in duration, pressure and energy per molecule. The immense local temperatures and pressures together with the extraordinary heating and cooling rates generated by cavitation bubble collapse means that ultrasound provides a unique method for generating high-energy in chemistry.

Ultrasound occurs at a frequency above 16 kHz, higher than the audible frequency of the human ear, and is typically associated with the frequency range of 20 kHz to 500 MHz. The frequency level is inversely proportional to the power output. Low-intensity, high frequency ultrasound (in the megahertz range) does not alter the state of the medium through which it travels and is commonly used for non-destructive evaluations in medical diagnosis. However, high-intensity, low-frequency ultrasound waves do alter the state of the medium and is the type of ultrasound typically used for the chemical applications.

4.1.1) Methods of producing cavitation

Cavitation can be generated within a fluid using transducers (devices which convert one form of energy to another). Gas-driven transducers, such as dog whistles, use high-velocity gas flow to generate ultrasound. Liquid-driven transducers, such as submarine propellers, force liquid across a vibrating plate or through an orifice, creating a cavitation zone. Electromechanical transducers, the most commonly used transducers in sound chemistry research, convert electrical energy to sound energy. The two main types of electrochemical transducers used in industrial applications are piezoelectric and magneto-restrictive.

Magneto-restrictive transducers were the first ultrasound generators used on an industrial scale. The magneto-restrictive effect, discovered by Joule, is the effect that some metals (nickel, cobalt and iron) and alloys have when placed in a magnetic field. Due to the magnetic field, the molecules in the substance rearrange themselves and the metal shrinks. When the magnetic field is removed the substance returns to its original size. The strength of the magnetic field determines the extent of change in size. Applying a magnetic field in short pulses gives a vibrating material which vibrates at the same frequency as that of the magnetic pulses.

Magneto-restrictive transducers have some disadvantages. The magnetic metals heat up fast when much energy is put into them. The conversion of energy into ultrasound is only 60%. The maximum frequency that can be reached with this technique is 100 kHz (9), but then cooling is essential. Recent developments have led to a new magnetic core based on an alloy of terbium, dysprosium and iron. With this core the magneto-restrictive transducer can generate more power and is more compact than other transducers, but this apparatus cannot produce frequencies above 70 kHz.

Piezoelectric crystals are the most common transducers used both for generation and detection of ultrasound. The piezoelectric effect was discovered in 1880 by the Curie brothers. They discovered that certain crystals without a centre of symmetry, develop a charge separation when pressure is applied to them. They discovered also that the reverse is true too. Some

crystals with this behaviour are: tourmaline, tartaric acid, Rochelle salt, ammonium di-hydrogen phosphate, barium titanate, and quartz. Of all these, quartz is the most common and the least susceptible to fracturing . Stronger and easier to manufacture is a transducer, based on ceramics, containing piezoelectric material. With these model there's the advantage of the possibility to choose which size and shape the transducer should have. Piezoelectric transducers are very efficient: over 95% of the input energy is converted into ultrasound. The frequencies that can be reached range from 20 kHz to over 5 MHz For these transducers also, cooling is necessary to avoid degrading the material used in the construction.

4.1.2) Types Ultrasonic Systems

4.1.2.1) Ultrasonic bath

Ultrasonic baths were originally manufactured for cleaning purposes. Typical baths have the transducers attached to the bottom, although the transducers can be submersed in a conventional tank to obtain similar effects. Bath systems are widely used in chemical sound research because they are readily available and relatively inexpensive. The reaction vessel is typically immersed in the coupling fluid contained in the bath (indirect sonication). However, the bath itself can be used as the reaction vessel and this would require additional mechanical agitation. In addition, the bath walls would be exposed to the reaction mixture and irradiation, making them susceptible to corrosion or erosion.

Since every bath has different characteristics, it is important to determine the optimum conditions for each bath and to place the reaction vessel in the same location for each experiment. In addition, it is important to use the same type of reaction vessel for each reaction because the shape of the bottom of the reaction vessel significantly influences the wave pattern, even when placed in the same position in the bath , (10).

4.1.2.2) Probe (HORN) systems

Probe systems, also called horn systems, are being more frequently used for chemical sound research in the laboratory. This may be because manufacturers are aware of the fact that this type of research is increasingly convincing and are providing equipment to meet the demand of researchers. In addition, probe systems are capable of delivering large amounts of energy directly to the reaction mixture which can be regulated by varying the amplitude delivered to the transducer. Disadvantages in using a probe system include erosion and pitting of the probe tip, which may contaminate the reaction solution (11). Fortunately probes are available with removable tips, making replacement relatively inexpensive. The vibrating motion generated by the piezoelectric transducer used in this equipment is normally too low for practical use and so it is necessary to magnify or amplify this motion. This is the function of the horn (or probe) attached to the transducer. Normally the horn is half a wavelength long. The most popular horn designs are show in Figure 5.

a) **Stepped**. For this design the magnification factor is the ratio of the end areas. The potential magnification is limited only by the dynamic tensile strength of the horn material. This is a useful and easy design to manufacture.
b) **Linear taper**. This is simple to make but its potential magnification is limited. It is approximately fourfold less.
c) **Exponential taper**. This design offers a higher magnification factor than the linear taper but its shape makes it more difficult to manufacture. Its length and the small diameter of the working end makes this design particularly suitable for micro applications.

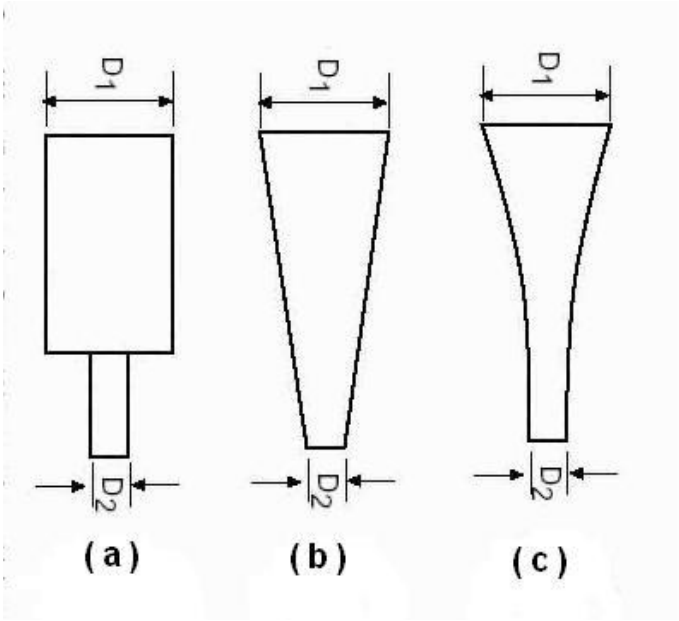

***Figure 5**: Horn designs*

The material used for the fabrication of acoustic horns should have a high dynamic tensile strength, a low acoustic loss, a high resistance to erosion caused by cavitation, and be chemically inert. The most suitable material tested so far, is a titanium alloy. The advantages of this method over a bath are therefore:

• A much higher ultrasonic energy available for use since energy losses during the transfer of ultrasound through the bath and reaction vessel walls are eliminated.

•These devices can be tuned to give optimum performance in the reaction mixture over a range of different energy levels.

•The ultrasonic intensity and the quantity of the sample to be irradiated can be matched fairly accurately for optimum effect.

The localized areas of ultrasonic intensity in a fluid is highly dependent on the energy delivered to the transducer. Contamine [12] observed that when the power delivered to the system is low (i.e., 8 W), the distribution of ultrasonic intensity is characteristic of a standing wave in the axial direction. However, as the power delivered to the system is increased, the wave pattern dissipates and the intensity becomes higher near the probe tip and decreases axially. In the radial direction, they found that at low powers (i.e., 8 W) the intensity is slightly higher at the centre of the reactor but is comparable over the cross section of the reactor. However, as the

power delivered increases, the ultrasonic intensity increases at the centre of the reactor and dissipates in the radial direction. At an input power of 200 W, the active region in the radial direction is equal to that of the horn (the remaining radial direction, had negligible activity). A minimum liquid height of 1 cm must be maintained in the reaction vessel, below which the transducer does not function properly [13].

4.1.2.3) Planar transducers

This type of setup is typically made in the laboratory and consists (see figure 6) of a planar transducer connected to a vessel which contains either the reaction mixture (a. Direct sonication) or a coupling fluid (b. Indirect sonication), into which the reaction vessel is immersed.

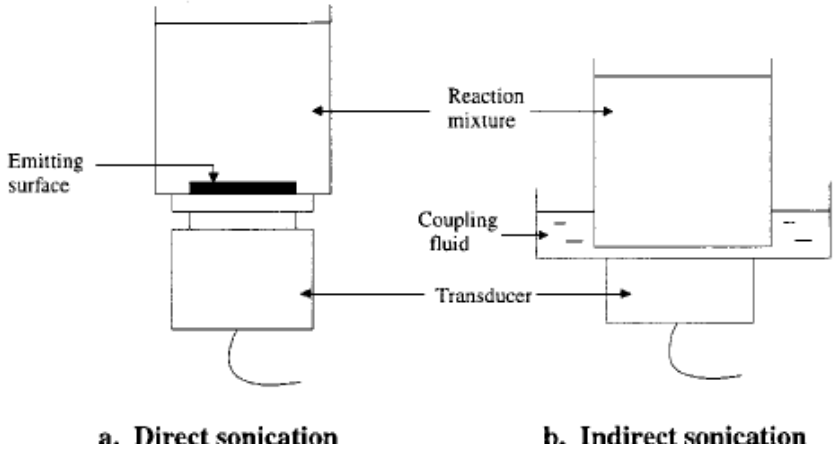

***Figure 6**: Planar transducer systems.*

There are several references available which provide a general overview of the field of sonochemistry and the types of chemical reactions which have been studied (5-13). Some authors have compared the various effects of ultrasound to other types of chemistry, such as electrochemistry (11).

4.1.3) Birth, growth and death of a cavity

Cavities can form when ultrasonic waves are transmitted through a solvent (see figure 7). The rarefactions correspond to low-pressure areas in the liquid.

When the pressure becomes sufficiently low the distance between the molecules will become larger than what is needed to hold the liquid intact [13]. Since the creation of vacuum cavities is energetically less favourable than the creation of a gas or vapour bubble, gasses dissolved in the liquid will be released into the cavity, leading to degassing, if the gas bubbles formed rise to the surface of the liquid.

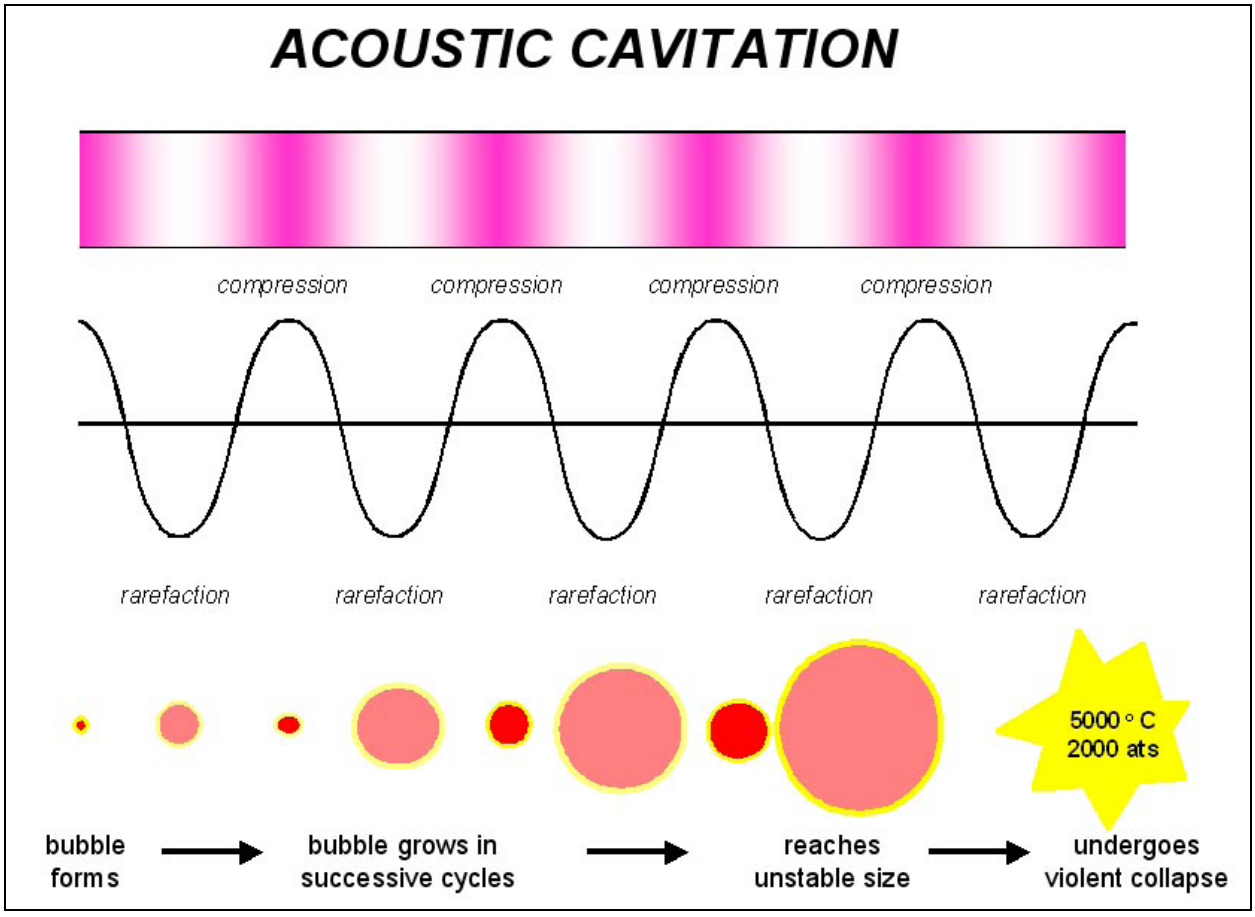

Figure 7: Schematic representation of a liquid under the influence of ultrasound.

Theoretically a negative pressure of the order of 105 atmospheres is needed to create a vacuum cavity. In practice the pressure necessary to create a cavity is much lower (in the

order of 104 atmosphere) due to liquid vapour filling the cavity and the presence of nucleation sites, like dissolved gas molecules and small dissolved particles. When there is no more dissolved gas in the solvent, the cavities cannot be filled with gas from the liquid. Then solvent will evaporate into the cavities, forming small bubbles of vapour [13]. The formed cavity grows over a number of cycles of the transmitted wave taking in gas or vapour from the liquid until a size is reached which equals the resonance size of the frequency of the wave. The formed cavities can be divided into two classes, stable and transient.

4.2) MIXED METAL CLUSTER FORMATION

4.2.1) Synthesis

Only a few metal clusters have been prepared by designed or rational synthetic procedures. Most clusters are prepared by placing together a variety of reagents, and allowing them to react. This reaction mixture is then examined to find out what compounds have been formed. This is particularly true for mixed metal clusters, and real need exists for the development of synthetic procedures, that can be used for designed synthesis of particular compounds. There are about four preparation methods generally used in preparing mixed metal clusters: (1) Pyrolysis, (2) Addition to coordinatively unsaturated compounds, (3) Redox condensations, and (4) Reaction of carbonyl metallates with metal halides.

1. **Pyrolysis Reactions**

Pyrolysis reactions generally involve the heating together of two or more stable compounds of different metals, presumably to give fragments that then combine to yield the mixed metal clusters. The amount of heat necessary to drive this reaction varies considerably, but in some cases , simply stirring the reagents at ambient temperature is sufficient. This reaction are

generally not adaptable to designed synthesis. An example could be the pyrolysis of two monomeric species:

$$H_2Os(CO)_4 + Pt(PPh_2Me)_4 \xrightarrow[3\ days]{25^\circ C} Os_2Pt(CO)_7(PPh_2Me)_3 \text{ (1,3\%)} \qquad [1]$$

Another example is the pyrolysis of metal carbonyl dimers. These have proven to be a useful reagent for mixed metal cluster synthesis, especially in the case of Fe and Co clusters since $Fe_2(CO)_9$ and $Co_2(CO)_8$ are easily obtainable materials. Predictions are usually unfruitful but examination of the available data shows that the initial unit dimer is preserved in approximately half of the reactions.

$$Fe_2(CO)_9 + Co(Cp)(CO)_2 \xrightarrow[Light\ petroleum]{65^\circ C, 15\ min} Fe_2Co(Cp)(CO)_9 \text{ (moderate yield) } [2].$$

The pyrolysis of metal clusters in the presence of monomers, dimers or other clusters usually requires much more severe reaction conditions. These higher temperatures and longer reaction time indicates the greater difficulty in fragmenting the clusters.

2. **Addition Of Coordinatively Unsaturated Species**

This synthetic method is becoming very important. It resembles the pyrolysis technique, as coordinatively unsaturated species are presumably formed during pyrolysis by dissociation of ligands or cleavage of metal-metal bonds. These species are apparently the key intermediates that condense to give the cluster. The addition of a metal nucleophile to a preformed coordinatively unsaturated compound occurs, in general, under milder conditions and they are much more adaptable to design synthesis. They also give a much higher yield in clusters than the pyrolysis method. The reactions of nucleophiles like Pt(0), Pd(0) and Ni(0) complexes, with unsaturated metal-metal bonds, have been extended to carbenes and carbyne derivatives, by Stone and co-workers.[14]

$$W[C(OMe)Ph](CO)_5 + Pt(C_2H_4)_2\{(PMe)t-Bu)_2\} \xrightarrow[toluene]{-20°C} WPt_2(\mu-C(OMe)Ph)(CO)_6\{PMe(t-Bu)_2\}_2\ (50\%) \quad [3]$$

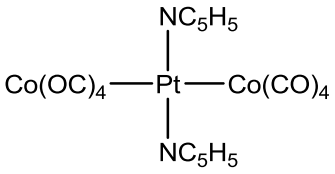

Fig. 8:

It is worth noting that the carbene ligand migrated from W to a position bridging the Pt-Pt bond during the course of the reaction. After these synthetic studies, Stoeet al. proposed a formal analogy between the addition of metal nucleophiles to olefins, metal carbenes, and doubly bonded metal-metal compounds.

3) Redox Condensation

The reaction between a carbonyl metallate and a neutral metal carbonyl has been termed "redox condensation", and has been widely used for synthesizing mixed metal clusters. Carbonyl metalates usually react rapidly with neutral carbonyls even under mild conditions. A large number of mixed metal hydride clusters have been formed through this reaction, primarily because the initial products are anionic clusters that in many cases can be protonated to give a neutral hydride derivative.

$$[Mn(CO)_5]^- + Fe(CO)_5 \xrightarrow[diglyme]{} [MnFe_2(CO)_{12}]^- \quad [4]$$

The reaction of carbonyl metalates with tri-nuclear clusters, provides a convenient synthetic via for tetra-nuclear clusters. Knight and Mays [15]explored this reaction, and on making $[Mn(CO)_5]^-$ and $[Re(CO)_5]^-$ to react with trimeric clusters of the Fe triad, obtained interesting tetra-nuclear clusters with particular mechanistic characteristics.

4) Reaction Of Carbonyl metallates With Metal Halides

The carbonyl metallate displaces the halide group from a metal halide complex, to give a metal-metal bonded specie. The configuration of the metal-metal bonded product depends on the nature of the starting complex.

$$[M(CO)_x]^{n-} + Cl - ML_n \rightarrow Cl^- + (CO)_x M - ML_n \qquad [5]$$

For example, the reaction of *trans*-$PtCl_2(pyridine)_2$ with $[Co(CO)_4]^-$ gives a linear specie, while the reaction of $PtCl_2(dppe)$ with $[Co(CO)_4]^-$ results in a Co_2Pt cluster.

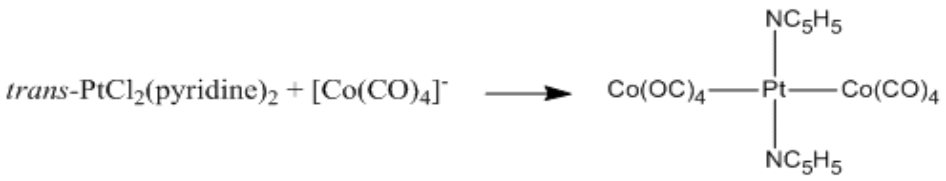

[6]

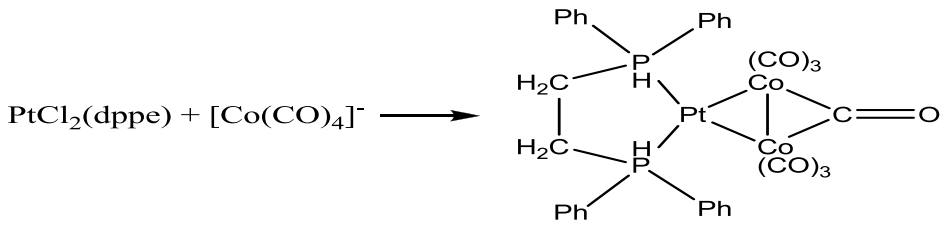

[7]

Some other types of reactions are used to create mixed metal clusters, although they don't fall into these categories. For example, photochemical reactions, and other reactions which could be considered addition of carbonyl metallates but with a resulting mechanism much more complicated. Although serendipity is the key force behind cluster synthesis, there's enough knowledge for strategic synthesis, especially in the case of tri-nuclear and tetra-nuclear clusters. It seems the most logical procedure is the step by step building of the clusters, beginning from the complex monomers. So, to build up a tetra-nuclear tetrahedron, the beginning material should be two metal-organic monomers, which react to give a metal-metal dimer.

CHAPTER FIVE

5) SYNTHETIC PROCESSES USED FOR CATALYTIC TESTS

5.1) Fischer-Tropsch Synthesis

Over the last three decades, there has been a growing interest in the use of coal as a potential source of both chemical feedstock and fuels. The rapid rise in the prices of crude oil and concern about the depletion of oil and natural gas reserves have triggered this interest. The major problem in the use of coal as a raw material for the chemical industry is the inability to convert coal directly into ethane and other desirable light olefins. However, the gasification of coal into a mixture of CO and H_2 could offer an alternative, provided that olefins could be produced from such a synthesis gas with a high selectivity.(14) The Fischer-Tropsch synthesis is the conversion of natural gas into liquid fuel, passing through syngas. After the first trials of Sabatier and Senderens, in the hydrogenation of CO, with the resulting product methane, using Co or Ni catalysts and working at temperatures between 80° to 200°C, in the year 1922, Franz Fischer and Hans Tropsch developed the Synthol process, where they obtained a wide range of hydrocarbons, accompanied by some oxygenated compounds. Working at 100 bars and 400 °C, they obtained a way of getting liquid, using catalysts based on iron, cobalt and nickel, with the aid of promoters. Towards 1927, the first fixed bed reactors were designed and brought about the industrialization of the process. During the second world war, this method of producing fuel was abandoned, because of the discovery of large oil fields. The recent petrol

crisis and the great need for new energy sources, have boosted the research, and increased the catalytic quality of this process. The main reactions involved in this process principally are the paraffin and olefin synthesis. Other minor reactions like alcohol synthesis, the Boudouard reaction and the water-gas shift reaction, are also present in the process, although the extent to which they occur depends on the reaction condition. For example, the Boudouard reaction, the carbon deposit formation and the redox reaction on the metal, causes deactivation of the catalyst. The presence of CO_2 on the surface of the catalyst is not always damaging for the catalyst, especially when the catalyst is able to convert CO_2 into hydrocarbons.

The paraffin synthesis	$nCO + (2n+1)H_2 \rightarrow C_nH_{2n+2} + nH_2O$	ΔH=-167 Kj/mol
The olefin synthesis	$nCO + 2nH_2 \rightarrow C_nH_{2n} + nH_2O$	ΔH=-147 Kj/mol
The alcohol synthesis	$nCO + 2nH_2 \rightarrow CnH_{2n+1}OH + (n-1)H_2O$	ΔH=-147 Kj/m l
The Boudouard reaction (dismutation)	$2CO \rightarrow C + CO_2$	
The water/gas shift reaction	$CO + H_2O \rightarrow CO_2 + H_2$	ΔH=-42 Kj/mol
Carbon deposit formation	$CO+H_2 \rightarrow C+H_2O$	
Oxydation and reduction reactions	$xM + yH_2O \rightarrow M_xO_y + yH_2$ $xM + yCO_2 \rightarrow M_xO_y + yCO$	

***Table 1**: The FTS reactions*

Essentially the Fischer-Tropsch synthesis can be divided up into three stages. The production and purification of syngas from different origin, like gasification of carbon, making a steam

reforming of methane in natural gas, and biomass, which can be anything organic, either vegetable or animal. The synthesis of hydrocarbons and waxes which is carried out industrially in two ways. Either at high temperatures (300-350°C), using Fe based catalysts to produce low molecular weight and linear hydrocarbons, or at low temperatures (200-250°C), using Co based catalysts to produce high molecular weight and linear hydrocarbons, i.e. waxes. The hydrocracking, which is a combination of hydrogenation and a catalytic cracking, for the selective conversion of heavy fractions into lighter fractions which are used as fuel.

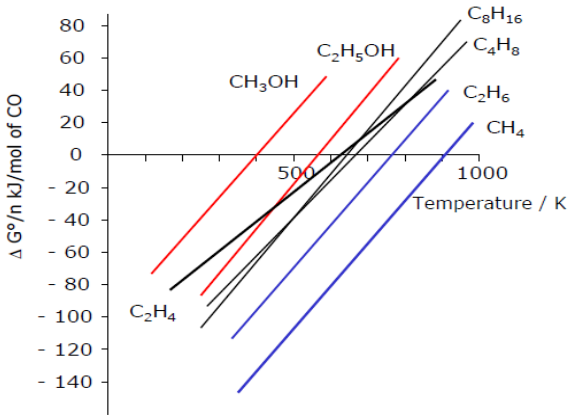

Graph 3: *The Francis' diagram for hydrocarbons*

A glance at graph 3 gives an idea of the ease of formation as temperature changes on the products of this synthesis. The first thing worth noting is how methane is the most favourable product. It can also be noticed that important or significant products are not very favoured. This means, if significant products are to be obtained, the process must be catalytically and kinetically controlled, for optimization. The mathematical model, generally accepted, which gives a good interpretation of the way products are formed in this process is the Anderson- Schultz-Flory model. This model was coined originally, for the free radical polymerization and poly condensation. It can be applied to the F-T synthesis, if the following assumptions are made: the chain growth reaction is supposed polymeric, with an addition of one carbon unit after the other; and that the probability of growth of the chain, is independent on the length of the chain itself. The A-S-F equation is as follows:

$$W_n = n(1-\alpha)^2\alpha^{n-1} \qquad [1]$$

This equation is known better in the linear form:

$$\ln\left(\frac{W_n}{n}\right) = \ln(1-\alpha)^2 + (n-1)\ln\alpha \qquad [2]$$

Wn = The weighted fraction of product with n number of atoms

α = The chain growth probability factor, and is equivalent to

$$\alpha = \frac{r_p}{r_p + r_t} \qquad [3]$$

The α factor varies from 0 to 1, and when it tends to 1 ,there's a production of waxes and long chain hydrocarbons. An effective distribution of products according to A-S-F model is shown in graph 4

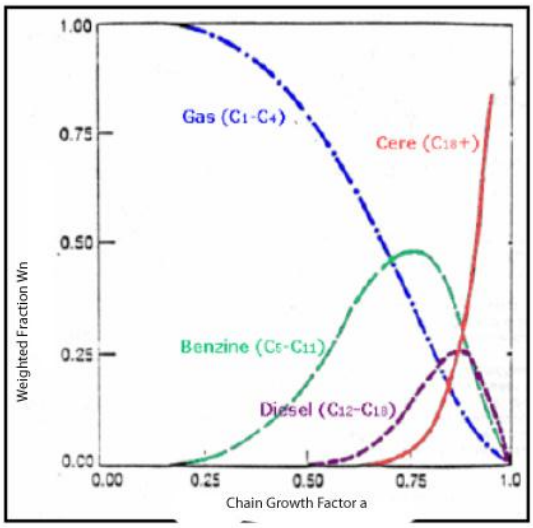

***Graph 4**: product distribution as a function of chain growth.*

5.1.1) Proposed Reaction Mechanisms

The three most popular reaction mechanism generally accepted for the Fischer-Tropsch synthesis are a) the surface carbide formation, b) formation of a "carbene" hydroxide, and c) a mechanism with a carbonyl insertion. All three methods have different initiations

- Formation of a Surface Carbide.

Initially there's a dissociative adsorption of CO on the surface of the catalyst.

Successively there's hydrogenation and the resulting metallo-vinyl compound acts as the monomer, for the polymerization reaction.

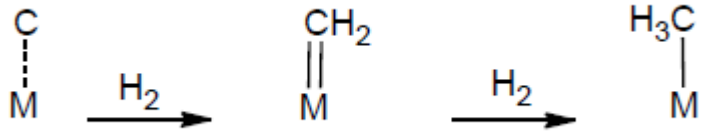

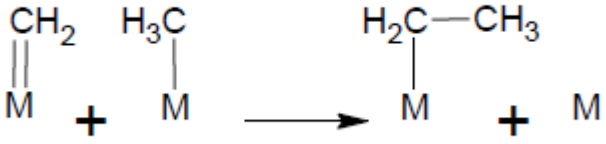

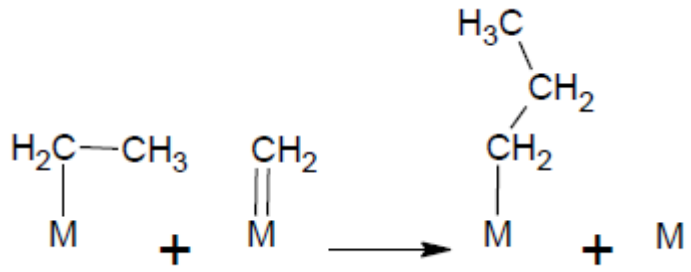

The termination of the polymerization is either by an elimination of hydrogen in β, which leads to the formation of a terminal alkene, or a hydrogen addition, which gives an alkane.(15)

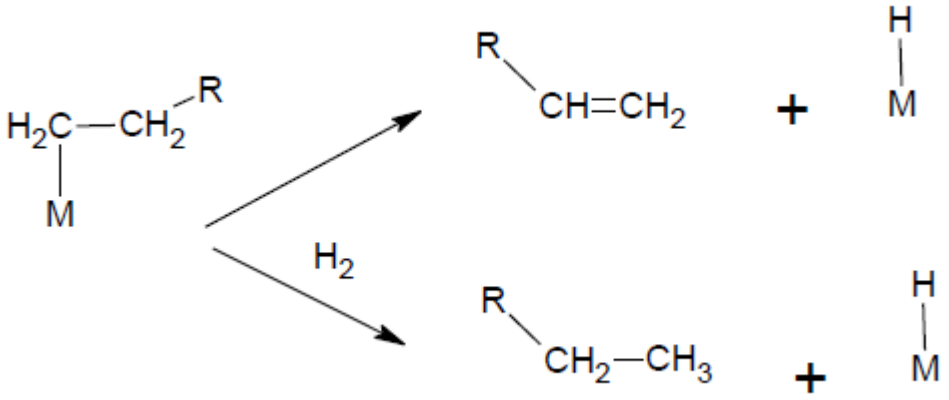

This mechanism is the most acceptable after observations with isotopically different Co, Ni and Ru.

- The “Carbene” Hydroxide Formation Mechanism.

In this mechanism CO is adsorbed chemically on the surface, without dissociation. The propagation is between two carbenes which react to lengthen the chain and produce water.

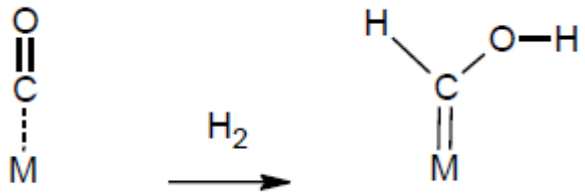

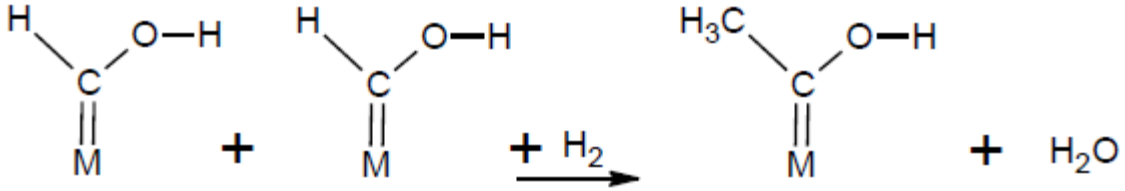

Termination is brought about by hydrogenation, with the formation of many types of product like, paraffins, olefins and alcohols.

- The carbonyl insertion.

This method requires an initial adsorption of CO in the molecular form, which is followed by hydrogenation, and subsequent formation of methyl-metallic species.

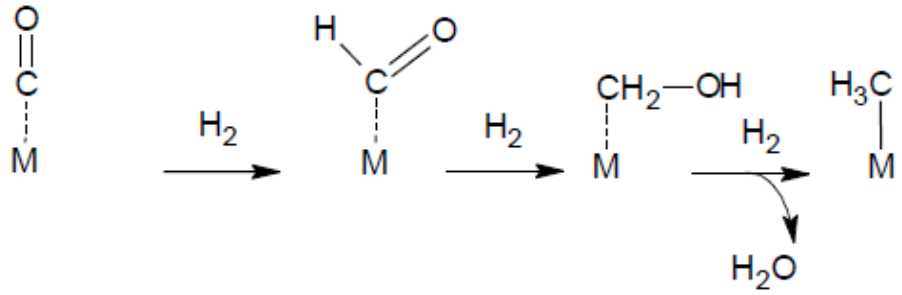

The most important step is the one where there's an insertion of a CO to the alkyl-metal bond for chain growth.

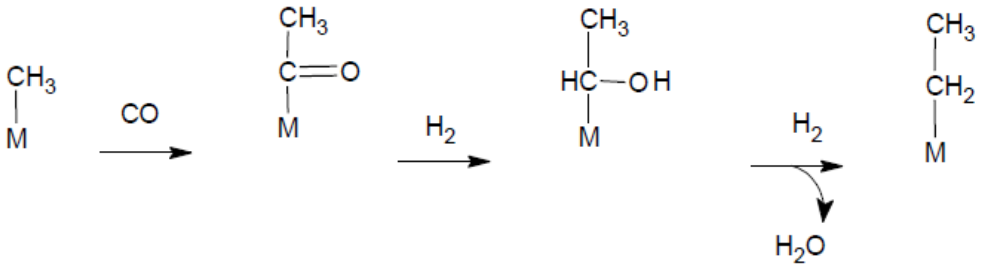

Even this mechanism terminates with a hydrogenation, which goes to confirm the resulting production of various species.

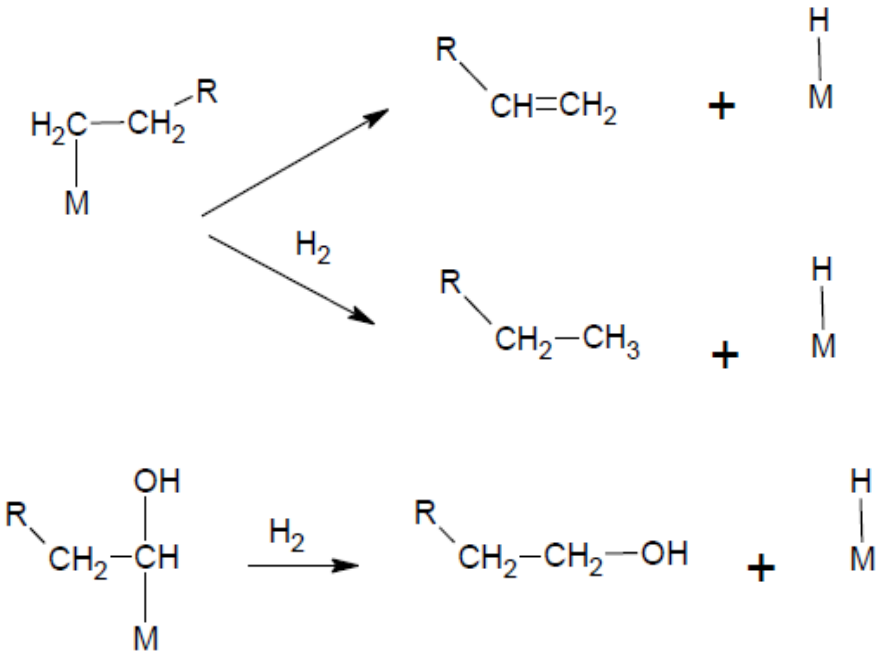

From the activity test results, all three types of mechanisms are justified. This gives a reason to think of a partial co-existence of all three mechanisms.

5.2) The Ammonia Synthesis

Since 1820, it was known that, there was the possibility to make ammonia directly from the elements, N_2 and H_2. This process was not possible because nobody succeeded in the realization of the reaction. Haber, under the following conditions, succeeded in laboratory conditions to carry out the reaction. These conditions were, firstly, there was a need for a catalyst to accelerate the reaction at relatively low temperatures, and secondly the unreacted reagents, should be recycled over the catalyst, so that the reaction can go on even at low conversions. So interesting were the results on laboratory scale that, BASF (Badische Anilin und Soda Fabrik) was convinced to buy the patent. The first industrial plant (1931), used iron oxide activated by an alkaline metal oxide, operating at 300°C and 200 atm., producing about 30 t/day. Since 1913, the amount of ammonia produce has greatly been increased but the fundamental aspects of the process has remained almost the same.

$$N_2 + 3H_2 \leftrightarrow 2NH_3 \qquad [4]$$

ΔH_{298}=-45.93 Kj mol^{-1}

ΔS_{298}=-99.37J K^{-1} mol^{-1}

$\Delta G°_{298}$<0 for Temperatures<200°C

This reaction is carried out with a diminishing volume, and it is exothermic, from where it can be deduced that, high pressures and low temperatures favour the forward reaction. That is the ammonia formation. This thermodynamically favourable reaction is kinetically so slow at low temperatures, that high temperatures are needed to kinetically increase velocity rates. Since $\Delta G°$ for this reaction becomes negative for temperatures less than 200°C , catalysis is the only other alternative to lower the activation energy. This synthesis, in which the forward reaction is difficult to realize, despite its thermodynamic favourability, presents some advantages.

- The reaction product is easily separated from the reagents, because of the differences in their liquefying points. -33°C for ammonia, and -196°C forH_2 and N_2.
- The direct reaction has a 100% selectivity. This means no secondary products.

A typical commercial catalyst has the following composition:

Fe_2O_3 94.8 % wt.,

K_2O 0.8 % wt.,

CaO 2.0 % wt.,

MgO 0.3 % wt.,

Al_2O_3 2.5 % wt.,

SiO_2 0.4 % wt.,

TiO_2, ZrO_2 and V_2O_5, in traces. This catalyst is either reduced in situ, at about 70 - 100 bars and at temperatures of about 450 - 500°C, or a pre-reduction is done elsewhere. The optimal situation would be, to find on the surface of the support (potash), a good dispersion of iron metal crystallites. This situation is probable only if heating does no go above 540°C.

Many reaction mechanisms have been proposed, to explain the reaction kinetics (even adsorption of molecules). Today the mechanism which seems to be the most probable provides a dissociative chemical adsorption of both hydrogen and nitrogen.

$$H_{2(g)} \rightarrow 2H_{(ads)}$$

$$N_{2(g)} \rightarrow N_{2(ads\gamma)} \rightarrow 2N_{(ads)}$$

$$N_{(ads)} + H_{(ads)} \rightarrow NH_{(ads)}$$

$$NH_{(ads)} + H_{(ads)} \rightarrow NH_{2(ads)}$$

$$NH_{2(ads)} + H_{(ads)} \rightarrow NH_{3(ads)} \rightarrow NH_{3(de-ads)}$$

A good reaction scheme could be represented as follows: (16)

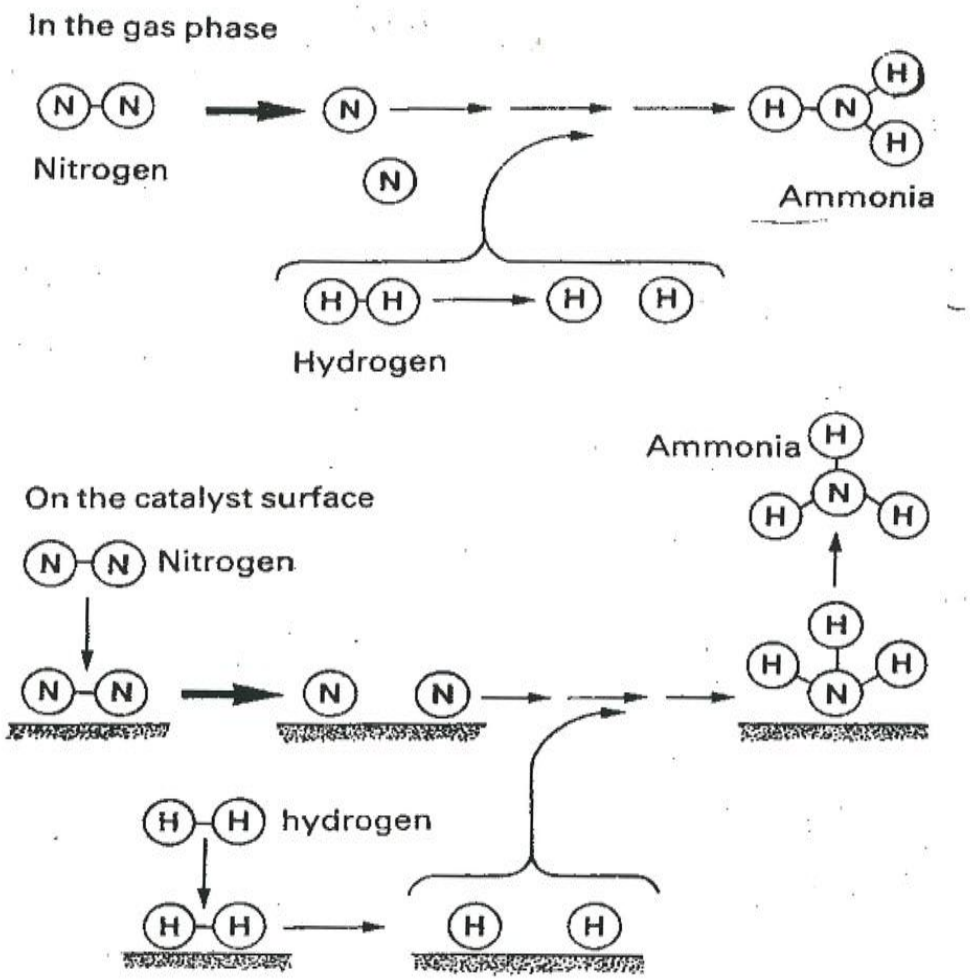
In the gas phase
Nitrogen
Ammonia
Hydrogen
On the catalyst surface
Nitrogen
Ammonia
hydrogen

CHAPTER SIX

6) CHARACTERIZATION METHODS

Various characterization methods were used to try to understand the organization of the texture on the surface. Some of them are: - TPR, TPO, TPD-H_2, Surface Area Measurements, IR, Raman, SEM-EDS, TEM, X-RAYS, Thermal Gravimetric Measurements.

6.1) TPR (Temperature Programmed Reduction)

Temperature-programmed reduction (TPR) is a widely used tool for the characterization of metal oxides, mixed metal oxides, and metal oxides dispersed on a support. The TPR method yields quantitative information of the reducibility of the oxide's surface, as well as the heterogeneity of the reducible surface. TPR is a method in which a reducing gas mixture (typically 3% to 17% hydrogen diluted in argon or nitrogen) flows over the sample. A thermal conductivity detector (TCD) is used to measure changes in the thermal conductivity of the gas stream. The TCD signal is then converted to concentration of active gas using a level calibration. Integrating the area under the concentration vs. time (or temperature) yields total gas consumed. Figure 1 shows a TPR profile for the reaction where M_xO_y is a metal oxide.

$$M_xO_y + yH_2 \leftrightharpoons xM + yH_2O \qquad [1]$$

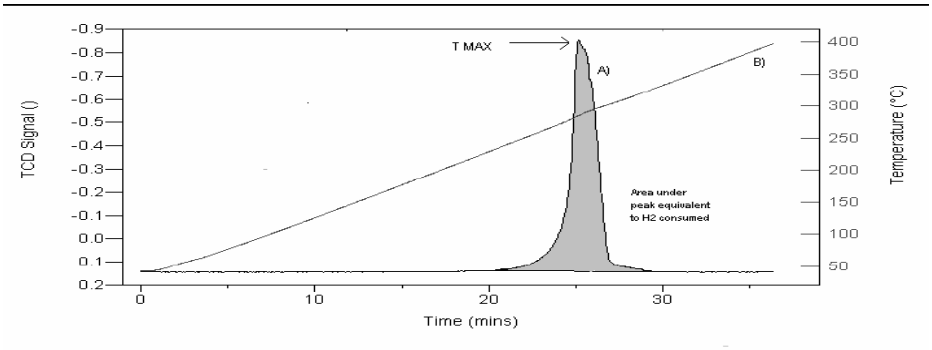

Graph 5. *Temperature-programmed reduction profile for a metal oxide. Trace A displays the TCD signal output as a function of time. Trace B displays the temperature as a function of time during a 10 °C heating rate from ambient to 400 °C.*

This figure illustrates a TPR spectrum where the peak maximum indicates the temperature that corresponds to the maximum rate of reduction. The TPR method provides a qualitative, and sometimes quantitative, picture of the reproducibility of the catalyst surface, as well as its high sensitivity to chemical changes resulting from promoters or metal/support interactions. Therefore, the TPR method is also suitable for quality control of different catalyst charges since deviations in manufacturing methods often result in different reduction profiles. Quantitatively correct areas of the reduction peak could be obtained constructing a calibration curve, using Ag2O as the standard sample, in different quantities.

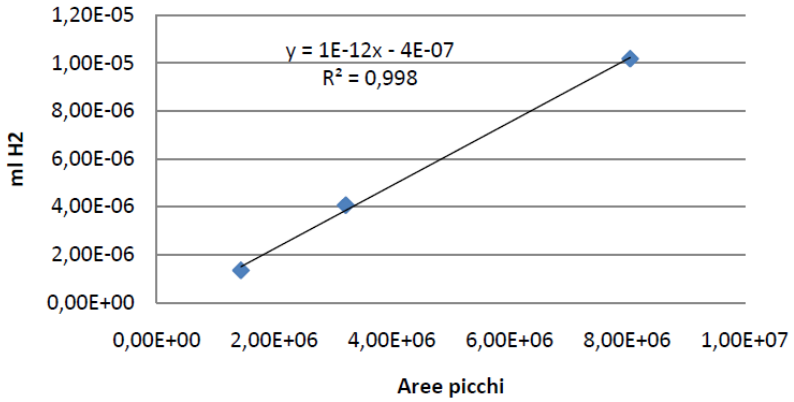

Graph 6*: TPR Calibration Curve*

6.2) TPO (Temperature Programmed Oxidation)

The temperature programmed oxidation analysis is made to give an estimation of the quantity of metals on the surface that can be re oxidised after reduction in the same conditions as used during activation. The same instrument used for the TPR measurements was used in this case too. Practically 10 mg of a sample is put into a U-tube, made of quartz. This tube is then heated to 400°C, while H_2 is flowing through at about 50ml/min. This reduction goes on for about 4 to 6 hours and then cooled to room temperature still under hydrogen flow. Then with a 30ml/min flow of the oxygenating gas (3.23% of O_2 in He), a temperature range from room temperature to800 °C, is scanned. A study of the area of the peak obtained, gives a measure of the amount of metal on the catalyst that can be reduced at the activation temperature. Obviously this interpretation can be done only after having constructed a calibration curve. In this case known quantities of different mixtures of O_2/He is injected into the instrument, and the following plot is obtained.

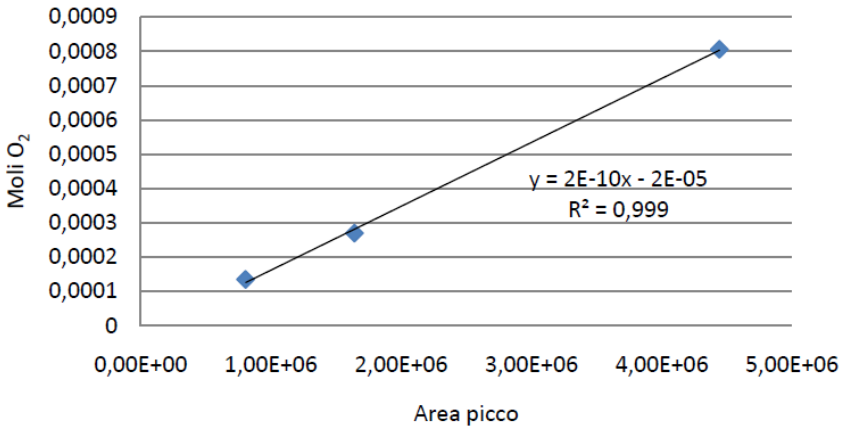

***Graph 7:** TPO Calibration Curve*

6.3) TPD-H_2 (Temperature Programmed Desorption With Hydrogen)

This is a method which goes to measure the amount of H_2 physically and chemically adsorbed on the surface of a catalyst. A 500 mg sample is heated in a U-tube sample carrier at 400°C

for 6 hours while hydrogen is flowing. The temperature is then lowered to 200°C, with a cooling rate of about 10°/min, still under hydrogen flow, and left there for about 30 minutes. Successively an isopropanol/nitrogen slurry mixture is used to cool down the sample to -80°C for 5 minutes. In the meanwhile the instrument is calibrated, injecting known quantities of a 10.22% mixture of H_2 in He. The areas of this pulse signals generated will be used to calculate the amount of hydrogen adsorbed. After the cooling with the slurry, hydrogen is substituted by an inert gas such as nitrogen or argon. The sample is then heated up to 400°C to allow all the adsorbed hydrogen to be released. From this analysis many useful information can be collected. For example

- The number of active sites on the surface of the catalyst.

$$n_{siti} = \frac{2*(molli\ H_2)*N_A}{w} \qquad [2]$$

Where N_A is the Avogadro number, and W is the weight in grams.

- The percentage of dispersion obtained on the surface.

$$\%\ Disp. = \frac{n_{active\ sites}}{n_{total\ sites}} * 100 \qquad [3]$$

Where total sites are meant to be, those obtained from the TPO reduction.

- An approximation of the sizes of the metal particles on the surface of the catalyst, using the Reuel and Bartholomew equation.

$$\theta_{nm} = \frac{96.2}{\%\ Disp.}. \qquad [4]$$

6.4) Surface Area Measurements

The instrument used is a Micrometric Pulse Chemisorb 2705, which uses the B.E.T. theory for single point adsorption. This implies an adsorption of a single layer of nitrogen on the surface.

The detector is a Wheatstone bridge, thermal conductibility detector. It measures the conductibility of the gas mixture at the entrance, and after it passes through the sample. The difference in the composition of the gas creates a difference in conductibility and this is registered. A sample of about 100 mg is weighed and transferred into a sample carrier (plexy glass tube). It is then pre-heated to about 200°C in order to eliminate eventually occurring humidity. The gas mixture made of 30.36% of nitrogenin helium, is made to pass over the sample while it emerged into liquid nitrogen, at a flow rate of about 10ml/min. the adsorbed nitrogen is then measured. Successively, the sample is brought to room temperature, and the amount of nitrogen desorbed is measured. This measure is supposed to be equal to the adsorption measurement.The B.E.T. theory supposes that at the temperature of liquid nitrogen, a monolayer of nitrogen is adsorbed on the surface of the catalyst. Since in the beginning of the analysis, a measure of the area covered by 1 ml of nitrogen is made and the number of molecules present in a monolayer is known, the surface area of the catalyst can be calculated, using the B.E.T. equation.

$$\frac{P}{P_o}\left[V\left(\frac{1-P}{P_o}\right)\right] = \left[\frac{1}{V_m C}\right] + \left[\frac{C-1}{V_m C}\right] * \left(\frac{P}{P_o}\right) \qquad [5]$$

V= The volume at the standard conditions of adsorption

P= Pressure

P_o= Vapour pressure of gas at the adsorption temperature

6.5) Vibrational spectroscopic techniques

There are many ways to obtain information on the physical/chemical properties of materials. Spectroscopic methods are based on certain excitations, electronic and nuclear, to which catalysts respond. For example, a catalyst can be irradiated with X-rays and the diffraction of these rays are studied (X-ray diffraction, XRD), or the energy distribution of electrons emitted from a catalyst as a result of photoelectric emissions can be studied (X-ray photoelectron

spectroscopy, XPS). Spectroscopic characterization can provide important information about the structure of catalysts and their precursors. Catalyst characterization allows identification of the active sites for reaction and reveals possible routes for optimization of catalyst structure. Both catalysis and spectroscopy are disciplines that demand considerable expertise. For instance, the state of a catalyst depends, often critically, on the method used for its preparation, its pre-treatment or its environment. It is therefore essential to investigate a catalyst under carefully selected, relevant conditions and after the proper treatment. Quick and easy experiments in catalyst characterization are difficult to find. Correct spectra interpretation requires experience based on practice and a sound theoretical background in spectroscopy, in physical chemistry and often in the solid state physics as well. It is always a good practice to keep in mind that, although many techniques undoubtedly provide valuable results on catalysts characterization, the most useful information almost always comes from a combination of several characterization techniques.

In conclusion, a successful outcome to any research on catalysts is most likely to be achieved by using a combination of spectroscopic techniques applied under conditions as close as possible to those of the reaction in which the catalyst operates and also by using an integrated approach in which experts from catalysis and spectroscopy work closely together.

In this study, we have used FT-IR and micro-Raman spectroscopic techniques.

6.5.1) FT-IR and micro Raman spectroscopy (4)

Raman and infrared spectroscopy are complementary methods for the study of molecular vibrations. The intensities of IR absorption bands depend on the change of the dipole moment brought about by variations in the molecular geometry for that vibration, while the intensities of Raman bands depend on the change of polarizability associated to the vibration. Infrared spectroscopy can be considered as the first important spectroscopic technique that has found general acceptance in catalysis. The most common application of infrared spectroscopy in catalysis is the identification of adsorbed species and the study of the ways in which these

species are chemisorbed on the surface of the catalysts. In addition, the technique is useful in identifying species that are present in precursor stages of the catalyst during its preparation. Sometimes the infrared spectra of adsorbed probe molecules such as CO and NO give valuable information on the adsorption sites that are present on catalyst.

Infrared radiation falls into three categories: Far Infrared (10 – 200 cm^{-1}), Mid-Infrared (200-4000 cm^{-1}) and Near-Infrared (4000-10000 cm^{-1}). We are interested in the mid-infrared region. A strong point of Raman spectroscopy for research in catalysis is that the technique is highly suitable for in situ studies. The spectra of adsorbed species interfere weakly with signals from the gas phase, enabling studies under reaction conditions to be performed. A second advantage is that typical supports such as silica and alumina are weak Raman scatters, with the consequence that adsorbed species can be measured at frequencies as low as 50 cm^{-1}. This makes Raman spectroscopy a powerful tool to study catalytically active phases on a support. A disadvantage of the technique is the small cross section of Raman scattering; most of the scattering intensity goes into the Rayleigh band. Of course, the use of an intense laser increases all intensities but, as disadvantage, the sample may heat up during measurement and surface species may decompose or de-adsorb. Finally, fluorescence of the sample, giving rise to spectral backgrounds, may seriously limit the detection capacity of weak signals. Twenty years ago only a handful of Raman spectroscopy publications appeared in the catalysis literature and none were in situ studies. Presently, the total number of Raman spectroscopy studies that have appeared in the catalysis literature amount to several hundreds publications, with a large number of in situ studies. Raman and infrared are complementary spectroscopic methods that are among the unique characterization techniques which provide fundamental molecular level information about the surface properties of supported metal oxide catalysts:

- the molecular structure of the surface metal oxide species
- crystallinity
- coordination of metal oxide sites
- the location of the surface metal oxide species

- surface coverage of the metal oxide over layer
- interaction with porous support (e.g. formation of silicate)

Raman spectroscopy is more versatile for catalysts characterization and in comparison with IR spectroscopy it presents at least two important advantages: there is no need of sample preparation and the spectra of water-metal interfaces are obtained easily and quickly. Thanks to the remarkable developments in Raman instrumentation, it is now possible to obtain good quality spectra even from very poor light scattering species using a few hundred micro watts or even less. The coupling of a Raman spectrometer to an optical microscope has further increased the versatility of the method by allowing the selective analysis of components of heterogeneous catalysts on a micrometer scale and by reducing greatly the amount of sample required from precious materials. Accordingly Raman microscopy has become a proven analytical technique in all the areas of scientific research, and especially to the characterization of catalysts.

6.5.1.1) Instruments

Infrared spectra were measured with a FTIR model IFS113V Bruker spectrometer, resolution of 1 cm^{-1} in the spectral region 370-5000 cm^{-1}. KBr pellets of different thickness (1 mm almost) were prepared to have best signal/noise ratio.

Micro-Raman sampling was made by an OLYMPUS microscope MOD. BX40 connected to an ISA Jobin-Yvon model TRIAX320 single monochromator, resolution 1 cm^{-1}. The exciting source was a MellesGriot 25LHP925 He-Ne laser used in single line excitation mode at 632.8 nm. The power focused on the samples was always less than 2 mW. The scattered Raman photons were detected by a liquid-nitrogen cooled CCD, JobinYvon MOD. SPECTRUM ONE.

Samples were not pre-treated but measured as a powder placed on a microscope slide: in this way it is possible to analyse the few microns grain size and not to focus on those regions where the presence of the support (silica or alumina) was predominant. The reproducibility of

the spectra was always controlled by sampling different points of the catalyst. Through the optical microscope analysis it was also verified that no local degradation occurred during laser irradiation.

6.6) Diffraction Methods

6.6.1) X-Ray Diffraction (XRD)

X-ray diffraction is one of the oldest and most frequently applied techniques in catalyst characterization. It is used to identify crystalline phases inside catalysts by means of lattice structural parameters, and to obtain an indication of particle size.

X-ray diffraction occurs in the elastic scattering of X-ray photons by atoms in a periodic lattice. The scattered monochromatic X-rays that are in phase give constructive interference. Figure 4.13 illustrates how the diffraction of X-rays by crystal planes allows to derive lattice spacing using the Bragg relation:

$n\theta = 2\,d\,\sin\theta$; n = 1,2, …..

where θ is the wavelength of the X-rays, d is the distance between two lattice planes, θ is the angle between the incoming X-rays and the normal to the reflecting lattice plane, n is an integer called the order of the reflection.

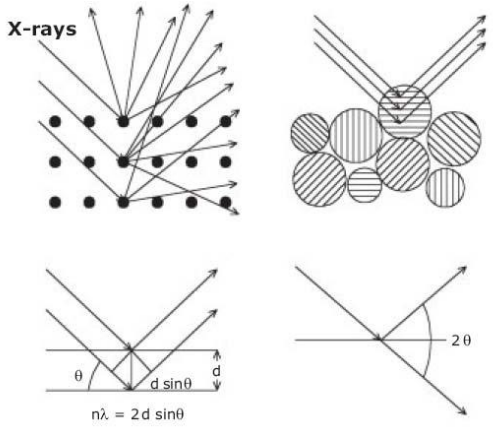

Figure 9: *X-rays scattering by atoms*

X-rays scattered by atoms in an ordered lattice interfere constructively in directions given by Bragg's law. The angles of maximum intensity enable one to calculate the spacing between the lattice planes and allow furthermore for phase identification. Diffractograms are measured as a function of the angle 2θ. When the sample is a polycrystalline powder, the diffraction pattern is formed by a small fraction of the particles only. Rotation of the sample during measurement enhances the number of particles that contribute to diffraction. If the angles, 2θ, under which constructively interfering X-rays leave the crystal are measured, the Bragg relation gives the corresponding lattice spacing, that are characteristic for a particular compound. When using powdered samples, a diffraction image occurs because a small fraction of the powder particles will be oriented in such a way that, a crystal plane is at the angle y to the incident beam for constructive interference.

In catalyst characterization, diffraction patterns are mainly used to identify the crystallographic phases that are present in the catalyst. X-Ray diffraction has an important limitation: Clear diffraction peaks are only observed when the sample possesses sufficient long-range order. The advantage of this limitation is that the width (or rather the shape) of diffraction peaks carries information on the dimensions of the reflecting planes. Diffraction lines from perfect crystals are very narrow. However, for crystallite sizes below 100 nm, line broadening occurs due to incomplete destructive interference in scattering directions where the X-rays are out of phase.

One of the great advantages of using X-rays is their penetrating power, such that XRD can be used to study catalysts under realistic conditions in specially designed in situ reactors. In this way it becomes possible to monitor solid-state reactions such as reduction, oxidation and sulphating, that play a role in the activation of catalysts.

The strength of XRD for catalyst characterization is that it gives clear and unequivocal structure information on particles that are sufficiently large, along with an estimate of their size, and it can reveal this information under reaction conditions. The limitation of XRD is that it can not detect particles that are either too small or amorphous. Hence, one can never be sure that

there are no other phases present than the ones detected with XRD. In particular, the surface, where catalytic activity resides, is almost invisible to standard XRD.

6.6.1.1) Instrument

The X-ray powder diffraction (XRPD) patterns were taken with a computerized Philips PW1710 diffractometer using the CuKα radiation, operating at 40 kV and 20 mA, step scan 1° min-1 and 1 s counting time in the 2-40° 2θ range at room temperature.

6.7) Analytical Electron Microscopy

Electron microscopy is a rather straightforward technique used to determine the size and shape of supported particles. Electrons have characteristic wavelengths of less than 1 amstrong, and come close to monitoring atomic detail.

Figure 4.19 summarizes what happens when a primary electron beam of energy between 100 and 400 keV hits a sample:

- Depending on sample thickness a fraction of the electrons passes through the sample without suffering energy loss. As the attenuation of the beam depends on density and thickness, the transmitted electrons form a two-dimensional projection of the sample.
- Electrons are diffracted by particles if these are favorably oriented towards the beam, enabling crystallographic information.
- Electrons can collide with atoms in the sample and be scattered back; backscattering becomes more effective as the mass of the atom increases. If a region of the sample contains heavier atoms (e.g. Pt) than the surroundings, it can be distinguished due to a higher yield of backscattered electrons.
- Auger electrons and X-rays are formed in the relaxation of core-ionized atoms.

- Electrons excite characteristic transitions in the sample, which can be studied by analyzing the energy loss suffered by the primary electrons.
- Many electrons loose energy in a cascade of consecutive inelastic collisions. Most secondary electrons emitted by the sample undergo their last loss process in the surface region.
- The emission of a range of photons from UV to infrared, called cathode luminescence, is mainly caused by the recombination of electron-hole pairs in the sample.

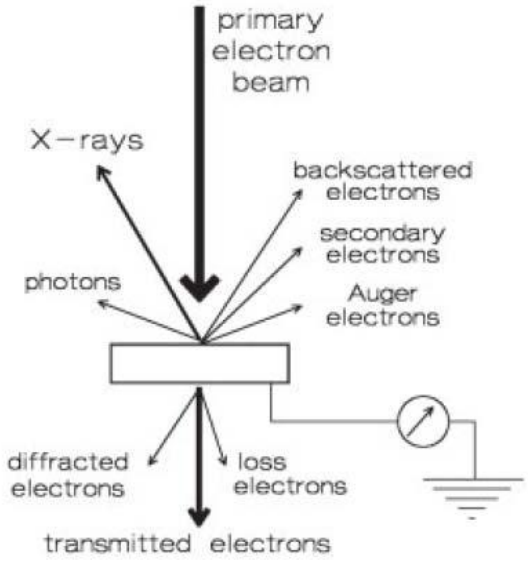

***Fig 10**: The interaction between the primary electron beam and the sample in an electron microscope leads to a number of detectable signals.*

Thus, the interaction of the primary beam with the sample provides a wealth of information on morphology, crystallography and chemical composition. Using transmission electron microscopy to make a projection of the sample density is a routine way to study particle sizes in catalysts. Typical operating conditions of a TEM instrument are 100-200 keVelectrons, 10-6 mbar vacuum, 0.5 nm resolutions and a magnification of 3 x 105 to 106.

Scanning electron microscopy (SEM) involves rastering a narrow electron beam over the surface and detecting the yield of either secondary or backscattered electrons as a function of the position of the primary beam. Contrast is caused by the orientation: Parts of the surface facing the detector appear brighter than parts of the surface with their surface normal, pointing away, from the detector. The secondary electrons have mostly low energies (5–50 eV) and originate from the surface region of the sample. Backscattered electrons come from deeper and carry information on the composition of the sample, because heavy elements scatter electrons more efficiently and appear brighter in images. Dedicated SEM instruments have a resolution of about 5 nm. The main difference between SEM and TEM is that SEM sees the contrast due to the topology and composition of a surface, whereas the electron beam in TEM projects all information on the mass it encounters in a two-dimensional image, which, however, is of a sub-nanometric resolution.

An electron microscope offers additional possibilities to analyze the sample. Diffraction patterns (spots from a single-crystal particle and rings from a collection of randomly oriented particles) enable the identification of crystallographic phases as in XRD. Emitted X-rays are characteristic for an element and allow for a determination of the chemical composition of a selected part of the sample. This technique is referred to as energy-dispersive X-ray analysis (EDX). Transmission electron microscopy is one of the techniques frequently used for the characterization of catalysts. In general, detection of supported particles is possible, provided that there is sufficient contrast between particles and support – a limitation that may impede applications of TEM on well-dispersed supported oxides.

The determination of particle sizes or of distributions therein is now a routine matter, although it rests on the assumption that the size of the imaged particle is truly proportional to the size of the actual particle and that the detection probability is the same for all particles, independent of their dimensions.

The electron microscopy present some limitations:

- In SEM and TEM microscopes the resolution is limited by the size of the electron probes.

- Microscopy is a local technique which does not provide global vision of the sample.
- The accuracy of TEM data depends on the number of images taken.
- Particle size measurements from electron microscopy could be performed accurately only for relatively dilute samples.
- The electron beam is potentially destructive; it could modify the catalyst structure and the size of nano-particles. All measurements in transmission and scanning electron microscopy have to be carried out in UHV, while it has been largely accepted that the presence of reacting molecules could affect the catalyst structure.

6.7.1) Instruments

SEM images were measured using a electron microscopy Philips XL-30 CP with RBS detector of back-scattered electrons and EDS analyser was used to describe the surface and elemental composition of catalysts. While the morphology of the catalysts particles dispersed in the micro-emulsion was studied using a Philips 208 Transmission Electron Microscope (TEM). A small drop of micro-emulsion was deposited on a copper grid pre-coated with a Formvar film and then evaporated in air at room temperature.

CHAPTER SEVEN

7) METHODS USED FOR THE ANALYTICAL EVALUATION OF CATALYSTS

7.1) The Laboratory Plant Scheme For The Fischer-Tropsch Synthesis (18)

This plant was projected and constructed for the realization of a Fischer-Tropsch synthetic process similar to the industrial plant. The following scheme was used for the F-T synthesis:

-

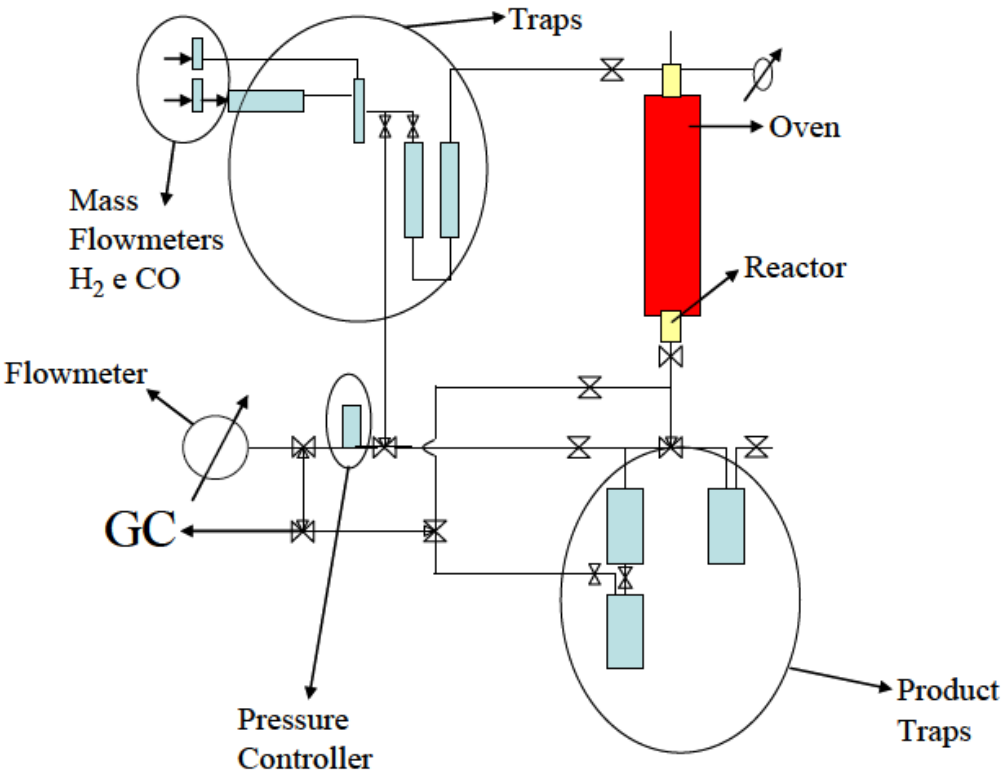

***Fig 11**: Laboratory Plant Scheme*

It is made of two mass flow metres, regulated to measure the flow respectively of CO and H_2. These are followed by molecular traps. One before the mixer, made of activated carbon. This is put directly on the CO line, for the elimination of carbonyl compounds which could be present in the CO gas bottle. A second trap positioned after the mixer filled with molecular sieves, to eliminate any traces of H_2O and CO_2 which could be present, even accidentally in the flow. The third trap is the oxygen trap. Along the line and between connecting parts, some valves are put, giving a possibility of excluding a part, or creating a directional flow. A tubular fixed bed reactor, made in stainless steel, and covered with a heating mantle made of resistances covered by the glass woollen mantle. This reactor leads to two collectors in series, with the first collector cooled with icy water. There's a by passing line which connects the line after the mixer to a point after the collectors. After this junction, there's a pressure controller to maintain pre-determined pressures. Then a bit further, a flow metre which measures the amount of fluid passing through the system. This has a bubble flow metre attached, for control. Before the terminal flow metres, there's a junction which leads to a gas chromatograph, to be able to analyse the exit gases, either from the collectors or from the by-pass.

7.1.1) The Way It Functions

It can all be divided into three principal zones:

The entrance:- This is the zone where the gases enter into the plant through the mass flow metres, and goes through the mixer and the traps for cleaning. These gases, CO and H_2, come from gas bottles and arrive at the flow metres at almost 30 bars. Here they are regulated to maintain a flow rate ratio of CO/H_2 being 1/2 giving a total of 12 l/h. The effective flow rates are controlled using the bubble flow metre. CO enters into the plant and goes through the first trap filled with activated carbon, where carbonyl traces coming from the gas bottles are eliminated. The two gases go through a mixer and then through the second trap, where traces of humidity which can be found in the flow are in turn eliminated. The gas mixture then goes

through the third trap which is the oxygen trap (Oxy-Trap, ALTECH). The gas mixture which comes out of the third trap is clean and can get into contact with the catalyst.

The Reaction zone:- This zone is made of a fixed bed reactor, the collectors and the pressure controller. At the reactor head there is a barometer for pressure control. The reactor is a stainless steel tube with an internal diameter of 10 mm, which is filled with a calculated quantity of catalyst. The catalyst is placed in the isothermal zone along the tube and the rest of the tube is filled with carborundum, which is an inert carbon. A filament which creates electrical resistance, is wrapped around tube for heating. Two thermocouples, one internal and the other external, are fitted for temperature control. It is all covered with a glass woollen mantle. The gasses and liquids together with waxes which are formed during reaction, all pass through the refrigerated collector where water, liquids and waxes are deposited and the gasses pass on to the pressure controller and through the flow metres, from where they are expelled from the plant. The pressure controller is an instrument which has an all or none valve. When it is set to permit the passage at a certain amount of bars, the valve opens when that pressure is reached. There's a connecting tube between the traps and the pressure controller. With the aid of this tube, pure gas coming from the flow metres can be conveyed to the gas chromatograph and be analysed for quantitative analytical reasons.

The control and analytical zone:- This zone is made of a central keyboard control unit, the control flow metre and the bubble flow metre and finally a gas chromatograph. The keyboard control unit is used to change, control and maintain the flow rates in the flow metres, the temperature readings of the thermocouples and the pre-set values of the pressure controller. The gasses which pass through this zone either leaves the plant or can be deviated to the loop of the of the gas chromatograph, from where they can be analysed.

7.1.2) Calculation Methods Used To Evaluate The Tests

The percentage of Conversion:- Since CO has the lower concentration, it is the limiting factor and can be easily used to control the degree of progress of the reaction, in the following way;

$$\frac{Q_{CO\,(IN)}-Q_{CO(OUT)}}{Q_{CO\,(IN)}} * 100 = \%\, Of\ CONV. \qquad [1]$$

The percentage of Selectivity:- The selectivity of a product x, which has n, number of carbon atoms, can be calculated with respect to the total quantity of CO reacted, with the following formula.

$$S_x = \frac{n*Q_x}{Q_{CO(in)}-Q_{CO(out)}} * 100 \qquad [2]$$

Q_x= It is the molar quantity of product x, which has n carbon atoms.

The percentage Yield R_x:- This can be calculated in the following way.

$$R_x = \frac{n*Q_x}{Q_{CO\,(in)}} * 100 \qquad [3]$$

The Carbon Balance:- This quantity can be obtained making a comparison or looking for the difference between all the carbon involved in product formation, including CO which did not react, and the total amount of CO put into the system. Therefore:

$$\%CO = \frac{(\sum nQ_x)+Q_{CO(OUT)}}{Q_{CO(IN)}} * 100 \qquad [4]$$

7.2) The Laboratory Plant Scheme For The Ammonia Synthesis (16)

The following lab plant was constructed for the ammonia synthesis:-

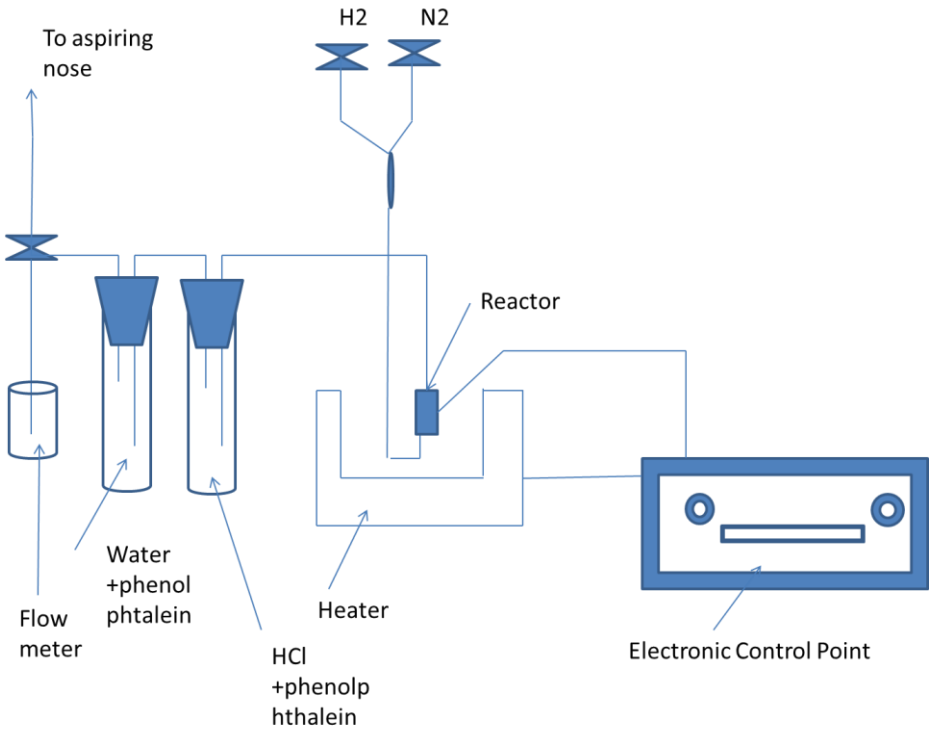

Fig 12: *Lab Plant For Ammonia Synthesis*

Two laboratory lines, the N_2 and the H_2 lines, are used with regulatory valves, as reagents. The flow rates are regulated with pin head valves and are measured with a bubble flow metre placed at the end of the plant. H_2 and N_2 from the line go through a mixer, then together in the stoichiometric ratio for the synthesis, they go across the reactor. Here in the presence of a catalyst and at the correct temperatures, they react and the product passes through two gas collectors. The first one is filled with a 0.1 N solution of HCl and a few drops of phenolphthalein. The second collector contains water and the indicator to demonstrate any possible passage of NH_3. After this, the exit gasses go into an aspiring nose connected to the global aspiring system of the laboratory.

PART TWO

EXPERIMENTALS

CHAPTER EIGHT

8) Prepared Catalysts

The catalysts listed in the tables below are examples of the various trials made during the course while trying to improve the method of binding the metal coming from the precursor (either Co in the case of the Fischer-Tropsch synthesis or Ru in the case of the ammonia synthesis), onto the surface of the support, which could be either alumina gel or silica gel. Some of them were repeated for reproducibility tests and some others came from other research groups with which we were collaborating. There are also some bimetallic ones too, together with those which have been drugged with Ru and Cs for catalyst promotion.

NAME	% IN WEIGHT	PREPATION METHOD
CAT 1 Co ON SILICA GEL	15	IMPREGNATION TO INCIPIENT WETNESS
CAT 2 Co ON SILICA GEL	10	ANCHORAGE IN BULK
CAT 3 Co ON ALUMINA GEL	15	BULK SOL-GEL
CAT 4 Co/Ru ON ALUMINA GEL	15/0.1	BULK SOL-GEL

CAT 5 Fe/Co ON SILICA GEL	5/5	BULK SOL-GEL
CAT 6 Fe/Co ON SILICA GEL	5.5 IN TOTAL	IMPREGNATION IN BULK
CAT 7 Co ON ALUMINA GEL	15	BULK SOL-GEL
CAT 8 Co ON SLILCA GEL	10	ANCHORAGE IN BULK
CAT 9 Co ON SILICA GEL	10	ANCHORAGE IN BULK
CAT 10 Co/Ru ON ALUMINA GEL	15/0.5	BULK SOL-GEL
CAT 11 Fe/Co ON ALUMINA GEL	15 IN TOTAL	BULK SOL-GEL
CAT 12 Fe/Co/Ru ON ALUMINA GEL	15 TOT. /0.5	BULK SOL-GEL
CAT 13 Co ON SILICA GEL	20	ULTRA SOUND
CAT 14 Co ON ALUMINA	15	ULTRA SOUND
CAT 15 Fe/Co ON ALUMINA	3.25/9.75	BULK SOL-GEL FROM CLUSTERS
CAT 16 Co ON ALUMINA GEL	20	IMPREGNATION TO INCIPIENT WETNESS
CAT 17 Co/Ru ON ALUMINA GEL	20/0.1	IMPREGNATION TO INCIPIENT WETNESS
CAT 18 Co ON ALUMINA GEL	20	BULK SOL-GEL

CAT 19 Co/Ru ON ALUMINA GEL	20/0.1	BULK SOL-GEL
CAT 20 Co ON SILICA GEL	15	ANCHORAGE TO INCIPIENT WETNESS
CAT 21 Co AND SILICA ON ALUMINA GEL	15	ANCHORAGE TO INCIPIENT WETNESS

Table 2: *Catalysts Prepared For Fischer-Tropsch Synthesis Tests*

NAME	PROCESS	% RATIO OF METAL	% RATIO OF SUPPORT	PREPARATION METHOD
CAT N1 Ru/Cs	AMMONIA SYNTHESIS	5/5	MgO/Al_2O_3 1/1	BULK SOL-GEL
CAT N2 Ru/Cs	AMMONIA SYNTHESIS	5/5	MgO/Al_2O_3 1/1	SOL-GEL AND IMPREGNATION
CAT N3 Ru/Cs	AMMONIA SYNTHESIS	5/5	MgO/Al_2O_3 1/1	SOL-GEL AND IMPREGNATION
CAT N4 Ru/Cs	AMMONIA SYNTHESIS	5/5	MgO/Al_2O_3 1/1	IMPREGNATION AND BULK SOL-GEL
CAT N5 Ru/Cs	AMMONIA SYNTHESIS	5/5	MgO/Al_2O_3 1/1	IMPREGNATION ON A MIXED SUPPORT

CAT N6 Ru/Cs	AMMONIA SYNTHESIS	5/5	MgO/Al_2O_3 1/1	IMPREGNATION
CAT N7 Ru/Cs	AMMONIA SYNTHESIS	5/5	MgO/Al_2O_3 2/1	IMPREGNATION
CAT N8 Ru/Cs	AMMONIA SYNTHESIS	5/5	MgO/Al_2O_3 3/1	IMPREGNATION

Table 3: *Catalysts Prepared For The Synthesis Of Ammonia*

8.1) CATALYSTS PREPARED FOR THE FISCHER-TROPSCH SYNTHESIS

8.1.1) CATALYSTS PREPARED BY IMPREGNATION "TO INCIPIENT WETNESS"

8.1.1.1) CAT 1

8.1.1.1.a) Preparation Procedure

The silica gel used in this preparation, was prepared diluting 58.89 g of TEOS in ethanol. Separately a solution of 1 g of NH_4F in 100ml of water is prepared and will be used as a catalyst for gelation. 10 ml of this solution is then added to the TEOS solution while agitating. Gelation occurs within an hour and the gel is left for ageing. It is then dried in an oven at 100 °C for one night. This gel is then smashed and sieved to obtain grains of about 45-125 mesh. With a gram of silica gel in a beaker, distilled water is added drop by drop, until the gel is wet without wetting the container. This is known as the "mud" point, which was exactly 0.89 g of H_2O/g of silica gel. With this reference in mind the amount of precursor solution to impregnate to incipient wetness the given amount of silica gel can be calculated.

Then, 11.13 g (0.0509 moles) of $Co(NO_3)_2*6H_2O$ are weighed and dissolved into 15 ml of water, which is the calculated quantity needed to get to the mud point. The needed amount of silica gel is weighed and distributed evenly at the bottom of a crystallizer. Then drop by drop the solution is poured into the crystallizer with mixing. This impregnated gel is then dried in an oven at 100 °C for one night and it is successively calcined in a muffle stove at 400 °C for 5 or 6 hours.

8.1.1.2) CAT 16

8.1.1.2.a) Preparation Procedure

On trying to make a reference catalyst on alumina, the choice of a method to use fell on impregnation. The reason being its large industrial usage. The metal precursor was cobalt nitrate ($Co(NO_3)_2.6H_2O$), and the support is alumina obtained from the (SNAMPROJECT). Calculations were made to produce a catalyst with a cobalt concentration of 20 %. To prepare 10 g of catalyst, 9.8649 g of $Co(NO_3)_2.6H_2O$ (i.e. 0.0339 moles) are dissolved in the minimum quantity of ethanol, about 15 ml, and the solution obtained is mixed drop wise to 8 g of Al_2O_3, which is heated to about 80 °C to accelerate the evaporation of the solvent. The wetted alumina is left to dry up in the air for a few days, and then it is dried in an oven for one night at 120 °C and then heated in a muffle stove at 400 °C for one night.

8.1.1.3) CAT 17

8.1.1.3.a) Preparation Procedure

Another Co based catalyst, supported on alumina is CAT 17. In this case instead there is a promoter, Ru. The precursors used are hexa hydrated cobalt nitrate and $Ru_3(CO)_{12}$ while the support used is a commercial alumina (SNAM PROJECT). The quantities used have been

calculated to give a catalyst with a 20 % in weight of Co and a 0.1 % in weight of Ru. Therefore 0.2110 g (0.0003 moles) of $Ru_3(CO)_{12}$ are weighed and dissolved into 15 ml of THF which is then heated in a reflux at 65 °C. When dissolution is completed, a solution made of 9.8649 g (0.0339 moles) of $Co(NO_3)_2*6H_2O$ in 15 ml of ethanol is added to the hot solution. Then 7.9 g of alumina is also added. The flask is left under agitation in reflux for one hour, then the solvents are taken off in a rotavapour, and afterwards in a vacuum pump. This is then dried in an oven at 120 °C for one night and then in a muffle stove for one night at 400 °C.

8.1.2) CATALYSTS PREPARED BY BULK IMPREGNATION

8.1.2.1) CAT 9

8.1.2.1.a) Preparation Procedure

In a 100 ml beaker, a solution made of 3.99 g of citric acid (C6H8O7.H2O), 20 ml of distilled water (H2O) and 37.5 ml of a 28 % ammonium solution (NH3), is prepared under agitation and cooled in an ice bath. Successively, 6.973 g of cobalt acetate (Co(CH3COO)2.4H2O)are added into the solution. Then, in a round bottom flask 15 g of SiO2 (Aldrich) are weighed. The acetate solution is then poured into the flask and then dried in a rotavapour, and afterwards in an oven at 100 °C for one night, after which it is being calcined in a muffle stove at 400 °C for one day.

8.1.2.2) CAT 5

8.1.2.2.a) Preparation Procedure

7.0202 g (0.0174 moles) of hydrated iron nitrate, Fe(NO3)3.9H2O, are weighed together with 5.0776 g (0.0175 moles) of hydrated cobalt nitrate, Co(NO3)2.6H2O, and were both dissolved

in 18 ml of ethanol. Preliminary tests were made to know how much ethanol was needed to dissolve this quantity of salt. 15 g of silica gel were then weighed and added into the mixture inside the round bottom flask. The quantities in excess of water and ethanol was removed using a “rotavapour”. After drying by evaporation, the catalyst was put into an oven at 110 °C for one night, and was successively calcined in a stove at 400 °C for another night. This catalyst prepared in this manner was intended to make an impregnation of a 1:1 ratio of Fe:Co, and a total metal:support ratio of 10:90.

8.1.2.3) CAT 6

8.1.2.3.a) Preparation Procedure

This catalyst was prepared by researchers of the group headed by Prof. Corrias of the University of Cagliari. They used the same precursors to make an impregnation on an aero-gel of silica. They obtained a final total concentration of metal:support of 5.5:94.5. After calcining at 500°C, a crystalline form named “cobalto ferierite” ($CoFe_2O_4$), was obtained which was very resistant to reduction in hydrogen. In fact reduction occurred at 800°C.

8.1.3) CATALYSTS PREPARED BY ANCHORAGE TO INCIPIENT WETNESS

8.1.3.1) CAT 20

8.1.3.1.a) Preparation Of The Support

146 ml of TMOS is mixed in a beaker with a double of this volume, i.e. 292 ml of methanol. 144 ml of distilled water is then added drop wise, under vigorous magnetic agitation. This amount of water is in an excess of 100 % with respect to the stoichiometric quantity needed for the hydrolysis reaction. Therefore the molar ratio between water and TMOS is 8 to 1. This mixture is then transferred into a crystallizer, where it is left to rest till the gel is formed. (24

h.). The gel is then smashed to obtain a powder with grains between 70-170 mesh, which is successively dried in an oven at 110 °C for one night. Almost 58 gm of gel was recovered.

8.1.3.1.b) Preparation Procedure For The Catalyst

7.59 ml of TMOS is added to a concentrated solution of 15.75 ml of $Co(NO_3)_2*6H_2O$ in 15 ml of ethanol, thus producing a 1 to 1 ratio between Si and Co in the solution. This solution is then used in a drop wise manner to wet the surface of 15 g of silica gel previously prepared, to incipient wetness. Everything is then left for one night in the open for evaporation to be completed, which is also a signal of the completion of grafting. Drying is then followed at 120 °C for 6 h., after which the catalyst is calcined in a muffle stove for 4 h. at 400 °C.

8.1.3.2) CAT 21

8.1.3.2.a) Preparation Of The Support

52.6 g of Tri sec-butoxide of aluminium was weighed in a dry box and dissolved in 300 ml of propan-2-ol. Into this solution the exact excess of 100% of water with respect to aluminium is added drop wise. Gelation occurs almost immediately, and the gel is left to age in a laboratory aspiring chimney. This gel is then dried at 110 °C in an oven.

8.1.3.2.b) Preparation Procedure For The Catalyst

In another study which is not included here for privacy, the ratio of TMOS to ethanol necessary to have the highest surface area and still dissolve the necessary quantity of cobalt nitrate, is 3 to 100. Then 11.173 g of $Co(NO_3)_2*6H_2O$ are dissolved in 18.42 ml of the TMOS/ethanol solution, which is the quantity needed to bring about an incipient wetness. This dissolving is done under vigorous agitation. The solution is then added drop wise onto 7 g of alumina gel

previously prepared. After a period of ageing of about 48 h. the catalyst is dried in an oven at 110 °C for one night and then calcined in a muffle stove at 400 °C for 4 h.

8.1.4) CATALYSTS PREPARED BY BULK ANCHORAGE

8.1.4.1) CAT 2

8.1.4.1.a) Preparation Procedure

Cobalt nitrate is used as the metal precursor, while tetramethylorthosilicate (TMOS) is used as the silica precursor in the gel. The molar ratio needed was 1:1. Calculations were made to prepare 10% in weight of cobalt on silica gel. Therefore to prepare 10 g of the catalyst, 4.9405 g of $Co(NO_3)_2.6H_2O$, (0.01696 moles), were weighed and dissolved in the minimum quantity of ethanol. Then into 15 ml of TMOS, were added 7.96 g of already prepared silica gel, and both solutions were mixed while agitating vigorously. Drop by drop, the gelation catalyst of this reaction, NH_4F (ammonium fluoride) is added until gelation occurs. The gel is left to age and then dried in an oven at 110 °C for one night. At the end it is calcined in a stove at 400 °C for 4 hours.

8.1.4.2) CAT 8

8.1.4.2.a) Preparation Procedure

The silica gel used, was prepared in the laboratory making a mixture of 76 ml of tetra ethyl ortho silicate (TEOS), with 78 ml of ethanol. The catalyst solution was prepared using a 1.3 g/100 ml of water concentration of NH_4F (ammonium fluoride). 48 ml of this solution was used to initiate gelation. The jelly mass obtained is left to dry and age. Successively this mass is

smashed and dried in an oven for four hours at 150 °C. In this way 20 g of silica gel was obtained.

Marostica 1 was prepared using the technique of anchorage, putting carbonyl cobalt on silica gel. This was done in an inert environment, (N_2), because of the instability of this carbonyl in the air. Initially tests are being made to verify the solubility of the metal precursor in ethanol, and it was noticed that 0.1106 g of $Co_2(CO)_8$, dissolve in 3 ml of ethanol. From this, to be able to make 10 g of the catalyst, 8 gm of silica gel and 2.907 g of $Co_2(CO)_8$, together with 3.53 g of TEOS, were weighed. The precursor was dissolved in 80 ml of ethanol, and in this solution was added the afore weighed silica gel and TEOS. Everything is left under agitation for gelation and evaporation of the solvent and at the end ageing, before the effective drying in an oven. Pellet forming is done by creating tablets and then breaking them up into particles of dimension between 0.5 to 2 mm in diameter..

8.1.4.3) CAT 3

8.1.4.3.a) Preparation Procedure

γ-alumina was prepared by precipitation of aluminium nitrate $[AL(NO_3)_3.9H_2O]$ and ammonium hydroxide (NH_4OH) in propan-2-ol at pH 10.8, measured by a pH-meter PHM82. The $Al(OH)_3$ obtained was calcined, to obtain γ-Al_2O_3. So 150 g of aluminium nitrate is dissolved in the least quantity of water and poured slowly into a round bottom flask. At the same time, the exact volume of an aqueous solution of a 30% of NH_4OH, is also poured into the flask to maintain the pH at 10.8. This precipitate is left to rest for one night and the next day it is filtered on a Buchner filter and then washed with propan-2-ol. During washing test are being made to verify the presence of nitrates. After washing, the precipitate is left to dry up in the air, and then put in an oven for 24 hours at 120 °C. A total weight of 30 g of $Al(OH)_3$ was obtained. Before preparing the catalyst, an example using small quantities was tried, to be able to know how much solvent is needed to avoid premature gelation. Then the afore prepared $Al(OH)_3$ is calcined at 500 °C, to measure the loss in weight, which has to be taken care of

during preparation. The various quantities necessary for the production of 10 g of catalyst, with a supported quantity of 15 % of cobalt, were calculated. 6.4 g of $Co(NO_3)_2.6H_2O$ were weighed and dissolved in 400ml propan-2-ol. Then in a dry box, 21 g of aluminium tri-sec butyl oxide is weighed and dissolved in 600 ml of propan-2-ol. 5.6 g of $Al(OH)_3$ are then weighed and dispersed into the aluminium solution, then the cobalt solution is added. Gelation occurs when the stoichiometric quantity of water is added, taking into consideration the water of hydration. It is then left to age for seven days and then put into an oven at 120 °C for 16 hours and calcined at 500 °C for 15 hours. After which the catalyst is characterized and formed into pellets of dimension of almost 2 mm.

8.1.4.4) CAT 4

8.1.4.4.a) Preparation Procedure

In this catalyst, 6.4 g of hydrated cobalt nitrate are weighed and dissolved in 400 ml of propan-2-ol, while 0.02 g of $Ru_3(CO)_{12}$ (ruthenium dodecacarbonyl) are weighed and dissolved in 25 ml of THF at 85 °C. Then in a dry box, 21 g of aluminium tri-sec butyl oxide are weighed and dissolved in 600 ml of propan-2-ol. In this solution 5.6 gm of $Al(OH)_3$ are dispersed while the other two solutions made of Co and Ru are mixed together and maintained at 80 °C. This last solution is put together with the aluminium solution and 2 ml of H_2O, which is the stoichiometric quantity of water needed for gelation, after taking into consideration that cobalt nitrate is hexa-hydrated. Ageing is done for seven days and then the catalyst is put into an oven where it is dried at 120 °C for 18 hours and then put into a stove for calcining at 500 °C for 15 hours.

8.1.5) CATALYSTS PREPARED BY BULK SOL-GEL METHOD

8.1.5.1) CAT 18

8.1.5.1.a) Preparation Procedure

This preparation was made to create a 20 % of Co on alumina. So, in a dry box, 38.6 g (0.1569 moles) of aluminium tri-sec butyl oxide (ASB) were weighed and dissolved in 60 ml of propan-2-ol, while 9.8649 g (0.0339 moles) of cobalt nitrate were also weighed and dissolved in 70 ml of propan-2-ol. The two solutions are then mixed together under agitation, then 4.8 ml (0.2673 moles) of water is added to the agitating mixture, and gelation occurs immediately. The quantity of water added has to be stoichiometrically double i.e. an excess of a hundred percent, with respect to the number of moles of ASB. This is considered taking into account the number of moles of the water of crystallization. The entire contents of the flask is then transferred into a crystallizing dish, where it is covered with a perforated paraffin film and left there to age. After all the solvents are evaporated, it is put into an oven at 120 °C for 4 days, and the in the stove at 400 °C for one night. After cooling it is formed into pellets of dimension, 0.5 to 2 mm mesh.

8.1.5.2) CAT 19

8.1.5.2.a) Preparation Procedure

This is another catalyst prepared using the bulk sol-gel method to obtain a catalyst supported on alumina, which is Co based and promoted by Ru in the ratio Co/Ru, of 20/0.1 %. 38.13 g (0.1550 moles) of tri sec-butoxide of alumina are weighed in a dry box and dissolved in 60 ml of propan-2-ol at 65 °C. In the same way, 0.2210 g (0.00030 moles) of dodecacarbonyl of ruthenium are weighed and dissolved in 15 ml of THF at 65 °C under reflux. The both solutions are mixed together, and finally a third solution is prepared weighing 9.8649 g (0.0339 moles)

of $Co(NO_3)_2*6H_2O$ and dissolving it in 70 ml of propan-2-ol. After the addition of this solution to the first mixture, a solution made of 4.7 ml (0.4646moles) of H_2O in 25 ml of propan-2-ol is then added and left for gelation. The formed gel is then dried in an oven at 120 °C for 4 days, then calcined in a muffle stove for 4 hours at 400 °C.

8.1.5.3) CAT 7

8.1.5.3.a) Preparation Procedure

42.7 ml of aluminium tri-sec butyl oxide is weighed in a dry box and transferred into a round bottom flask. This precursor is dissolved in 348.7 ml of ethanol while N_2 was flowing through the flask. This solution is heated to 80 °C, while vigorously agitating. A white suspension is obtained. A mixture of 232.5ml of ethanol, 0.3 ml of HNO_3 and 1.5 ml of H_2O is added to the precursor solution and heating at 80°C is continued for two hours. At this point the solution becomes colourless. It is then cooled and left to rest for the night. Successively, a solution containing 7.398 g of Hexa-hydrated cobalt nitrate $[Co(NO_3)_2*6H_2O]$ in 29.6 ml of ethanol and 10 ml of water is then added under agitation. The entire content of the flask is transferred into a crystallizer and left to rest for seven days. It is then dried in an oven for four hours at 120 °C and then calcined in a stove at 500 °C for one night. 9.3454 g of catalyst were obtained, giving a 93% yield.

8.1.5.4) CAT 10

8.1.5.4.a) Preparation Procedure

52.6 g of aluminium tri-sec butyl oxide is weighed in a dry box and dissolved in 300 ml of propan-2-ol. 0.108 g of $Ru_3(CO)_{12}$ (ruthenium dodeca-carbonyl) is also weighed and dissolved in a warm THF (60°C) and finally 7.38 g of hexa-hydrated cobalt nitrate $[Co(NO_3)_2*6H_2O]$ is weighed and dissolved in 60 ml of propan-2-ol. This solution is heated to the temperature of

the THF solution. At 60° C, the ruthenium carbonyl solution is added to the aluminium solution under rigorous agitation. At the end, a drop by drop addition of the cobalt nitrate solution is carried out. At the beginning a light precipitate is noticed, but it disappears with agitation. This is jellification caused by the water of hydration on the cobalt nitrate molecule. 3.5 ml of water in 20 ml of propan-2-ol is then added into the container, while the whole of its content is transferred into a crystallizer. Here the catalyst is left to rest while it jellifies. When all the solvent is evaporated, it is put in an oven at 120°C for one night. After cooling it is calcined in a stove at first at 250°C for 2 hours and then at 500°C for one night. The stove is then put off, and the so prepared catalyst is allowed to cool down in the stove.

8.1.5.5) CAT 11

8.1.5.5.a) Preparation Procedure

51 g of aluminium tri-sec butyl oxide is weighed and dissolved in 300 ml of propan-2-ol, in a dry box. While 5.6084 g of $Co(NO_3)_2$*6H2O and 2.7341 g of $Fe(NO_3)_3$*$9H_2O$ are being dissolved in 80 ml of propan-2-ol. The cobalt/iron solution is then added drop wise into the aluminium solution under vigorous agitation. The contents of the container is then transferred to a crystallizer where it is left to rest and to become gel. At the end of solvent evaporation the catalyst is put into an oven, at 110°C for one night. After this drying, it is put into a stove at the temperature of 250°C for 2 hours, and then carried up to 500°C for one night. At the end it is cooled down in the stove.

8.1.5.6) CAT 12

8.1.5.6.a) Preparation Procedure

50 g of aluminium tri-sec butyl oxide were weighed and dissolved in 300 ml of propan-2-ol, in a dry box. Then still in the dry box, 0.106 g of $Ru_3(CO)_{12}$ were weighed and dissolved in 8 ml

of anhydrous THF (tetrahydrofuran). Aside 2.7335 g of $Fe(NO_3)_3*9H_2O$were weighed and dissolved in 50 ml of propan-2-ol. 5.6088 g of $Co(NO_3)_2*6H_2O$ were also weighed and dissolved in 50 ml of propan-2-ol. All four solutions were heated in a warm water bath to 80 °C, then the solution containing THF is added to the aluminium solution. The Fe and Co solutions are mixed together at first and then under vigorous agitation poured slowly into the aluminium solution. All the contents of the round bottom flask is poured into a crystallizer and left to rest and start jellification. When all the solvents are evaporated, the crystallizer is put into an oven at 110 °C for one night. Afterwards a two-step calcination is done in a stove. At first, at 200 °C for one night then at 400 °C for seven hours.

8.1.5.7) CAT 15

8.1.5.7.a) Preparation Procedure

This is a catalyst prepared by Dot. Vidick D. of the University of Louvain la neuve, in Belgium. It is prepared using the bulk sol-gel technique, and the metal precursor is a cluster ($HFeCo_3(CO)_{12}$) prepared by herself in a previous research program. The relationship between Fe and Co in the cluster is 3.25 to 9.75. After the preparation the catalyst was not calcined to avoid cluster destruction. The catalyst is then activated in micro reactors in batches of 2.5 g at a time at 400 °C for 6 h. This is done to avoid weight loss and shrinkage in a fixed bed reactor during activation. This activated catalyst is then formed into pellets and the fixed bed reactor is charged.

8.1.6) CATALYSTS PREPARED BY ULTRA SONIC METHODS

8.1.6.1) CAT 13

8.1.6.1.a) Preparation Procedure

This was the first attempt of Dot. Di Michele A. of the University of Perugia to prepare metal based supported catalyst. The precursors used were cobalt carbonyl and Aldrich commercial silica gel. These compounds were mixed together in hexane and then treated with ultra sound waves. The solid obtained was filtered, washed and dried and then calcined at a low temperature (300 °C). The obtained catalyst is a 20 % in weight of Co on SiO_2.

8.1.6.2) CAT 14

8.1.6.2.a) Preparation Procedure

PG4 is a catalyst prepared by Dot. Di Michele A. of the University of Perugia using the ultra sound technique. It is a Co based catalyst supported on commercial alumina and promoted by Ru. The Co and Ru components are in the relationship 15 to 0.5 % in weight, and they come from the carbonyl compounds. The precursors are dissolved in n- decane, then the commercial alumina is added to the mixture and then treated with ultra sound waves for 4 h. The solid is then filtered and washed with dry hexane. The catalyst is then dried and calcined at 300 °C for 10 h.

8.2) CATALYSTS PREPARED FOR THE AMMONIA SYNTHESIS

8.2.1) PREPARATION METHOD FOR CAT N1 (16)

0.571 g of $Ru_3(CO)_{12}$ was dissolved in 460 ml of dry THF, and agitated cold for 30 hours in a 500 ml round bottom flask. In another 100 ml flask, a cold solution of 3.5 g $Mg(OC_2H_5)_2$ in 50 ml of methanol. In a third flask, 0.47 g of $Cs_2(C_2O_4)$ is dissolved in a methanol/water mixture of composition 45 ml/5 ml. This mixture is heated lightly, working under a nitrogen flow, to enhance the solubility of the oxalate salt. The ruthenium solution and the caesium solution are mixed together cold and agitated until a homogenous solution is obtained. Afterwards in a dry box 17 g of $Al(sec\text{-}OBu)_3$ are dissolved in 50 ml of propan-2-ol, then into this solution, the Ru/Cs mixture and Mg solutions are simultaneously added. It is all left under agitation for one hour, after which the mixture is transferred into a crystallizer to ease evaporation, and left for gel formation and ageing for three days. The formed gel is then dried in an oven for 24 h. and then calcined in a muffle stove for 4 h. at 400 °C in a nitrogen environment.

8.2.2) PREPARATION METHOD FOR CAT N2 (16)

The carbonyl ruthenium solution in THF and the caesium oxalate solution in the water/methanol mixture are prepared in the same manner as in the catalyst R_{11}. Then in a dry box, 17 g of $Al(sec\text{-}OBu)_3$ are dissolved in 50 ml of propan-2-ol,andit is left under agitation till a white solution is obtained. Then 10 ml of water (corresponding to a 150 % excess) are slowly added to the solution to favour gelation. The $Mg(OC_2H_5)_2$ solution is mixed with the gel and agitated for some time before drying with the rotavapour. This alumina gel on which the alkyl oxide of Mg is anchored, is then impregnated with the ruthenium carbonyl solution. After drying with the rotavapour, caesium oxalate is then added and a final drying is done, still with the rotavapour. It is then dried in a vacuum pump and afterwards in an oven at 120 °C for 24 hours and in a muffle stove for 4 hours at 400 °C.

8.2.3) PREPARATION METHOD FOR CAT N3 (16)

A 17 g weight of aluminium tri sec-butyl oxide is dissolved in 50 ml of propan-2-ol, in a dry box and left under agitation until a white solution is obtained. 6 ml of water is then addedto initiate and favour gelation. The solution is then left to age for 4 days. In an advanced stage of gelation, the magnesium alkoxide solution is then added and agitated, with a successive drying in a rotavapour. Before this mixture gets completely dry, 0.52 g of ruthenium carbonyl dissolved in a hot 120 ml of THF is added and then the drying is completed. A solution of 0.21 g of $Ba(NO_3)_2$ dissolved in 20 ml of a solvent made of methanol and water in the ratio 1:1, is prepared. This solution is refluxed in a nitrogen flushed environment. The solution is added to the mixture under agitation and then dried in a rotavapour. Drying is continued in an oven at 120 °C for 24 h. and the calcining in a muffle stove at 400 °C for 4 h.

8.2.4) PREPARATION METHOD FOR CAT N4 (16)

Both the solutions of magnesium ethoxide in methanol and caesium oxalate in a methanol/water mixture are prepared as usual. In a 250 ml flask, 3.7 gm of commercial alumina which has been preventively crushed and sieved to control the grain size, is weighed. The magnesium solution is then added and agitated for 1 hr. The hot ruthenium carbonyl solution is then added, and once this mixture becomes homogeneous, i.e. a homogeneous suspension, the caesium oxalate solution is added and the suspension left under agitation for 4 days, so that gelation occurs with a slow evaporation. The great excess of solvents are taken off, with the help of a rotavapour and a vacuum pump. Then the catalyst is dried in an oven at 120 °C for 24 hrs. and successively in a muffle stove for 4 hrs. at 400 °C.

8.2.5) PREPARATION METHOD FOR CAT N5 (16)

8.2.5.a) Preparation Of The Mixed Metal Oxide Support

3.5 g of $Al(sec\text{-}OBu)_3$ is weighed and dissolved in 10 ml of propan-2-ol, and left under agitation until the whitish solution is formed. Then 85 ml of magnesium methoxide are added and a suspension is formed which disappears with the vigorous agitation and the whitish solution shows up again. Afterwards 2 ml of water are added to favour the gelation of both Al_2O_3 and MgO, which is the necessary stoichiometric quantity needed. It is all transferred into a crystallizer, where it is left under agitation until gelation occurs. It is all left to dry and age at room temperature.

8.2.5.b) Impregnation Of The Mixed Support

2.02 g of mixed metal gel for support is weighed and put into a 250 ml flask. Then in a second flask, 0.23 g of $Ru_3(CO)_{12}$ are dissolved in 60 ml of THF under reflux, in a nitrogen environment. Still under reflux but in air, 0.19 g of $Cs_2(C_2O_4)$ are dissolved in a 20 ml mixture of H_2O/MeOH, in the ratio 50/50. The ruthenium carbonyl solution is poured into the flask containing the mixed metal gel, and after agitation it is dried using a rotavapour. In the same way the caesium solution is added and dried. After drying in a vacuum pump the built up catalyst is put into an oven at 120 °C for 24 h. and then in a muffle stove at 400 °C for 4 hours in a nitrogen environment.

8.2.6) PREPARATION METHOD FOR CAT N6, CAT N7 AND CAT N8 (18)

These three catalysts were prepared in the same way varying the percentage ratio of MgO and Al_2O_3. CAT N6 has a ratio 1:1, while CAT N7 has a ratio 2:1 and lastly CAT N8 has a ratio 3:1.

They were all impregnated with the same 5 % in weight of Ru with respect to the support and an atomic relationship of 1 to 1between Ru and Cs.

8.2.6.a) Preparation of the ratio 1 to 1 mg in MgO/Al_2O_3 in CAT N6

In a 500 ml flask with three openings, 1.6447 g of magnesium ethoxide is weighed and deposited. Then 8 ml of ethanol are added and the flask heated to about 70 °C, under agitation. 2 ml were further added when it was noticed that it was not dissolving. Successively, 0.1130 g of oxalic acid, previously dissolved in a minimum quantity of water is added and the ethoxide immediately dissolves into a whitish suspension. All is left in reflux for 3 h. and afterwards 7.1045 g of tri sec-butoxide of aluminium are added to the suspension and immediately a colloidal phase is observed. Then to favour gelation, 3 ml of water are added drop wise into the solution and it is all left in a crystallizer for the night. The next day everything is dried up in an oven for 24 hours at 110 °C, then in a muffle stove, at first at 250 °C for one hour, then at 500 °C for 4hours.

The two other supports are prepared as above, changing only the variating quantities to obtain the desired ratio:

8.2.6.b) IMPREGNATION OF THE SUPPORT

In a 500 ml flask, 0.2083 g of ruthenium carbonyl are dissolved in 167.50 ml of THF at room temperature. Then the calcined support is added to the flask. The flask is then mounted on a rotavapour where rotation is maintained for one hour. After which the solvent is sent away with the application of a vacuum into the flask. In another 250 ml flask 0.1614 g of oxalates of caesium are mixed with 83 ml of a 9/1 solution of ethanol/H_2O. the contents of this flask is transferred to the 500 ml flask, and then rotation for one hour followed by evacuation of the solvents. The catalyst is then dried in a vacuum pump.

The impregnation procedure is the same for the other two catalyst with the only difference, the support.

CHAPTER NINE

9) SOME CHARACTERIZATION RESULTS

9.1) CHARACTERIZATION OF CAT 1

9.1.1) SURFACE AREA MEASUREMENT

The measured surface area for CAT 1 using the B.E.T. single point method gave 242 m^2/g

9.1.2) TPR ANALYSIS

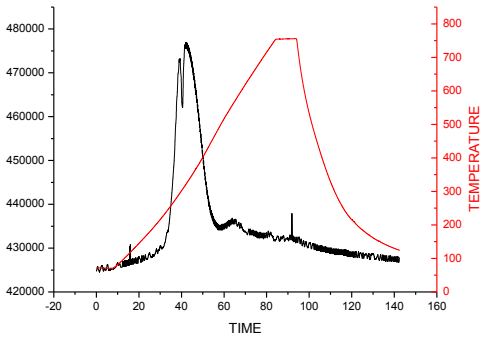

***Graph 8**: TPR Trace For CAT 1*

This catalyst presents all reduction peaks between 300 and 400 °C. These could be interpreted as the successive reductions from Co_3O_4 to CoO and then to the metallic state. The low temperatures could be explained as the ease of reduction.

9.1.3) TPO ANALYSIS

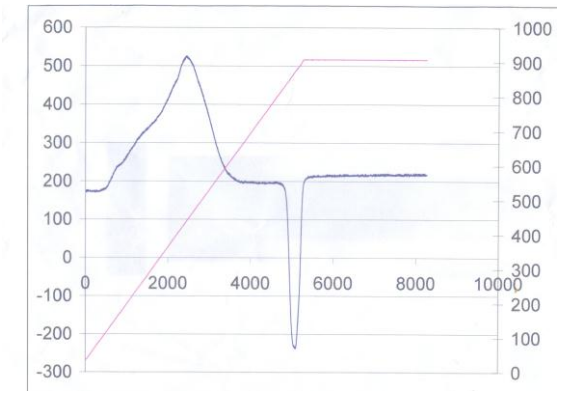

***Graph 9**: TPO Trace For CAT 1*

The TPO trace goes to confirm the TPR results because there's an almost complete re-oxidation at temperatures around 400 °C. The measured reducibility is total.

9.1.4) H_2-TPD ANALYSIS

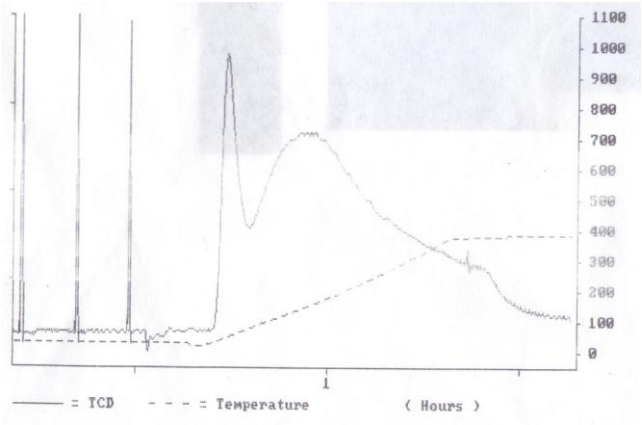

***Graph 10**: H_2-TPD Trace For CAT 1*

Here the hydrogen desorption peaks so evidently occur at temperatures lower than 400 °C.

9.1.5) FT-IR SPECTRSCOPY

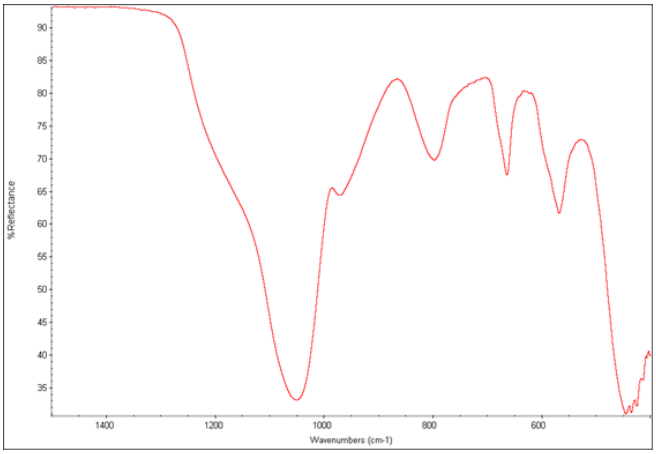

***Graph 11**: FT.IR Spectrum (400-1500 cm^{-1}) For CAT 1*

The band which occurs around 1050 cm^{-1} could be attributed to the stretching of Si-O-Si bonds which normally occur at 1080 cm^{-1}, but has been shifted due to the contemporary presence of Si-O-Co bands, which normally occur at 1025 cm^{-1}. In fact a very pronounced shoulder is noticed. The band between 780-800 cm^{-1} can also be referred to as a Si-O-Si stretching band. While the bands at 650 and 580 cm^{-1} could be attributed to the presence of cobalt oxides. (Co_3O_4).

9.1.6) RAMAN SPECTROSCOPY

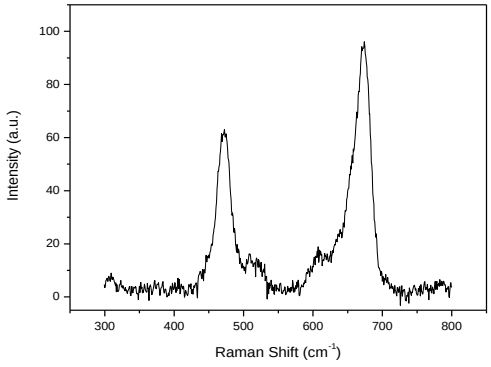

***Graph 12**: RAMAN Spectrum For CAT 1*

The bands at 486 cm^{-1} and 679 cm^{-1} with their respective shoulders at 524 and 612 cvm^{-1}, most probably show the presence of Co_3O_4.

9.1.7) TEM IMAGES

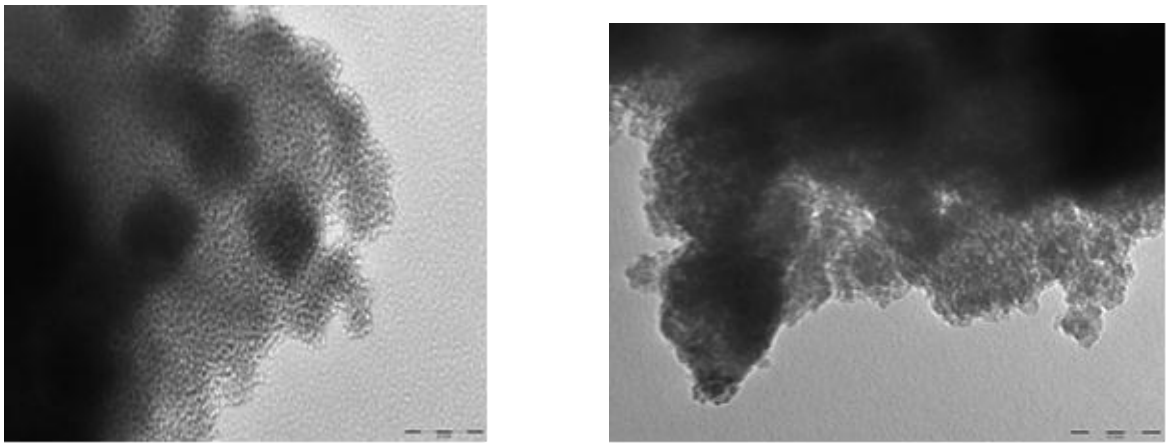

***Image 1**: TEM Images For CAT 1*

The images which have been magnified to 200000x, show zones of highly dispersed metal on the support, although the dispersion is not very homogeneous.

9.1.8) SEM IMAGE

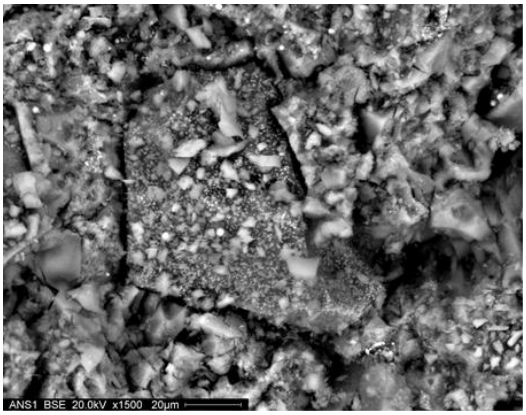

***Image 2**: SEM image For CAT 1*

The SEM image confirms the high and inhomogeneous dispersion of the catalyst.

9.2) CHARACTERIZATION OF CAT 9

9.2-1) TGA (Thermal Gravimetric Analysis)

In the results of a TGA analysis for CAT 9. it is noticed that after the first section where the weight loss can be attributed to drying, weight loss due to real decomposition begins at almost 250 °C and finishes at almost 500 °C.

9.2.2) TPR ANALYSIS

Looking at the graph of the TPR analysis for CAT 9, the first thing that calls for attention is the almost absence of a reduction peak at 300 °C, or at least at some other low temperature. There's just a great reduction peak at 750 °C, which can be attributed to the formation of strong interactions between support and catalyst precursor. This interactions create bonds that render the precursor very difficult to reduce. The reduction percentage is just 14 %.

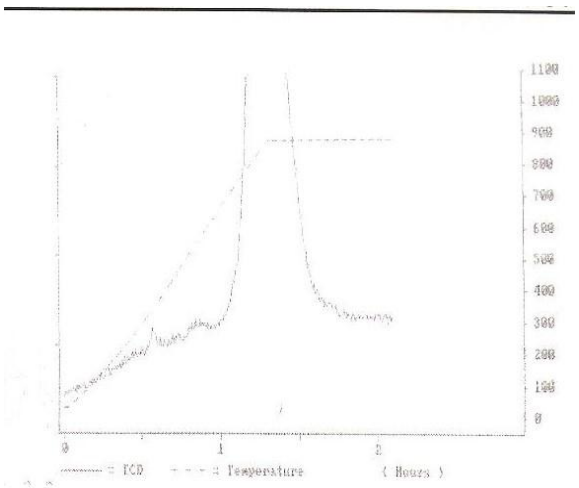

***Graph 13**: TPR For CAT 9*

9.2.3) TPO ANALYSIS

The TPO analysis for LIZ01, shows a very low re-oxidizing capacity. The degree of reduction is just about 19 %. This is most probably due to the difficulty in reducing at low temperatures.

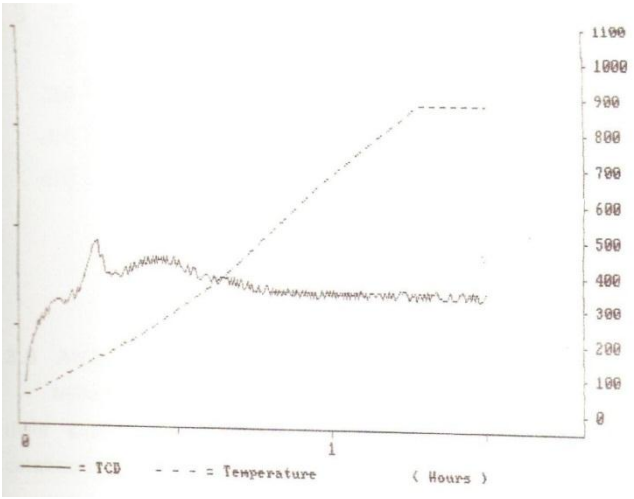

Graph 14: *TPO for CAT 9*

9.2.4) H_2-TPD ANALYSIS

From the desorption peaks of this analysis for CAT 9, it can be noticed that very little quantities of hydrogen are being desorbed, and from calculations the following results are obtained:

- Number of sites per gram of catalyst; 2.14 x 10^{18}.
- The percentage of dispersion; 1.44 %.
- Particle diameter (nm); 66.58.

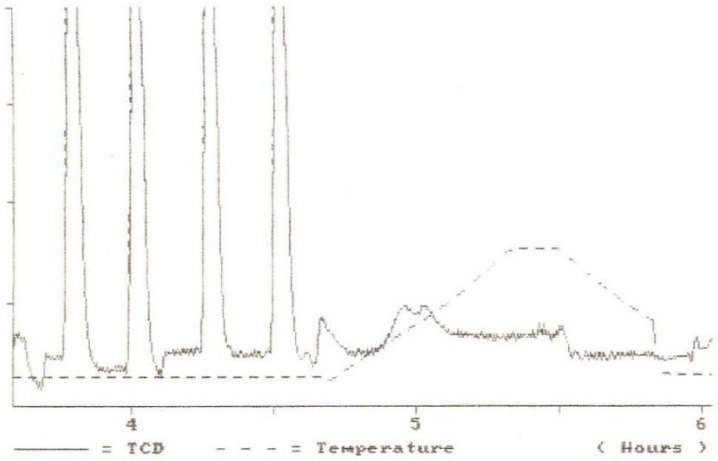

***Graph 15**: H_2-TPD Trace For CAT 9*

9.2.5) FT-IR SPETROSCOPY

The FT-IR spectrum for CAT 9 shows in a very relevant manner the presence of vibrational bands at 790 cm^{-1} and 1080 cm^{-1}, which are normally attributed to Si-O-Si stretchings. There are no evident bands that can be attributed either to oxides or to silicates of cobalt.

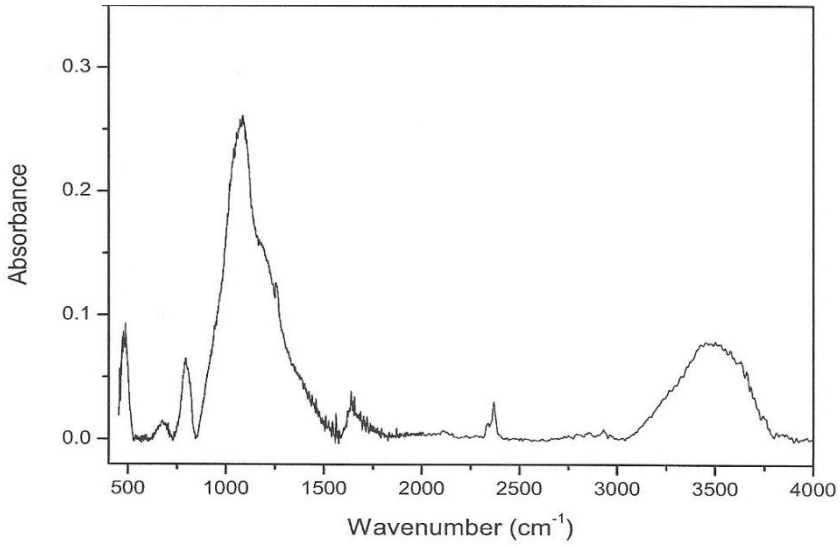

***Graph 16**: FT-IR Spectrum For CAT 9*

9.2.6) TEM IMAGES

From these images it is difficult to distinguish between the support and the metal particles. Only metallic islands can be seen.

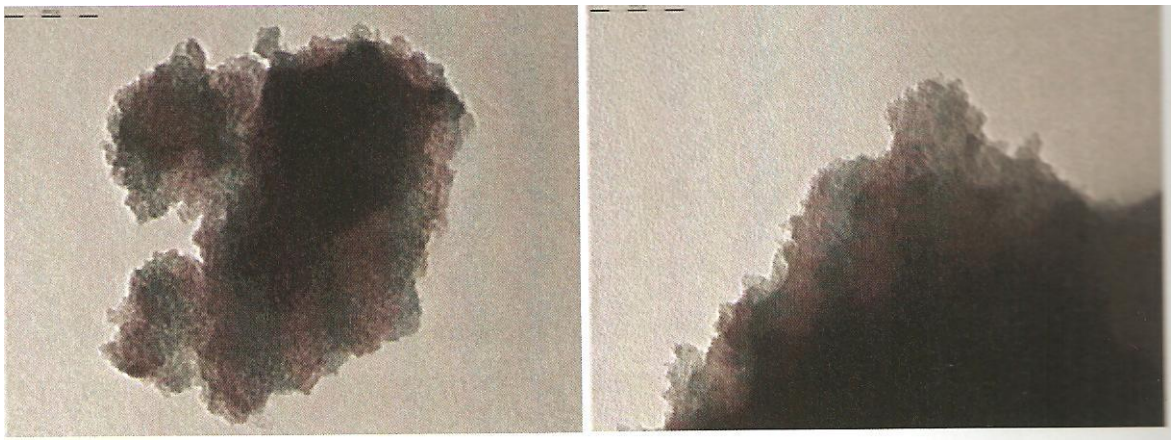

A) B)

***Image 3**: A) TEM Image For CAT 9 B) Enlarged TEM Image*

9.2.7) SEM And EDS ANALYSIS

From the SEM images the very poor dispersion is evident. The micro-analysis EDS gives 12.6 % of Co on a point.

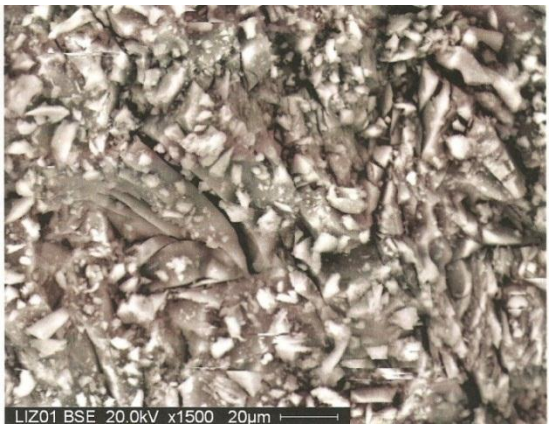

***Image 4:** Enlarged SEM Image For CAT 9*

9.2.8) XRD ANALYSIS

The x-ray diffraction graph for CAT 9 gives evidence of an amorphous powder.

9.3) CHARACTERIZATION OF CAT 8

9.3.1) TGA (Thermal Gravimetric Analysis)

The greater part of the weight loss is noticed at temperatures between 30 and 100 °C. This loss can be attributed to solvent evaporation and carbonyl decomposition. The second weight loss peak near 300 °C, is much more difficult to interpret because of the ignorance in the decomposition products of carbonyl cobalt. A possible hypothesis could be made on the release of CO coming from the strong interactions between silica gel and cobalt carbonyl, that is the silicates. This hypothesis is noticed in the TPR analysis too.

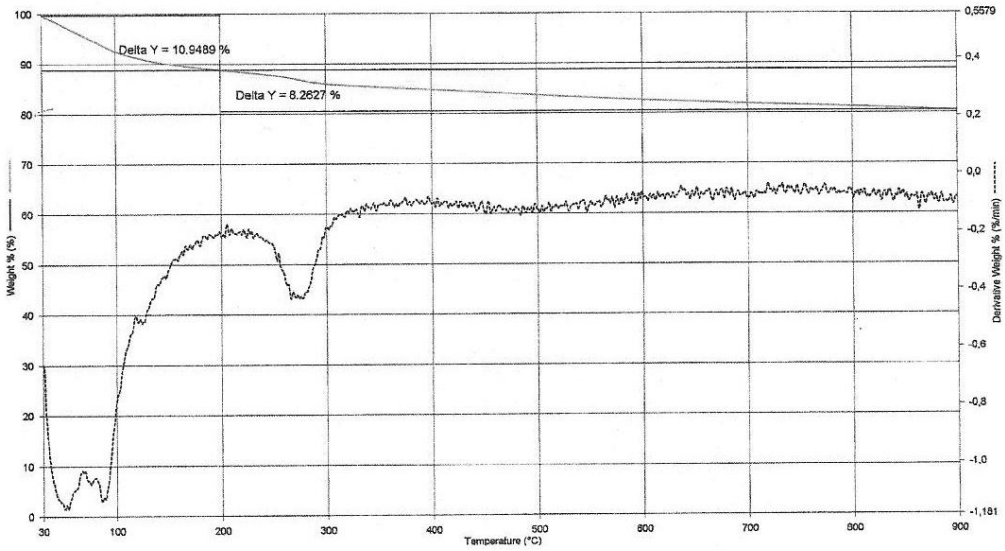

***Graph 17**: TGA Trace For CAT 8*

9.3.2) SURFACE AREA MEASUREMENT

The surface area was measured, both on the supporting silica gel and the already supported catalyst. This gave 137 m^2/g for the support and 125 m^2/g on the supported catalyst.

9.3.3) TPR ANANLYSIS

The results of the TPR analysis can be divided up into two zones, the first zone goes from 200 °C up to 400 °C, and presents a very pronounced peak followed by a shoulder. This peak most probably is due to consumed hydrogen, which goes to react with CO in a sort of methane formation reaction. The last peak around 750 °C, most probably belongs to the reduction of cobalt silicates.

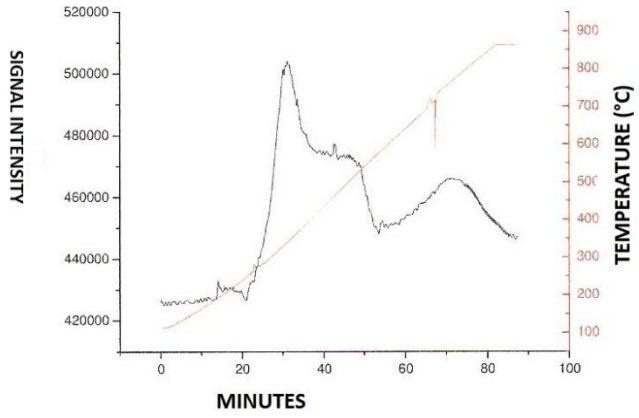

***Graph 18**: TPR Trace For CAT 8*

9.3.4) TPO ANALYSIS

The two peaks in the graph represent the reduced metal on the surface thatis being oxidized. The first is at 150 °C and the second is at 210 °C. They both give a reducing ability of about 75 %.

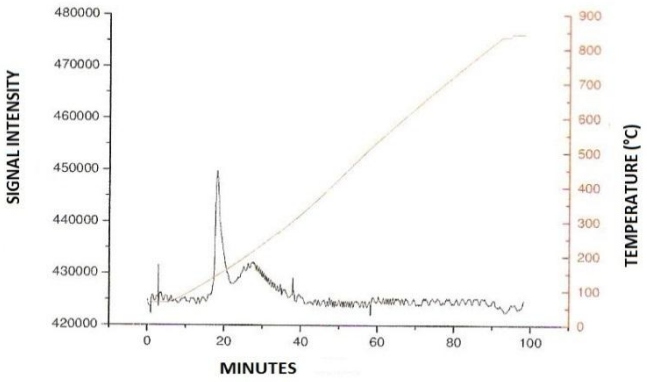

***Graph 19**: TPO Trace For CAT 8*

9.3.5) H_2-TPD ANALYSIS

From the graph, two desorption peaks can be detected. One at almost 100 °C and the other at around 200 °C. From calculations, a 0.9 % dispersion is obtained. This very low dispersion can be attributed to metallic aggregations. Consequently, a low number of active sites will result.

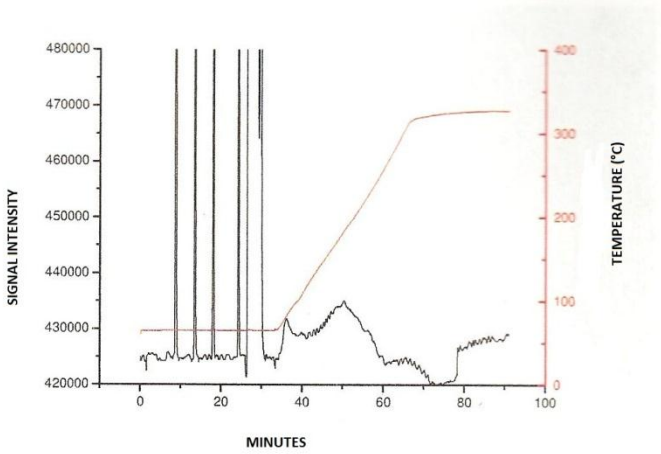

***Graph 20**: H_2-TPD Trace For CAT 8*

9.3.6) FT-IR SPECTROSCOPY

The FT-IR spectrum gives a large band at 3447.9 cm^{-1} which can be attributed to the stretching of the Si-OH bond. The other bands like those around 3000 cm^{-1} can be attributed to vibrations of alkyl groups present in the solvent. Another interesting band which is characteristic of the carbonyl compound $[Co_2(CO)_8]$ is seen at 2012.2 cm^{-1}. Finally, around 1097 cm^{-1},there is an intense absorption which is characteristic of Si-O-Si.

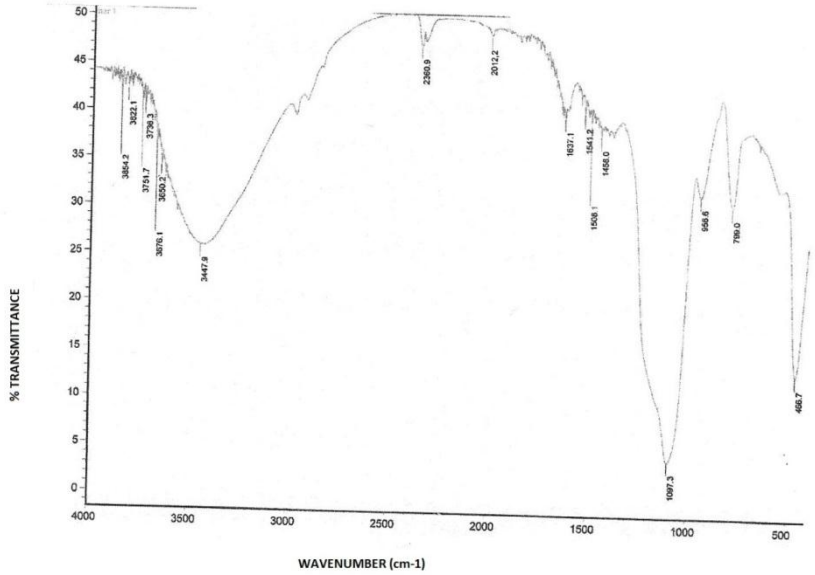

***Graph 21**: FT-IR Trace For CAT 8*

9.3.7) MICRO RAMAN (x: Raman Shift(cm^{-1}) y: Intensity (a.u.))

The bands registered at 675.5 cm^{-1}, 511.3 cm^{-1} and 469.7 cm^{-1}, are characteristic of Co_3O_4, which goes to show that the sample was analysed in the air because the carbonyl group is oxidized to an oxide group.

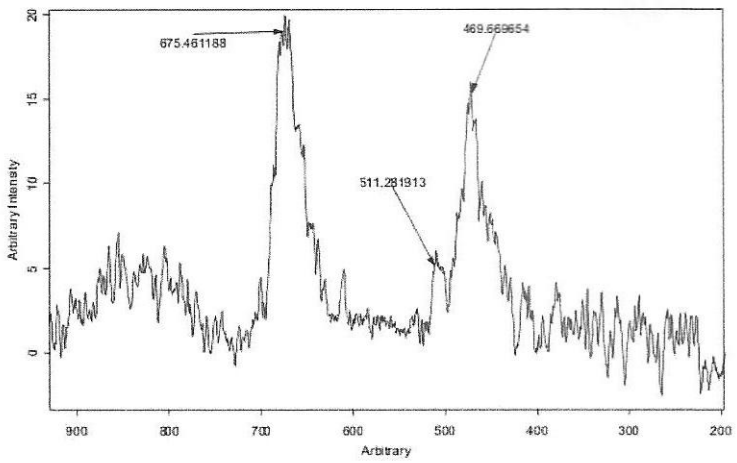

***Graph 22**: Raman Spectrum For CAT 8*

9.3.8) SEM IMAGE

The SEM image shown and the EDX studies on the bright granular area and on the dark zone, do confirm the formation of metallic aggregates. On the clear zone, a 13 % of Co is observed, while on the dark zone, a bit less.

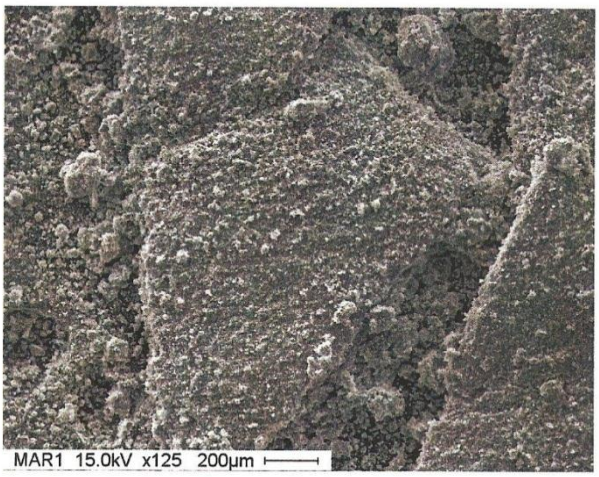

***Image 5**: SEM Image For CAT 8*

9.3.9) TEM IMAGE

The TEM photograms also show how the cobalt particles are not very well dispersed. The dark zones indicate cobalt particles while the clear zones do indicate the support in silica gel.

9.4) CHARACTERIZATION OF CAT 5

9.4.1) TGA (Thermal Gravimetric Analysis)

At 400 °C and above, there's a complete decomposition of CAT 5.This is also seen because of the almost 45 % of total weight loss, as seen on the graph.

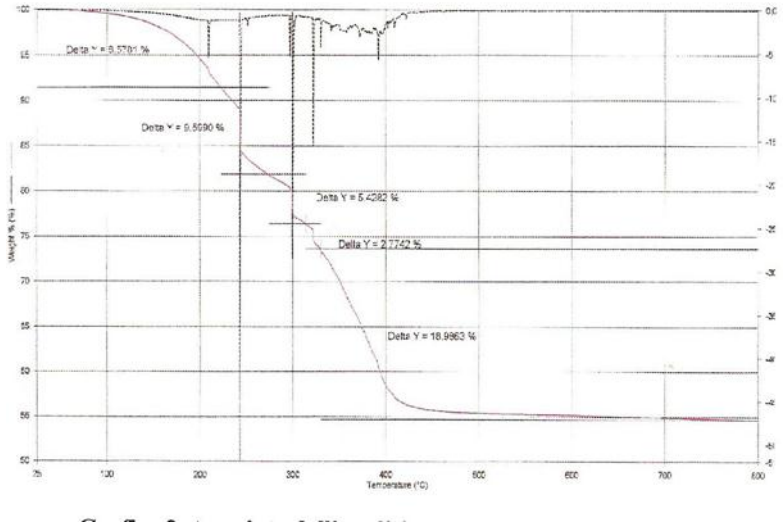

***Graph 23**: A TGA trace of CAT 5*

9.4.2) SURFACE AREA MEASUREMENT

As it is expected from the preparation method, the surface area is very high. 380 m^2/g. This is an index of a good and homogeneous surface coverage.

9.4.3) TPR ANALYSIS

The TPR analysis gives a complex trace. There is a first peak at 500 °C, then around 700 °C there's a shoulder peak and two distinct peaks at 800 and 900 °C. The complex nature of this peak could be attributed to the formation of mixed metal oxides like cobalt "ferrierite" ($CoFe_2O_4$), which give the first peak. The last two peaks could be attributed to the formation of silicates of both Co and Fe, which are much more resistant to reduction than the mixed oxides.

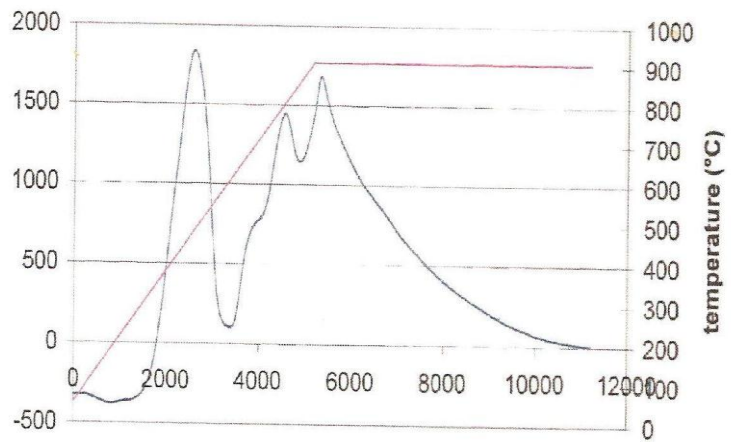

***Graph 24**: TPR analysis trace for CAT 5*

9.4.4) TPO ANALYSIS

After a pre-treatment of CAT 5 at 400 °C in a hydrogen flow, the resulting peak is interesting because it shows a total oxidation. In fact it gives a maximum oxidation at 400 °C, with a 100 % reducing ability.

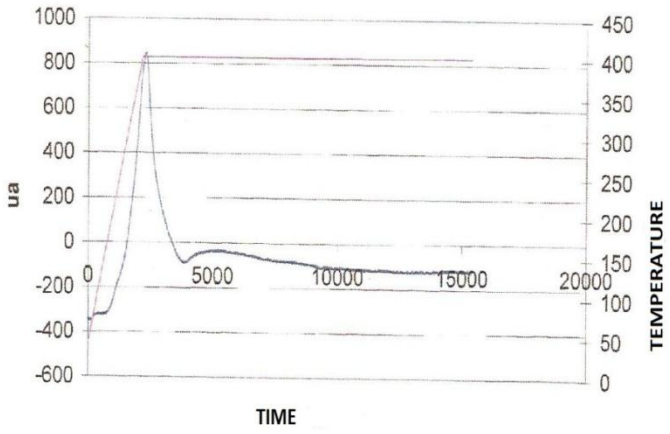

***Graph 25**: A TPO trace for CAT 5*

9.4.5) H_2-TPD ANALYSIS

This analysis shows a first peak at very low temperatures, and two others at 200 °C and 400 °C respectively. But from the calculations the dispersion percentage is so low, just 14 %.

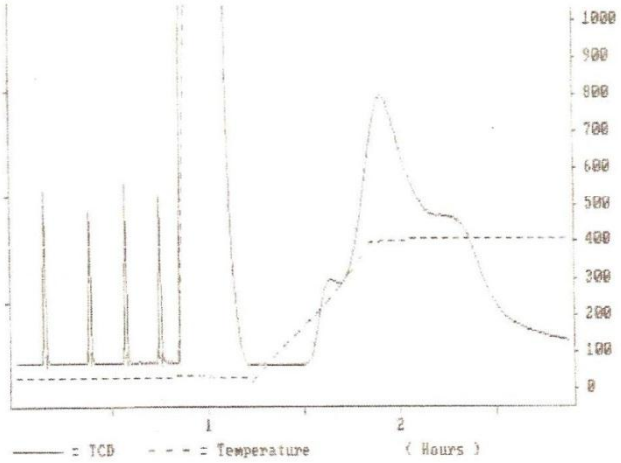

***Graph 26**: H_2-TPD for CAT 5*

9.4.6) FT-IR SPECTROSCOPY

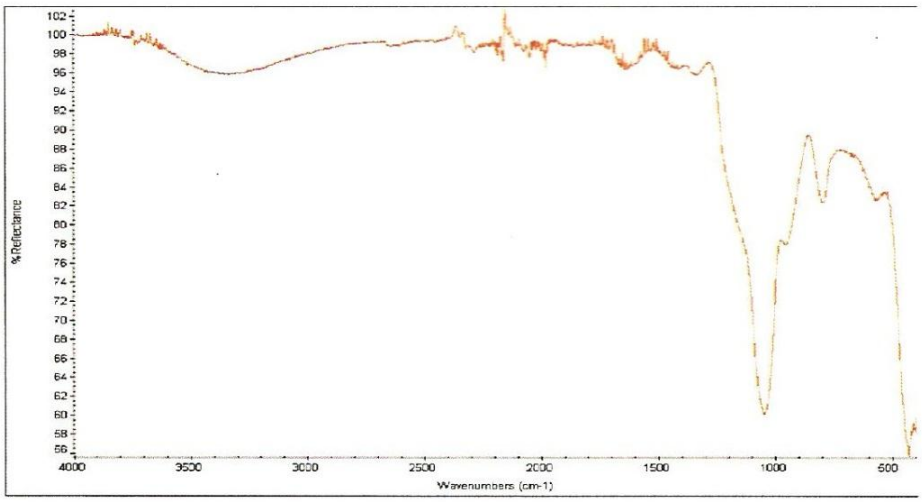

***Graph 27**: FT-IR Spectrum Of CAT 5 Before Calcining*

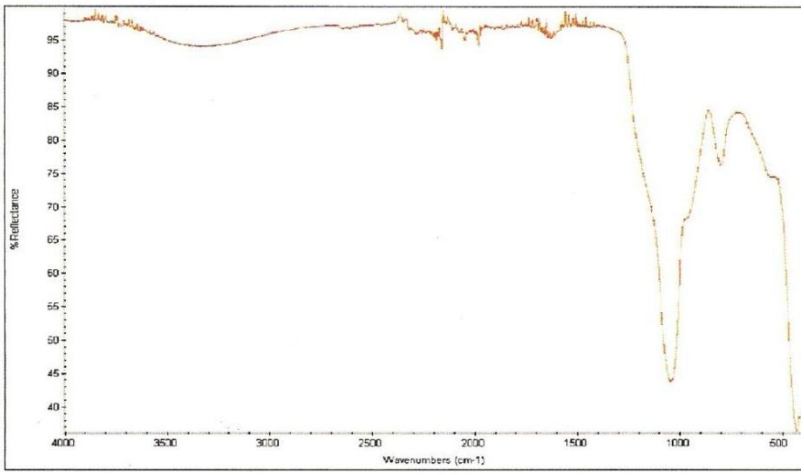

***Graph 28**: FT-IR Spectrum Of CAT 5 After Calcining*

The two spectra of CAT 5 are shown to make evidence of the presence and the absence of vibrational bands for nitrates and water. In fact before calcining, although it is not very evident because of dilution in the support, some hunches can be seen around 1400 cm^{-1}, these give the evidence of the presence of nitrates. Then between 3000 and 3500 cm^{-1}, the band for water is evident. In the spectrum made after calcining, the hunches are completely absent and

the water bands are greatly reduced. The bands at 1080 cm^{-1} and 1050 cm^{-1} are attributed to Si-O-Si stretching and the shoulder at 950 cm^{-1} can be attributed to Si-O-M, where M is either Fe or Co. While the large band between 550 and 600 cm^{-1} and the signal at 825 cm^{-1}, can all be attributed to vibrations of Fe-O.

9.4.7) XRD ANALYSIS

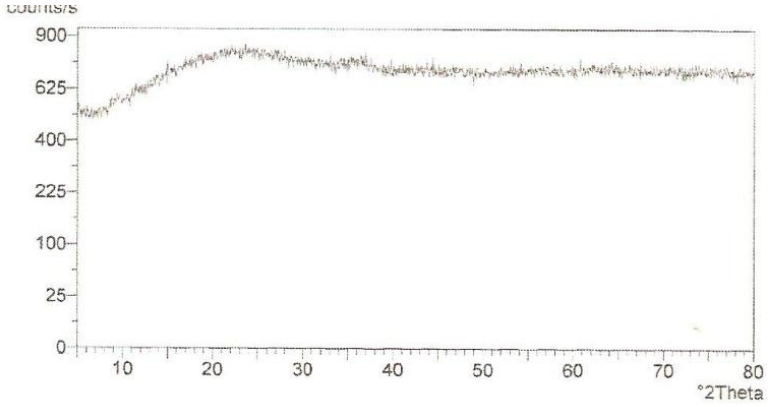

***Graph 29**: XRD Trace For CAT 5*

As can be seen from graph x, the x-ray diffraction pattern shows a sample completely amorphous, as it was also expected from the preparation method.

9.5) CHARACTERIZATION OF CAT 6

9.5.1) TPR ANALYSIS

This TPR trace shows a first reduction peak at 500 °C. This is already a temperature that is not possible to manage on a laboratory plant. The second peak reduces at 900 °C.

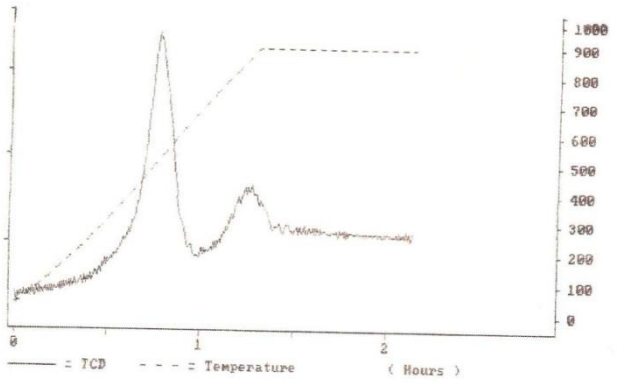

***Graph 30**: TPR Trace For CAT 6*

9.5.2) TPO ANALYSIS

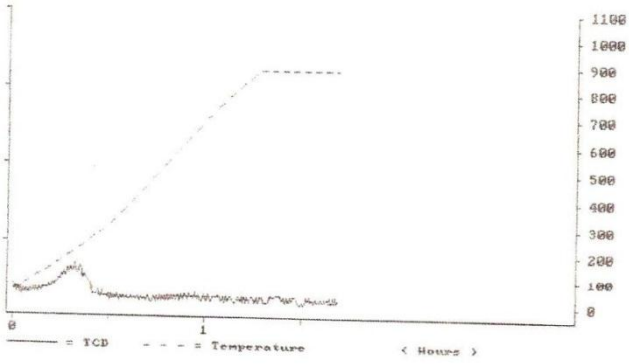

***Graph 31**: TPO Trace For CAT 6*

This TPO results confirms that there is little or no Co oxides reduced at 400 °C. Hence a 100 % reducibility.

9.5.3) H_2-TPD ANALYSIS

From the H_2-TPD analysis, a 28 % dispersion is obtained which can be attributed to the type of support used in the preparation. An aero-gel was used.

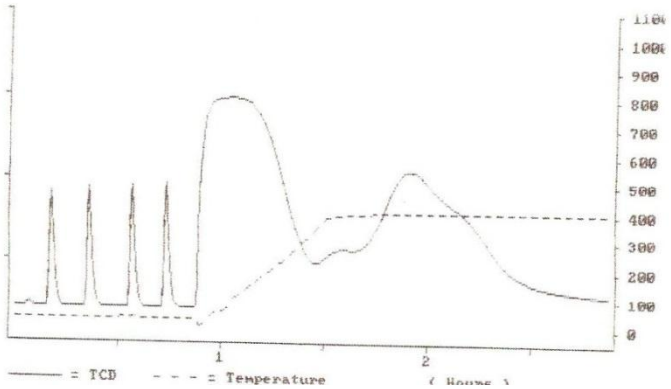

***Graph 32**: H_2-TPD Trace For CAT 6*

9.5.4) XRD ANALYSIS

Here the peak seen on the x-ray diffraction trace could be explained as the presence of Fe-Co alloys.

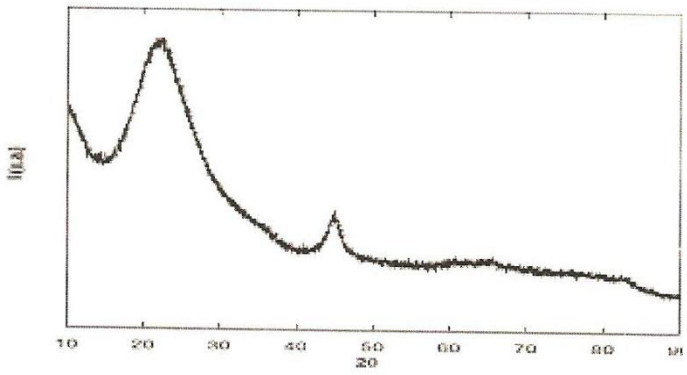

***Graph 33**: XRD Trace For CAT 6*

9.6) CHARACTERIZATION OF CAT 16

9.6.1) TGA (Thermal Gravimetric Analysis)

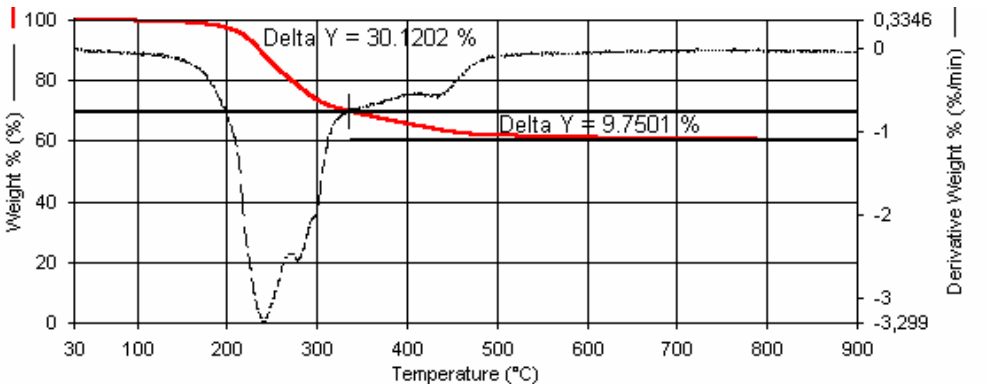

***Graph 34**: TGA Of Dry CAT 16*

A very great weight loss of about 30 % is noticed already, before even 300 °C and a further 10 % weight loss is noticed between 300 and 500 °C. This is the reason for the decision to calcine the catalyst at 400 °C.

9.6.2) SURFACE AREA MEASUREMENT

The surface area of CAT 16, determined by the BET single point method was 269 m^2/g.

9.6.3) TPR ANALYSIS

The TPR trace for CAT 16 shows two clear peaks. One at 430 °C which can surely be attributed to the reduction of mixed cobalt oxides, like Co_3O_4 and CoO. The second peak falls at 680 °C, which goes to indicate species formed from interactions between Co and the support, and are much more difficult to reduce.

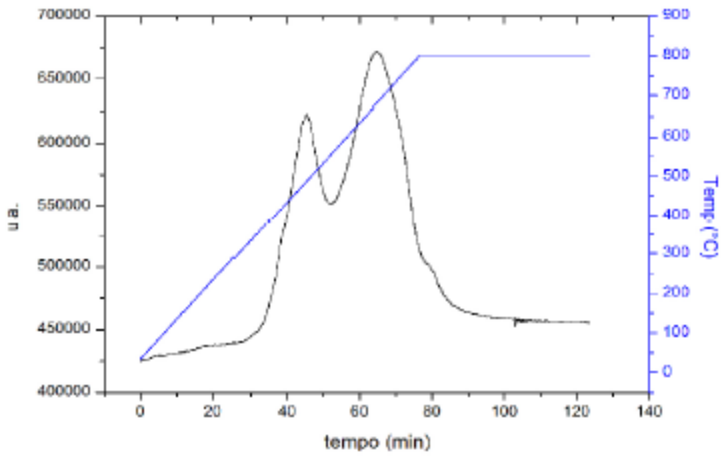

***Graph 35**: TPR Trace For CAT 16*

9.6.4) TPO ANALYSIS

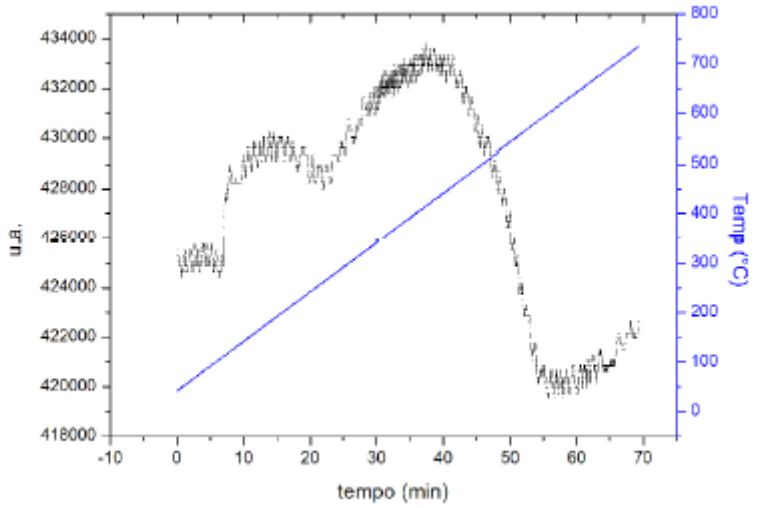

***Graph 36**: TPO Trace For CAT 16*

After reduction for 4 hours at 400 °C, a re-oxidization gives peaks at temperatures lower than 600 °C and a reducing capacity of 59 %. The maximum of oxygen consumption is seen at 375 °C.

9.6.5) H_2-TPD ANALYSIS

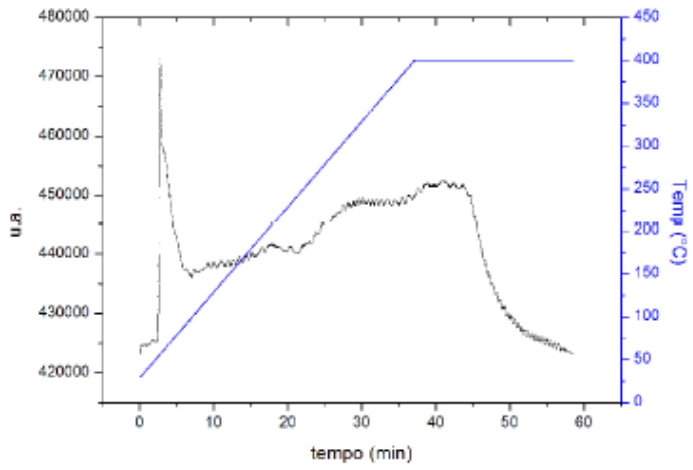

***Graph 37**: H_2-TPD For CAT 16*

9.7) CHARACTERIZATION OF CAT 17

9.7.1) SURFACE AREA MEASUREMENT

A study of the surface area of CAT 17 gives a value of about 281 m^2/g.

9.7.2) TPR ANALYSIS

The shoulder at 225 °C could be interpreted as a reduction of Co_3O_4 to CoO, and the peak at 425 °C could be the total reduction to Co in the metallic state. The lowering of the reduction temperatures could be attributed to the promotion effect of Ru. The little peak present around 800 °C could be explained as a residue of aluminates formed.

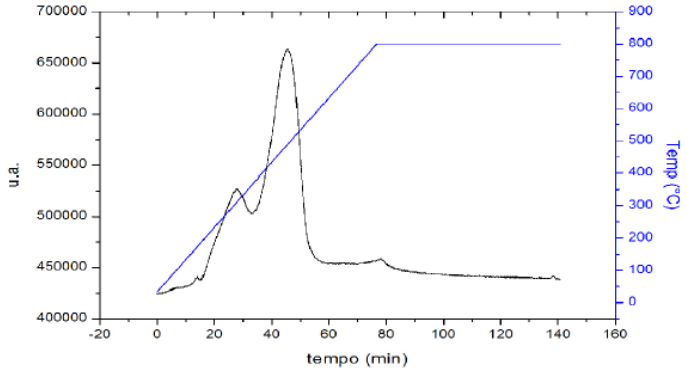

***Graph 38**: TPR Trace For CAT 17*

9.7.3) H_2-TPD ANALYSIS

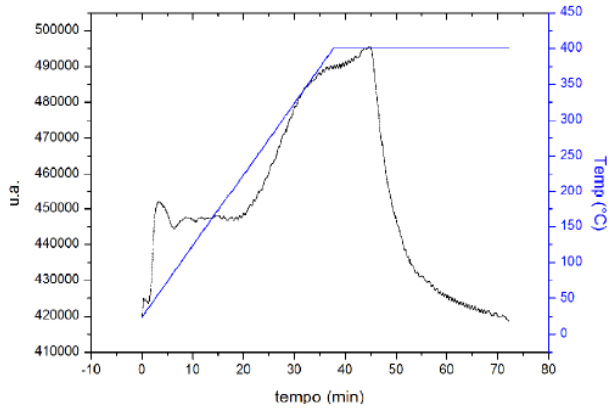

***Graph 39**: H_2-TPD Trace For CAT 17*

In this case two evident adsorption peaks could be identified. One at 33 °C and the other at 350 °C.

9.8) CHARACTERIZATION OF CAT 3

9.8.1) TGA (Thermal Gravimetric Analysis)

As can be deduced from graph 40, which was carried out in a static environment to simulate the stove, and heated at 19 °C/min beginning from 30 °C up to 900 °C, at 500°C the catalyst has already undergone a total decomposition with a loss in weight of about 43.9%.

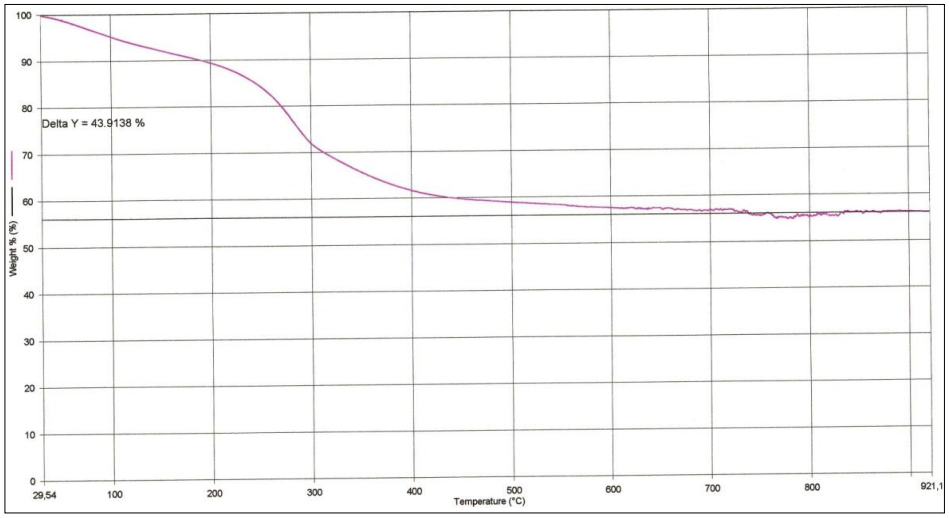

***Graph 40**: TGA Trace For CAT 3*

9.8.2) SURFACE AREA MEASUREMENT

CAT 3 demonstrated a relatively high surface area of about 379 m^2/gm, which is easily explained, since this method of preparation has always given products with a normally high surface area.

9.8.3) TPR ANALYSIS

Looking at the TPR peak for CAT 3, a single peak is seen which begins at 300 °C and has a maximum at almost 600 °C. Then there's a little shoulder at a higher temperature. Although these peaks give a total ability to reduce of almost 51% the reduction temperature is so high, and still this percentage is not so high. This would imply that at the activation temperature in a Fischer-Tropsch plant, very little Co is reduced.

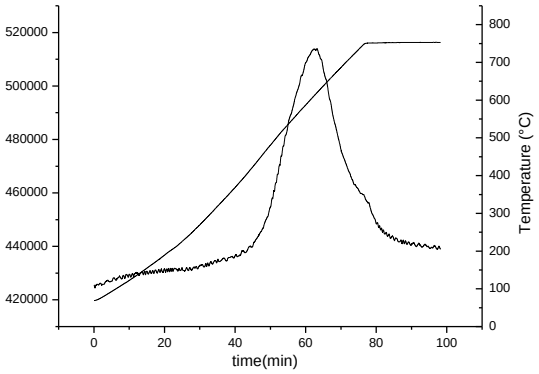

***Graph 41**: TPR Trace For CAT 3*

9.8.4) FT-IR SPECTROSCOPY

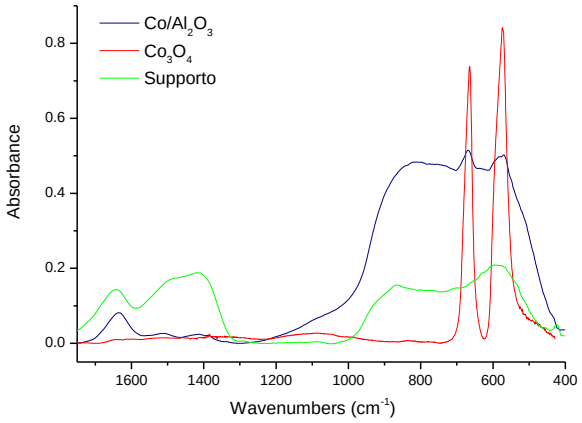

***Graph 42**: FT-IR Spectrum For Calcined CAT 3*

Graph 42 puts together the support, a trace of a Co_3O_4 and a trace of the catalyst CAT 3, in absorbance. The Co_3O_4 vibrational bands are evident.

9.8.5) XRD ANALYSIS

This analysis conducted at the University Of Perugia, put into evidence the diffractional peaks centred at 2θ=31.3°; 36.9°; 44.9°; 59.6° and 65.3° which are characteristic of Co_3O_4 crystalline forms.

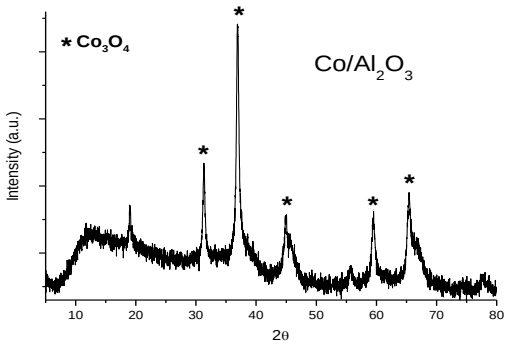

***Graph 43**: XRD Trace For CAT 3*

9.8.6) RAMAN-SPECTROSCOPY

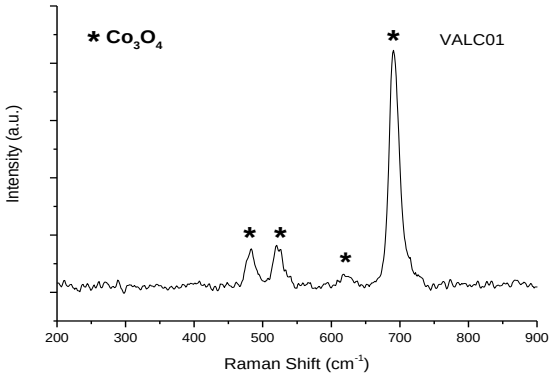

***Graph 44**: RAMAN Spectrum For CAT 3*

The four bands identified on the Raman trace, i.e. 483 cm^{-1}, 523 cm^{-1}, 621 cm^{-1} and 694 cm^{-1}, are characteristic of Co_3O_4.

9.8.7) SEM AND EDS ANALYSIS

These analysis were also conducted at the University Of Perugia, and they showed a surface deposition, not very homogeneous, though the EDS gave a point concentration of about 14.79% of Co on the surface.

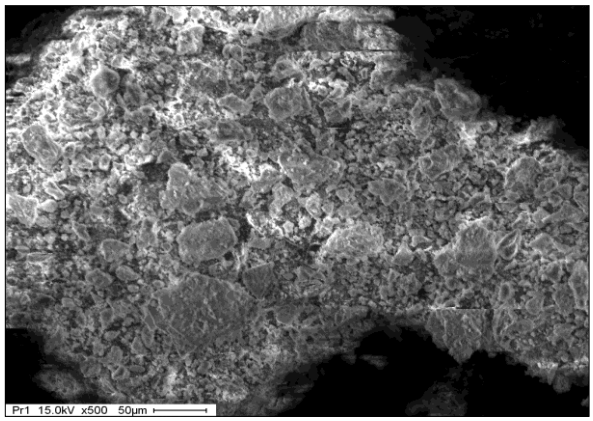

***Image 6**: Enlarged SEM Image For CAT 3*

9.9) CHARACTERIZATION OF CAT 4

9.9.1) TGA (Thermal Gravimetric Analysis)

In this thermal gravimetric analysis the heating is done at the rate of 10 °C/min, going from 30 °C up to 900 °C, in a static environment to be able to simulate the calcining conditions. In this way the weight loss can be estimated. It is noticed that before 500 °C the weight reduction is completed, with a total weight loss of 41.1%.

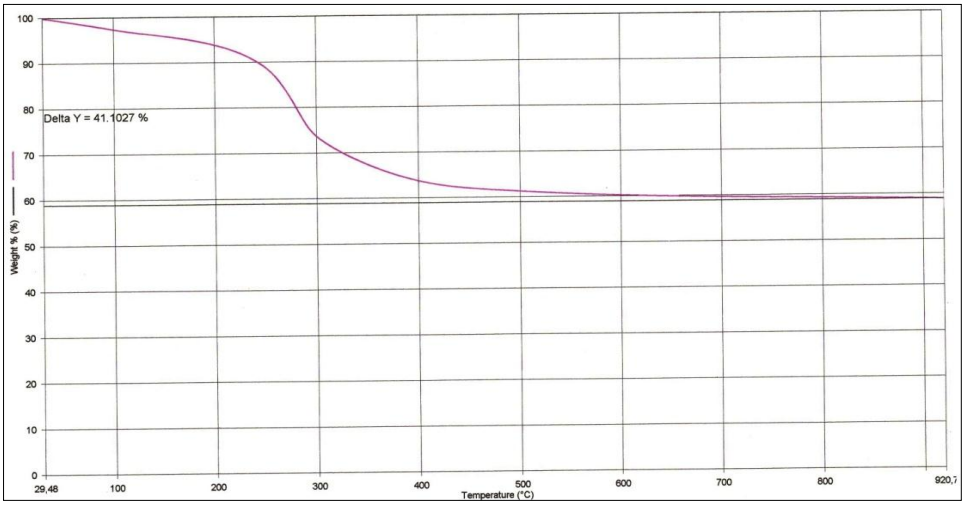

***Graph 45**: TGA Trace For CAT 4*

9.9.2) SURFACE AREA MEASUREMENT

The surface area measured using the BET single point method, gave an area of about 374 m^2/g, which is congruous with the preparation method.

9.9.3) TPR ANALYSIS

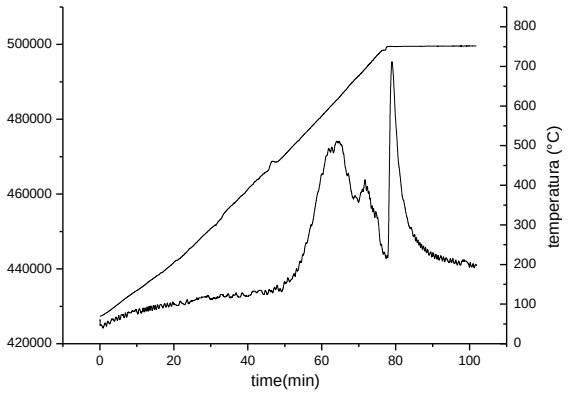

***Graph 46**: TPR Trace For CAT 4*

The results of this analysis shows three peaks between 600 °C and 800 °C the first two could be attributed to the reduction of oxides of Co and Ru. The third peak instead, can be attributed to the reduction of aluminates. These are strong bonds between Co and Al-O.

9.9.4) FT-IR SPECTROSCOPY

Here in graph 47, the presence of the mixed Co oxides are not so evident.

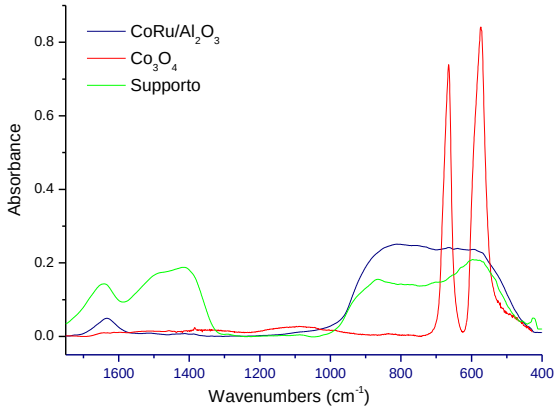

***Graph 47**: FT-IR Spectrum For CAT 4*

9.9.5) XRD ANALYSIS

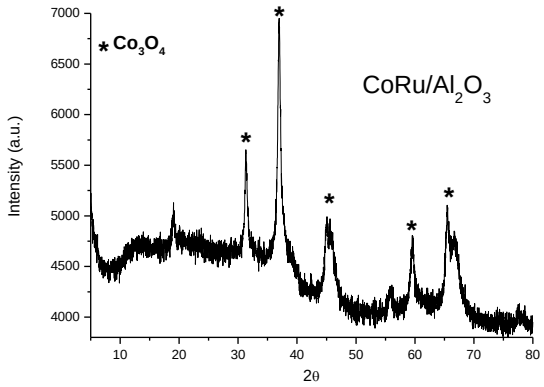

***Graph 48**: XRD Trace For CAT 4*

Here the only diffractional peaks that are recognised are those centred at 2θ=31.3°; 36.9°; 44.0°; 59.6° and 65.3°, which are attributed to the presence of Co_3O_4.

9.9.6) RAMAN SPECTROSCOPY

Here, the only evident peaks are the ones attributed to Co_3O_4. They are those resulting at 483 cm^{-1}, 523 cm^{-1}, 621 cm^{-1} and 694 cm^{-1}.

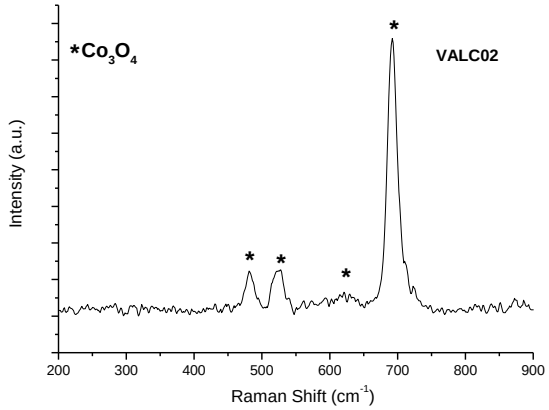

***Graph 49**: Raman Spectrum For CAT 4*

9.9.7) SEM AND EDS ANALYSIS

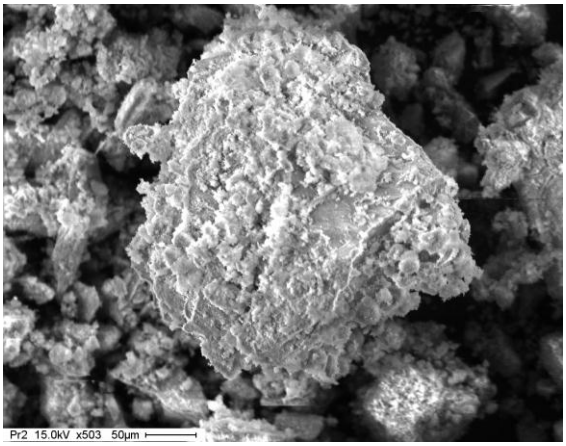

***Image 7**: Enlarged SEM Image For CAT 4*

From this image, a striking situation jumps to the eye. The nonhomogeneous distribution of cobalt oxides on the surface. In fact, in the EDS point study in point A and point B, the following results were obtained. Point A, 2.7 % of Co and 0.15 % of Ru, while in point B, 13.91 % of Co and 0.32 % of Ru were observed.

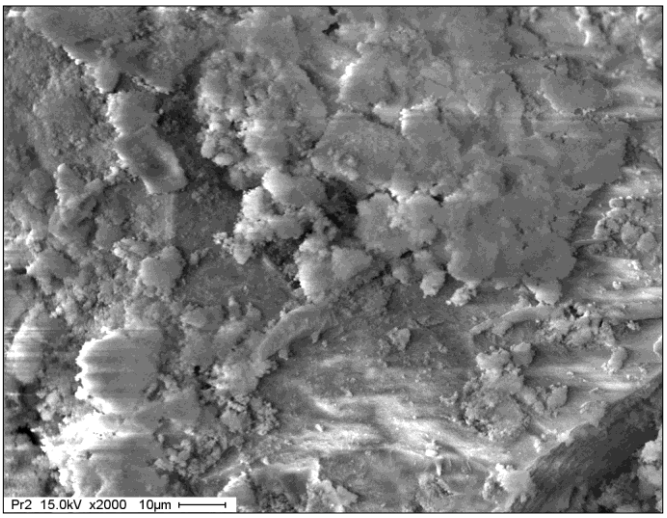

***Image 8**: SEM Image and EDS Analysis For CAT 4*

9.10) CHARACTERIZATION OF CAT 18

9.10.1) SURFACE AREA MEASUREMENT

The surface area obtained for CAT 18, using the BET single point method, gave an area of 172 m^2/g. This low surface area can be attributed to the high surface covering of the bulk sol- gel method of preparation.

9.10.2) TPR ANALYSIS

The TPR graph shows a large peak with a maximum at 695 °C with two shoulder peaks at 340°C and 420°C. This is an index of the scarcity of the mixed oxides like Co3O4 and CoO. The principal peak instead, which has the maximum at 695 °C, is indicative of the presence of species very difficult to reduce.

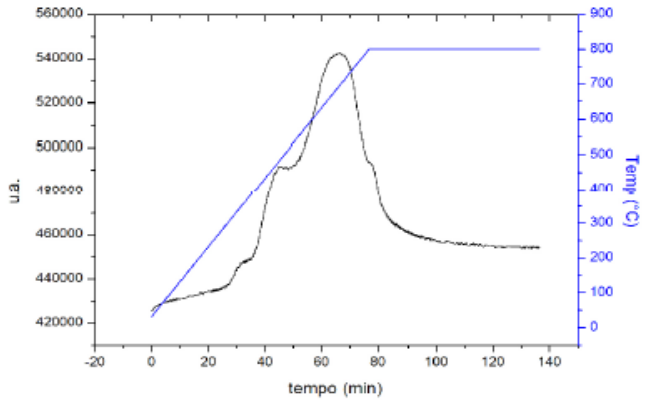

Graph 50: *TPR Trace For CAT 18*

9.10.3) TPO ANALYSIS

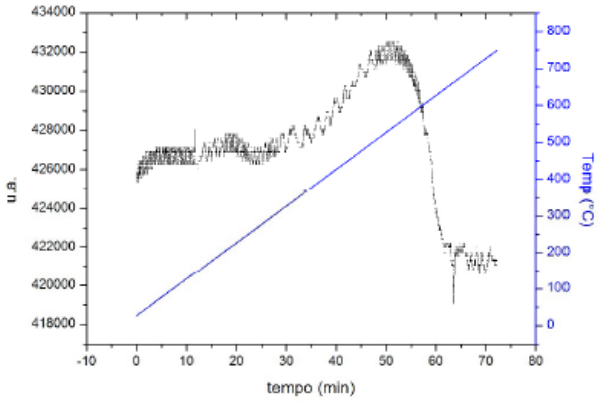

Graph 51*: TPO Trace For CAT 18*

Always keeping in mind that the pre-treatment used for TPO is similar to the activation condition of the catalyst, a 37 % of reducing capacity is obtained. This quantity is totally oxidized on meeting oxygen and at temperatures below 650 °C.

9.10.4) H_2-TPD ANALYSIS

This trace shows an intense peak at almost 25 °C and two other smaller peaks at 120 and 325 °C.

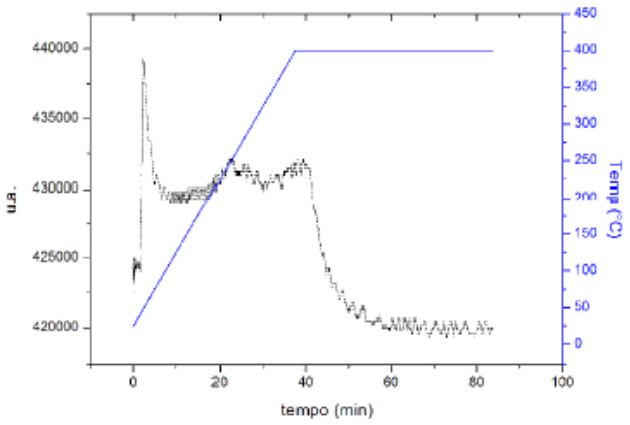

***Graph 52**: H_2-TPD Trace For CAT 18*

9.10.5) FT-IR SPECTROSCOPY

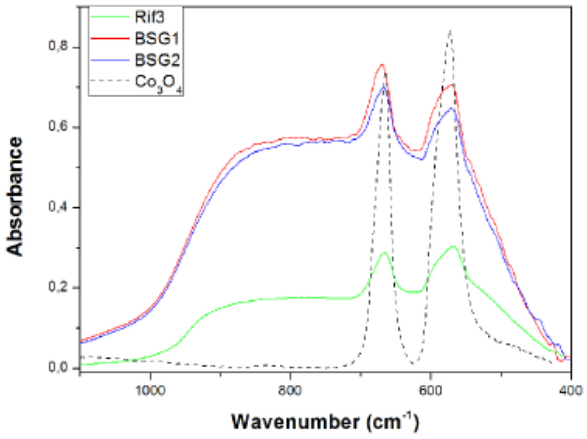

***Graph 53**: FT-IR bands For CAT 17, CAT 18, CAT 19, And Co_3O_4 For Comparison.*

The spectrum shows two distinct vibrational bands. One at 570 cm^{-1} which is attributed normally to vibrations of the type OB_3, where B is Co^{+3}, in octahedric sites. The second band at 670 $^{cm-1}$ can be attributed to vibrations of the type ABO_3, where A is Co^{+2} in a tetrahedric site.

9.10.6) RAMAN SPECTROSCPY

All three spectra show bands in the regions normally attributed to Co_3O_4. These bands fall at 670 cm^{-1}, 610 cm^{-1} and 487 cm^{-1}. The band at 510 cm^{-1} is not very evident for morphological reasons. The analysis was done on powder.

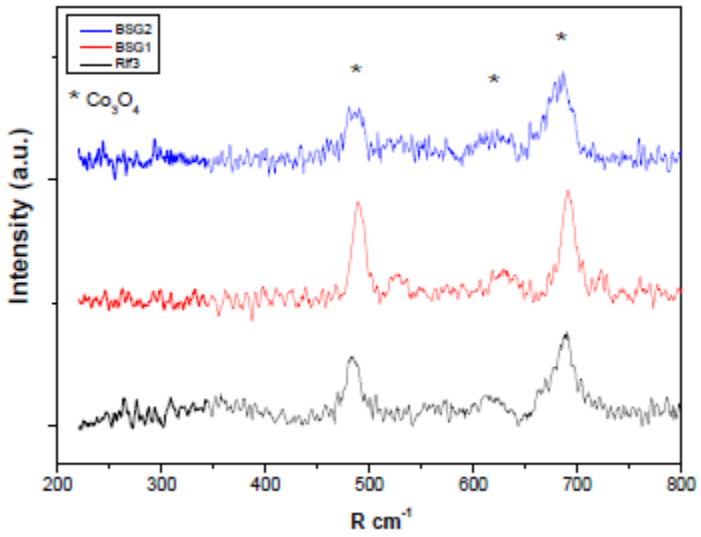

***Graph 54**: RAMAN Spectra for CAT 17, CAT 18 and CAT 19*

9.10.7) XRD ANALYSIS

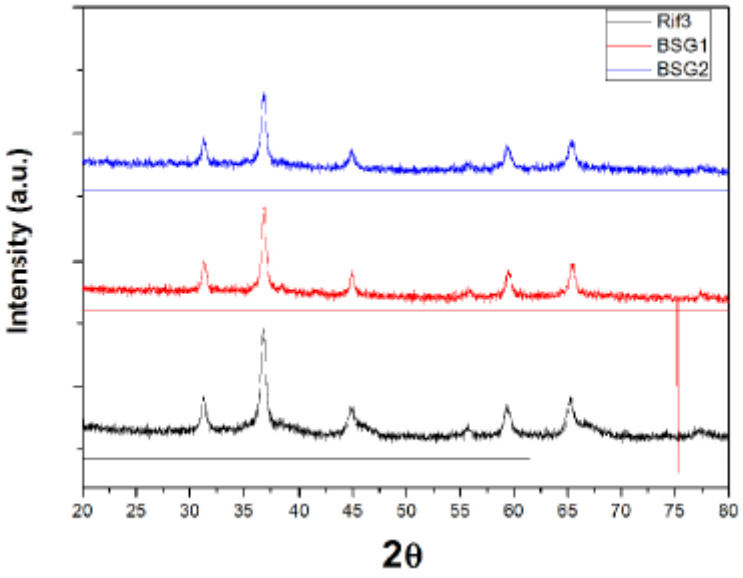

***Graph 55**: XRD Traces For CAT17, CAT 18 and CAT 19*

The peaks on the graph are very similar for all three samples. Those centred at 2θ= 31.3°, 36.8°, 44.8°, 59° and 65.2°, demonstrate the presence of Co_3O_4, on the surface of the catalysts.

9.10.8) SEM IMAGE

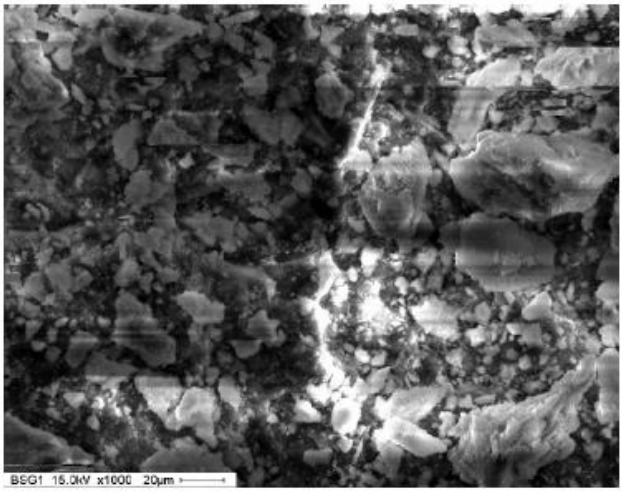

***Image 9**: SEM Image For CAT 18*

The sample used showed up to be very homogeneous because an EDS study revealed a 7.5 % of Co on a point which corresponds to 19.3 % in weight.

9.10.9) TEM IMAGE

This image gives an ulterior confirmation of the homogeneity of CAT 18, and the fact that with the bulk sol-gel method the distribution on the surface is homogeneous.

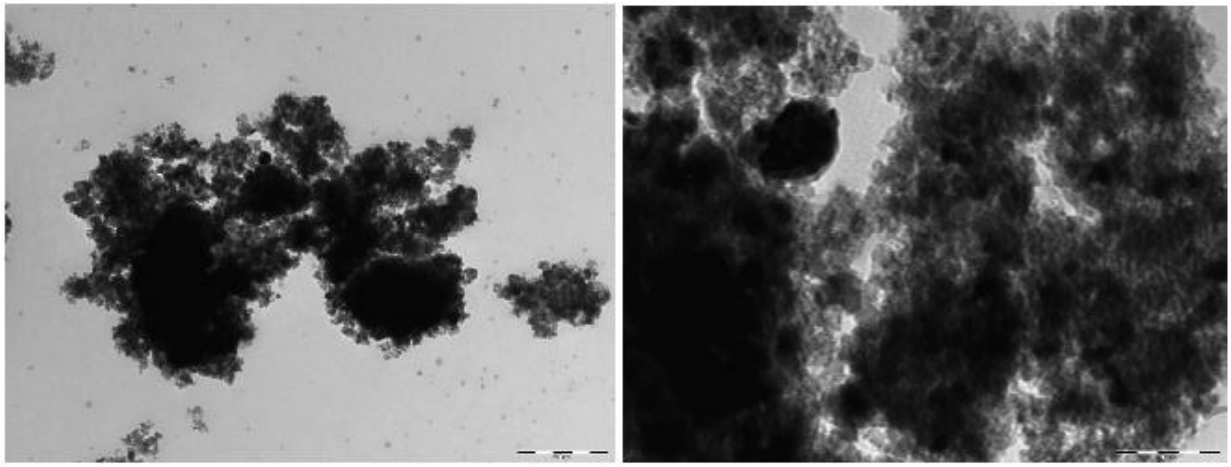

***Image 10**: TEM Images For CAT 18*

9.11) CHARACTERIZATION OF CAT 7

9.11.1) SURFACE AREA MEASUREMENT

A measure of the surface area using the BET single point method gave 157 m^2/g, while a sample sent to the University of Cagliari, where they use the BET multiple points method with a complete isotherm, gave 170.6 m^2/g. This same instrument permits an evaluation of the pore distribution on the surface of the catalyst.

The steepness of the curve indicates a homogenous distribution of pores on the surface of the catalyst, which is exactly what was desired. It gave a medium pore diameter of about 35 Å, that is 3.5 nm.

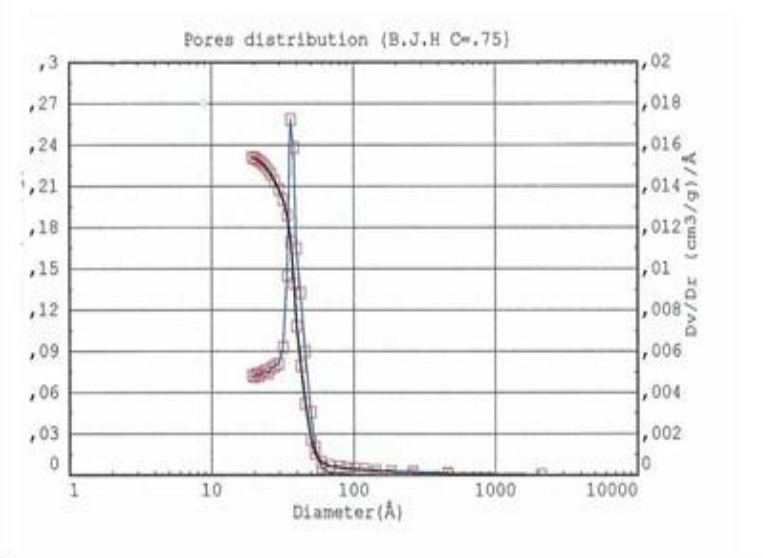

***Graph 56**: Pore Distribution On CAT 7*

9.11.2) TPR ANALYSIS

The absence of peaks at the lower temperature area gives an idea of a complete absence of species that can be easily reduced like the oxides of Co^{2+} or Co^{3+}. The peak at 600 °C instead induces a thought of strongly tied up species between cobalt and support. It seems during calcining, instead of the formation of oxides, there's the formation of aluminates. Under these conditions, a reduction capacity was calculated and it gave 40% of the total quantity of metal on the catalyst.

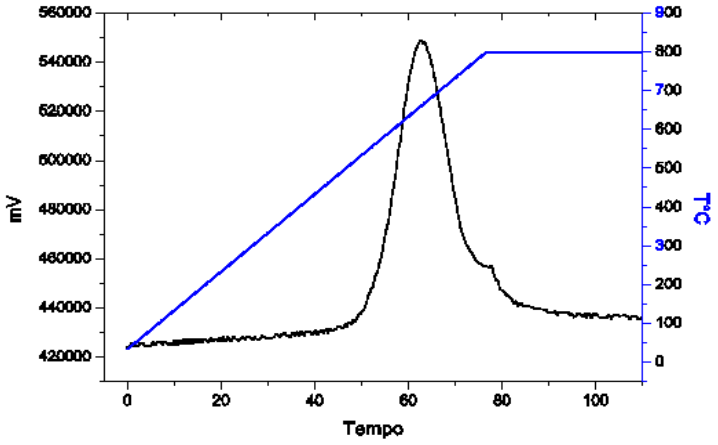

***Graph 57**: TPR Trace For CAT 7*

9.11.3) TPO ANALYSIS

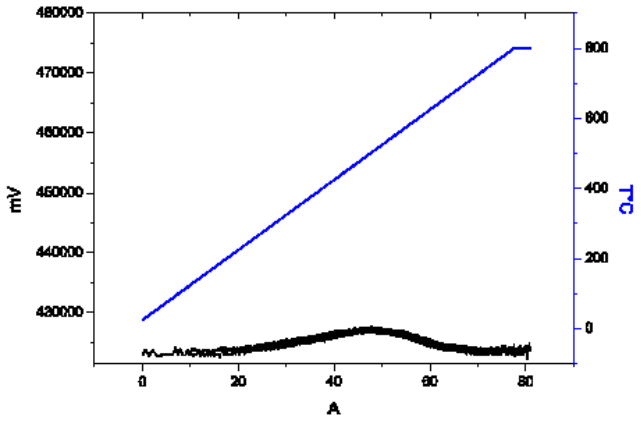

***Graph 58**: TPO Trace For CAT 7*

Following the suggestions of the TPR analysis, a TPO analysis was made, taking the activation temperature to be 600 °C. A broad peak was obtained at 580 °C, from whose integration, a 47% oxidation capacity could be deduced.

9.11.4) H_2-TPD ANALYSIS

After having treated a sample in the activation condition of the laboratory plant, that is 400 °C for six hours, the H_2-TPD trace shows no desorption peaks. Therefore no H_2 was adsorbed.

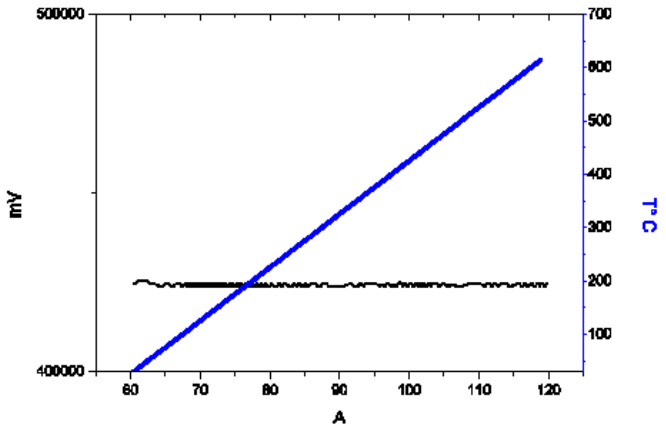

***Graph 59**: H_2-TPD Trace For CAT 7*

9.12) CHARACTERIZATION OF CAT 10

9.12.1) FT-IR SPECTROSCOPY

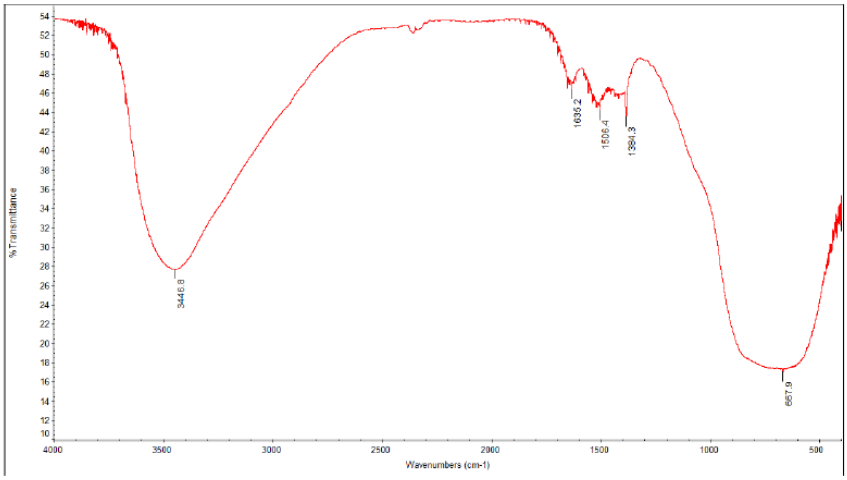

***Graph 60**: FT-IR Spectrum for CAT 10*

Graph 60 indicates the presence of water around 3446 cm^{-1}, and a large peak in the area between 800 and 1000 cm^{-1}. This peak most probably comes from an overlap of many peaks in the vibration region of the metal-oxide bond.

9.12.2) SURFACE AREA MEASUREMENT

The surface area of the catalyst CAT 10, as measured with the aid of "Micrometrics Pulse Chemisorb 2705", using the BET single point method, gave 241 m^2/g.

9.12.3) TPR (Temperature Programmed Reduction) ANALYSIS

This analysis shows a three peak trace corresponding to three distinct temperature ranges which could be attributed to different reduction types. The peak at 206°C can be attributed to the reduction of ruthenium oxide to the metallic form. The second peak at 404°C can be

attributed to the reduction of a mixture of cobalt oxides, like Co_3O_4 and CoO. The third peak at 745°C is normally attributed to very strongly bonded species, not very easy to reduce. These species are termed aluminates, and are formed during calcinning. From this analysis, it could be calculated that, the total amount of surface metal reduced during activation of the catalyst is only 7.4% of the total, while the amount of metal that can be reduced on the surface is about 39.2% of the total amount deposited.

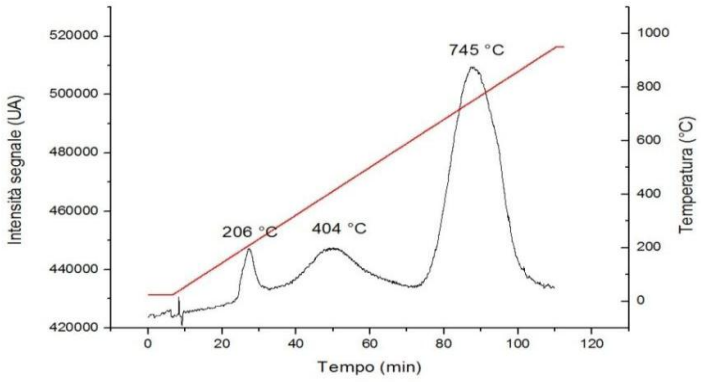

***Graph 61**: TPR Analysis For CAT 10*

9.12.4) TPO (Temperature Programmed Oxidation) ANALYSIS

The TPO trace shows how active metal is not easily re-oxidized in the working conditions of the lab. plant. In any case there's a shoulder peak at 250°C which shows the beginning of oxidation. The oxidation of reduced metal occurs at 400°C. In this analysis it can be calculated that, the amount of surface metal that can be oxidized is only about 7.4%.

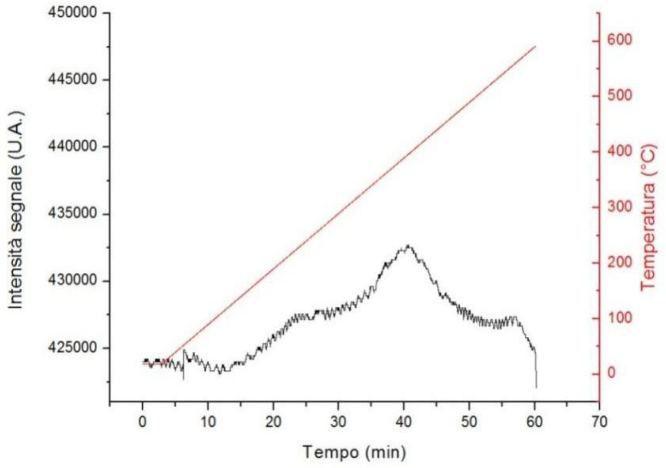

***Graph 62**: TPO Analysis For CAT 10*

9.12.5) H_2-TPD (Temperature Programmed Desorption Of Hydrogen) ANALYSIS

The H2-TPD analysis of MAR 01, gives a single desorption peak at 400°C with a shoulder peak at 330°C. From the areas under the peak, a very scarce percentage of dispersion is calculated. (1.7%), and the calculated particle dimension about 57 nm. The number of active sites resulting from this surface distribution are 2.3*1019. Eventually here there's a very low value of H2 adsorbed for every gram of catalyst, just 19 µmol/gm.

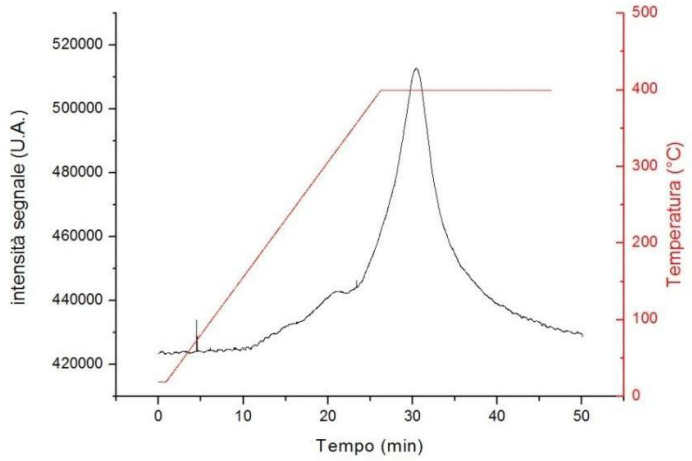

***Graph 63**: H_2-TPD Analysis For CAT 10*

9.12.6) XRD (X-Ray Diffraction) ANALYSIS

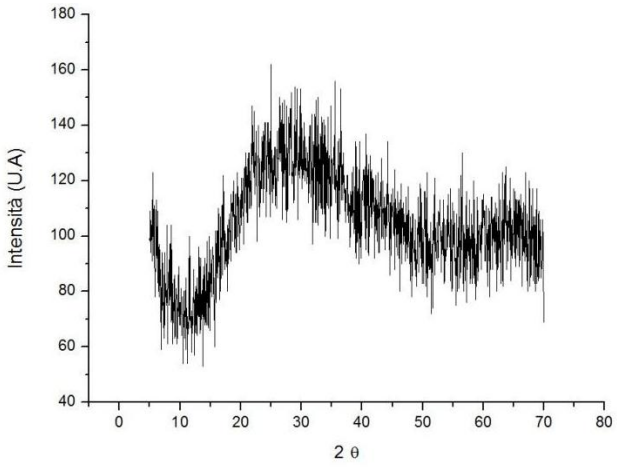

***Graph 64**: XRD Analysis For CAT 10*

The only important information we can obtain from this analysis is fact that it is amorphous. In fact, the bulk sol-gel method of preparation produces amorphous compounds over a large temperature range.

9.12.7) SEM (Scan Electron Microscopy) IMAGE WITH EDS

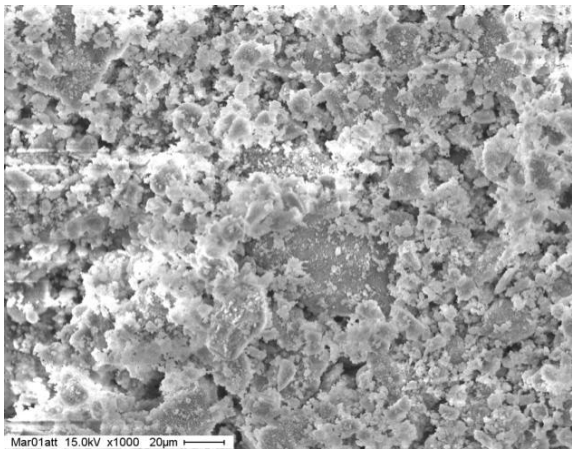

***Image 11**: SEM Image For CAT 10*

The SEM picture above gives evidence of a general surface covering, which is supposed to give good catalytic activity, but the point analysis carried out shows this superficial covering is not homogenous. Really at the examined point there is a 20.31% by weight of Co particles. There's also a complete absence of Ru at the point.

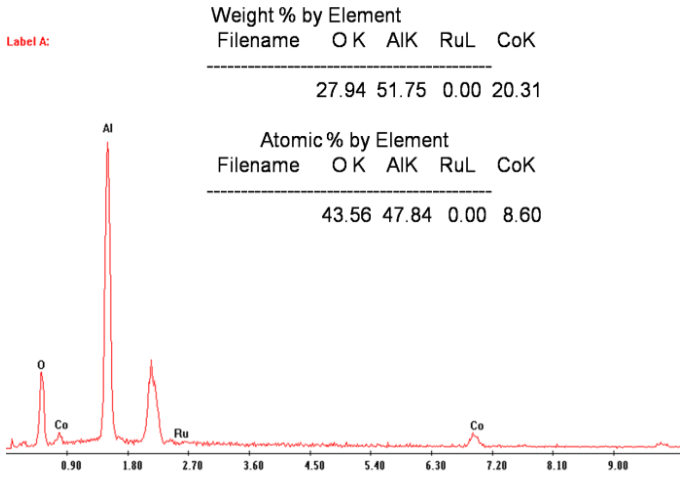

***Graph 65**: EDS Results For CAT 10*

9.13) CHARACTERIZATION OF CAT 11

9.13.1) SURFACE AREA MEASUREMENT

The B.E.T. single point method of measuring the surface area, using the Micrometrics Pulse Chemisorb 2705, gives a surface area of 264 m^2/g for CAT 11.

9.13.2) FT-IR SPECTROSCOPY

A superimposition of the two situations: before and after calcining, which are the blue and the red curves respectively, brings to our attention some interesting characteristics like, a decrease in the band around 3500 cm^{-1}, which could be attributed to the decrease in the water content. Then, there's an almost complete disappearance of the band at the 1384 cm^{-1} area, which can

be attributed to the burning out of (NO_3)- group during calcining. An idea strongly supported by the appearance of the bands at 725 and 664 cm-1, which could imply the formation of metal-oxides like Co3O4.

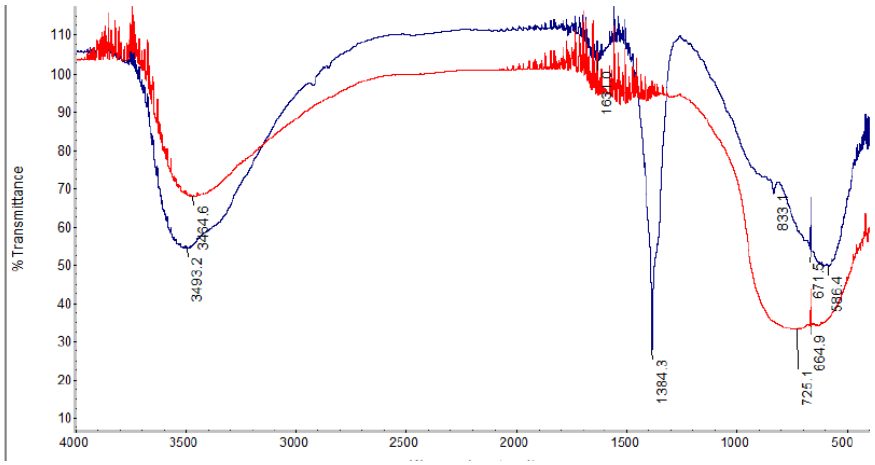

***Graph 66**: FT-IR Spectrum For CAT 11*

9.13.3) TPR ANALYSIS

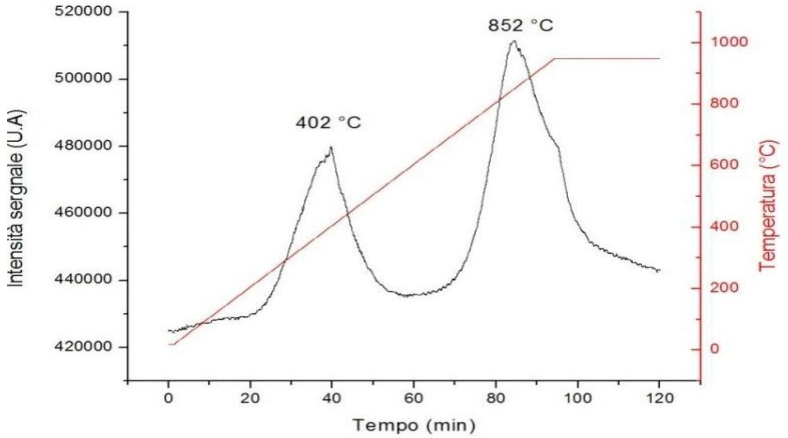

***Graph 67**: TPR Analysis For CAT 11*

The TPR trace for CAT 11 shows two distinct peaks. The first one at 402°C, and can be attributed to the reduction of mixed oxides of cobalt and iron. The second peak comes up at 852°C, which can be attributed to the reduction of the species much more difficult to reduce

like the aluminates. From these peaks, a reduction capacity of 11.3% is calculated, around the activation temperature. The total reducing capacity is about 31.7% of the total quantity of deposited metal.

9.13.4) TPO ANALYSIS

The oxidation as seen on the trace begins at 400°C and reaches maximum 550°C. There's a single oxidation peak, without shoulders or addition of peaks which can be expressed as a one stage oxidation of the active phase. This could be due to strong bonding interactions with the support.

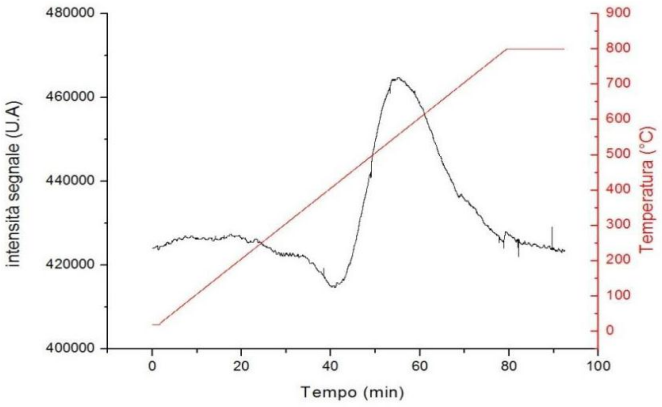

***Graph 68**: TPO Analysis For CAT 11*

9.13.5) H_2-TPD ANALYSIS

In this case, there is a desorption peak at 400°C, a very low dispersion of about 1.5%. The active sites are very few, about $2.4*10^{19}$, and a total desorption of about 19.7 $\mu mol\, H_2/gm$ of catalyst.

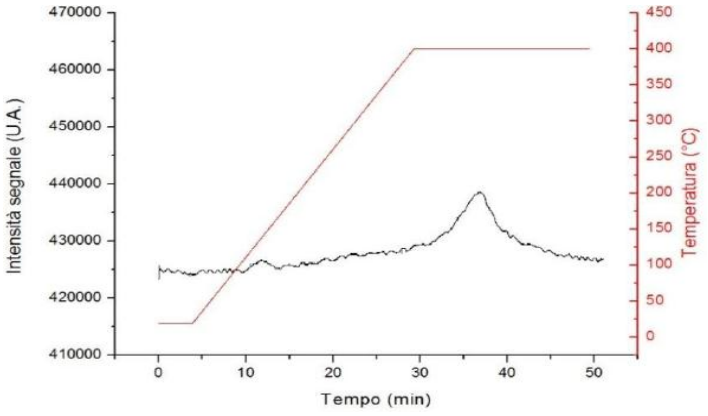

Graph 69: *H_2-TPD Analysis For CAT 11*

9.13.6) XRD ANALYSIS

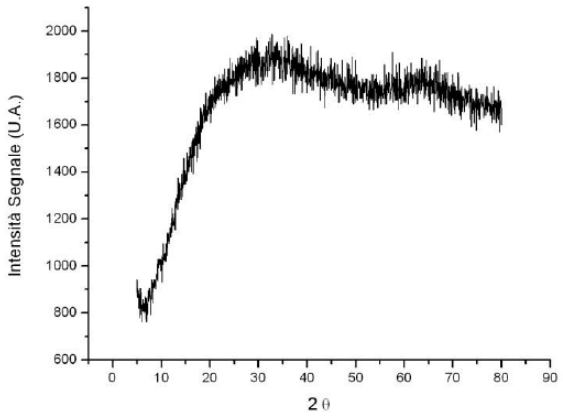

Graph 70*: XRD Trace For CAT 11*

This graph goes to confirm the amorphous nature of the bulk sol-gel products. There are just no peaks to justify any crystalline structures.

9.13.7) SEM IMAGE WITH EDS ANALYSIS

The SEM image give a good coverage on the surface of the catalyst, though an EDS study on a point in this case, shows a Co concentration higher than expected. In fact, 18.81% instead of 11.25%. Therefore, only a non-homogenous covering can be suggested.

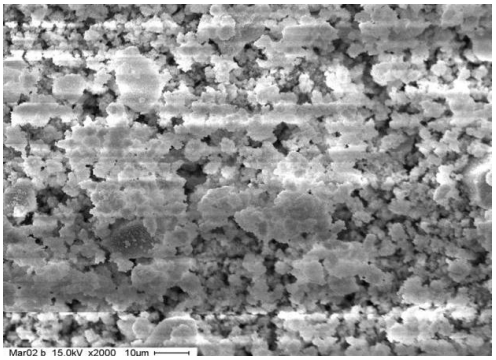

Image 12: *SEM Image For CAT 11*

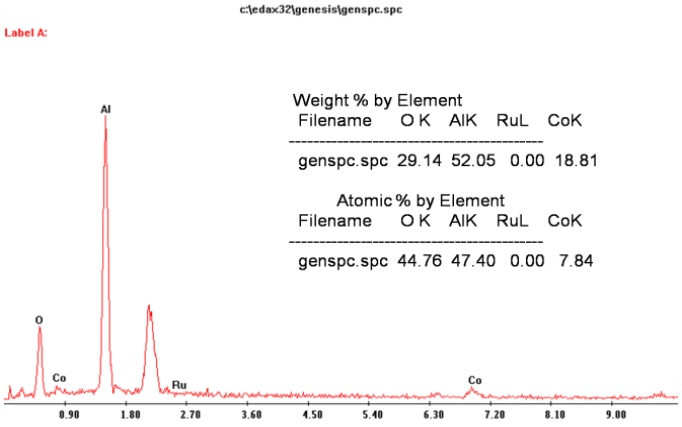

Graph 71*: EDS Study For CAT 11*

9.14) CHARACTERIZATION OF CAT 12

9.14.1) SURFACE AREA MEASUREMENT

The surface area shown by CAT 12 is a bit different from the other two, giving a value of 110 m^2/g.

9.14.2) FT-IR SPECTROSCOPY

With CAT 12, there is an evident demonstration of the effect of calcination. There's almost the complete disappearance of the water band at the 3515 cm-1 area, and at 1384 cm-1 there's also an evident burn out of NO_3-. Finally around the 772 and 672 cm-1 area, typical metal oxide vibration bands are evidenced.

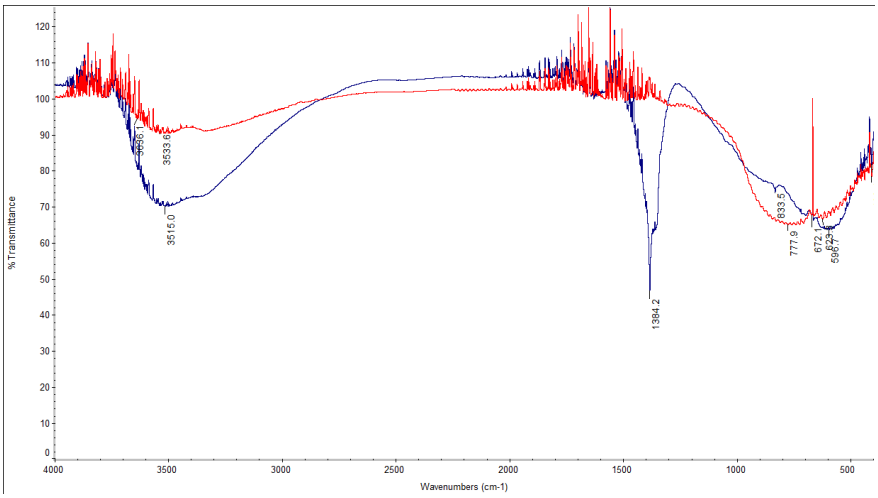

***Graph 72**: FT-IR Spectrum For CAT 12*

9.14.3) TPR ANALYSIS

In the case of CAT 12, the TPR trace comes out with tree peaks. The first of which can be attributed to the reduction of reduce-able specie of ruthenium (154°C). The second peak at 451 °C can be attributed to the reduction of oxides of Co and Fe. Then there's the third peak which at these higher temperatures, is usually attributed to strongly bonded metal-support species. In the temperature zone where activation is normally done, CAT 12 has a reducing capacity of about 16.6% and a total capacity of 34.1%.

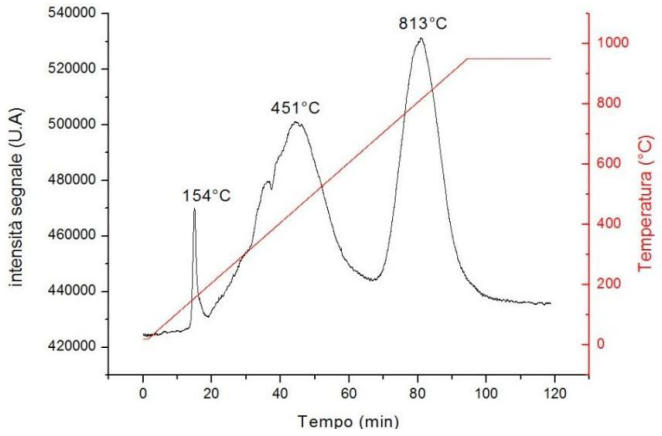

***Graph 73**: TPR Trace For CAT 12*

9.14.4) TPO ANALYSIS

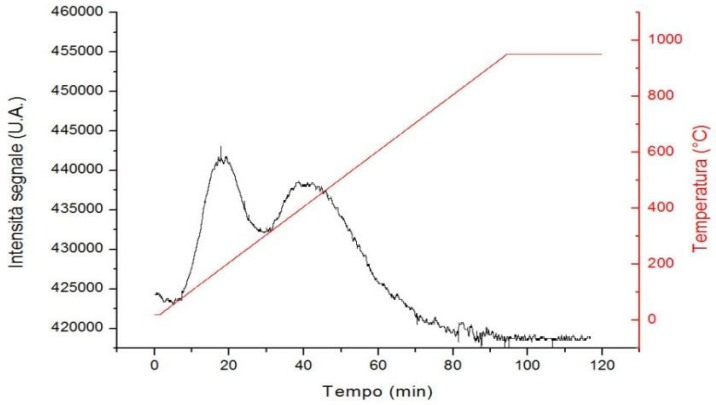

***Graph 74**: TPO Trace For CAT 12*

The TPO analysis gives two peaks, and none of them can be specifically attributed to the formation of particular oxides. They both in any case, give a total oxidation capacity of about 40.6%.

9.14.5) H_2-TPD ANALYSIS

This trace has a peak with three crests, showing how the three metal types desorb hydrogen at three different temperatures. The promotion effect of Ru is seen from the increased amount of

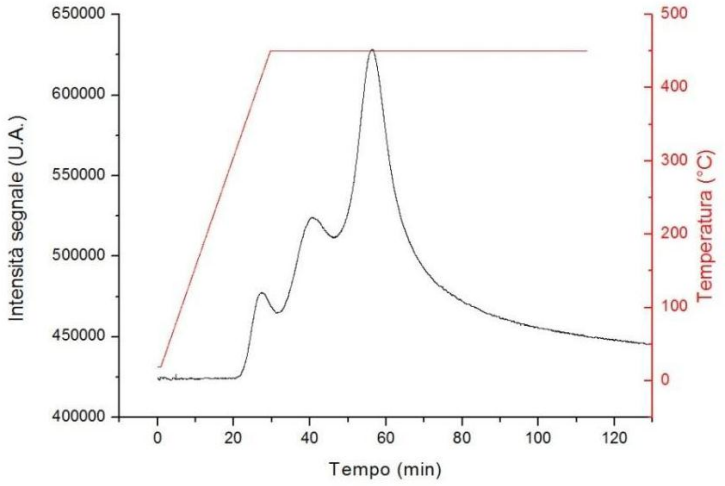

***Graph 75**: H_2-TPD Trace For CAT 12*

adsorbed H_2, almost 166 µmol./gm. It is also interesting to see how the dispersion and the number of active sites increase.

9.14.6) X-RAY DIFFRACTION ANALYSIS

In this case too, there's a confirmation of the absence of crystalline structures, because of the amorphous nature of the bulk sol-gel products.

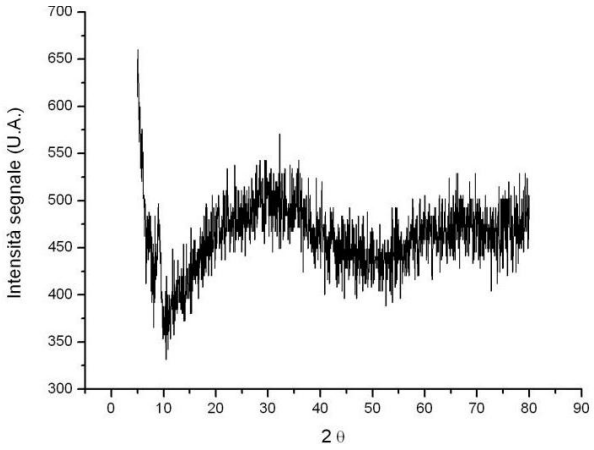

***Graph 76**: XRD Trace For CAT 12*

9.14.7) SEMIMAGE WITH EDS ANALYSIS

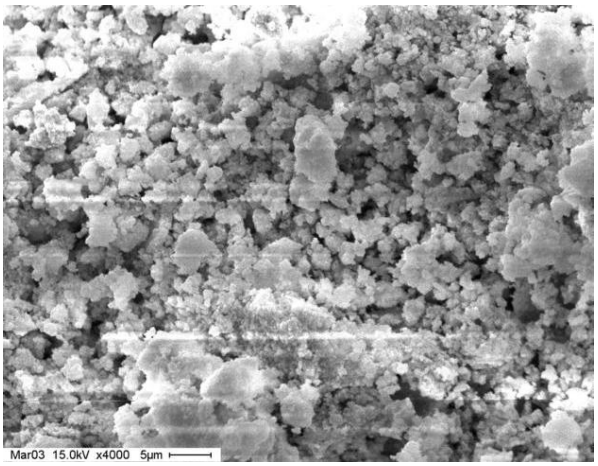

***Image 13**: SEM Image For CAT 12*

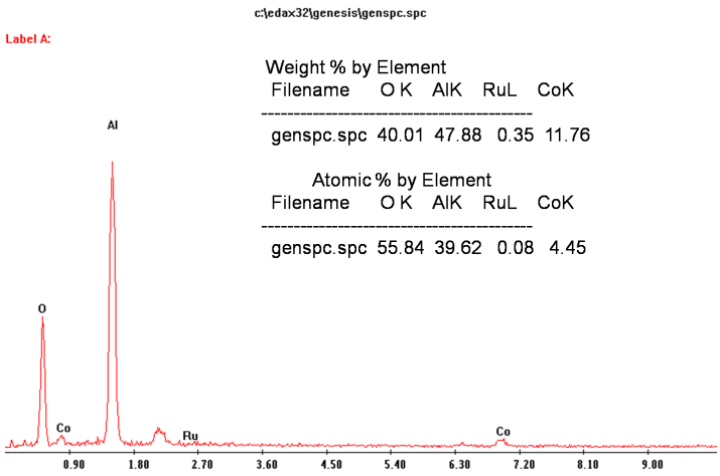

***Graph 77:** EDS Study For CAT 12*

Even in this case, there's a good surface coverage, although the bulk sol-gel method as usual does not give a uniform dispersion. In this case the EDS study gives an11.76% of metal on a point, instead of 11.25% as expected. This could mean a dispersion on the surface, much better than expected. A similar result is obtained for ruthenium too. There's a 0.35% on the same point instead of the 0.5% deposited.

9.15) CHARACTERIZATION OF CAT N8

9.15.1) FT-IR SPECTROSCOPY

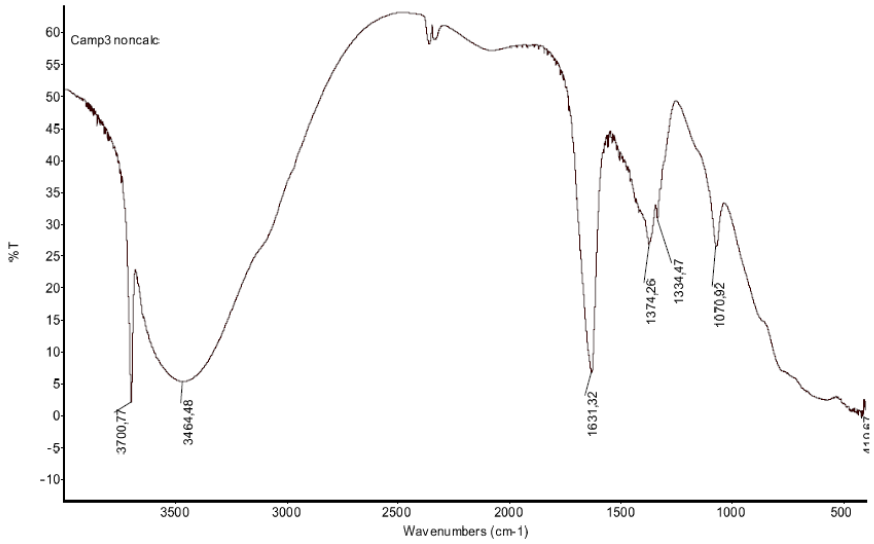

***Graph 78**: FT-IR Spectrum For CAT N8 Support Uncalcined*

On this spectrum, which is CAT N8 not yet calcined, the band at 3701 cm^{-1}could be attributed to the presence of OH groups which do not participate in hydrogen bond formation, while the band at 3464 cm^{-1} could be attributed to OH groups implicated in hydrogen bonds. The band at 1631 cm^{-1} could be attributed to the bending of water molecules still present in the structure, while the band at 1374 cm^{-1} with a little shoulder could be the vibrations of C-O and C-H bonds of the precursors with a possible interference of CO_2. The 1071 cm^{-1} band is attributable to the Al-O stretching of the precursor. Graph 79, on the following page shows the disappearance of the bands at 3701 cm^{-1} and those at 1071 cm^{-1}, while the band at 1635 cm^{-1} is reduced. Graph 80 instead shows the spectrum of the support on which $Ru_3(CO)_{12}$ has been impregnated. Effectively some new peaks are noted at 2046 cm^{-1} and 1973 cm^{-1}, which could evidently be attributed to the presence of ruthenium carbonyl.

Finally graph 81 is a spectrum of CAT N8 when it has been impregnated with $Cs_2(COO)_2$.

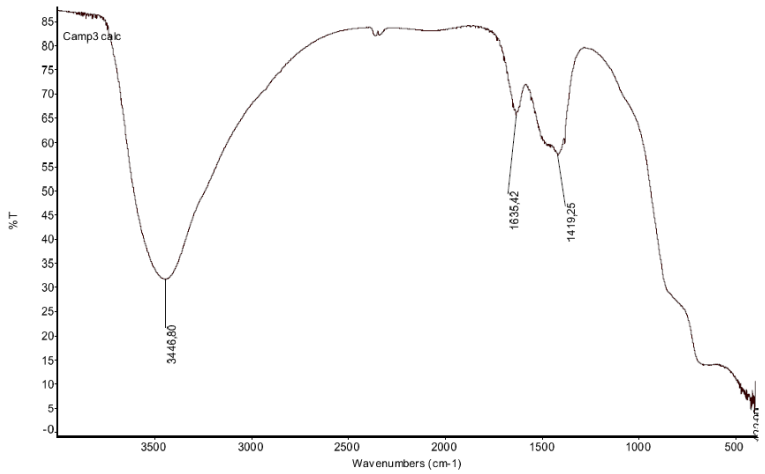

Graph 79: *FT-IR Spectrum For CAT N8 Support Calcined*

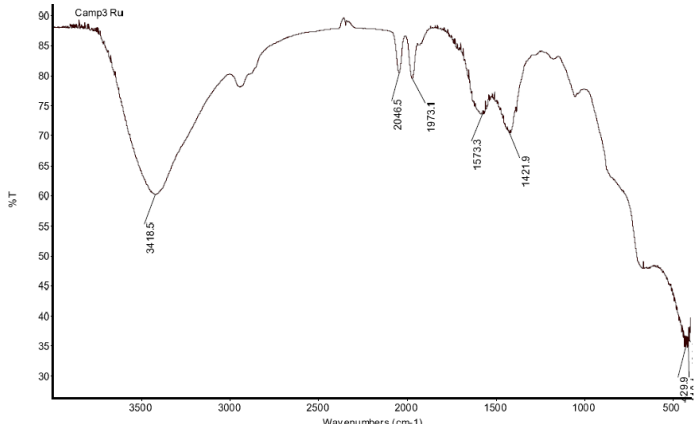

Graph 80*: Support of CAT N8 Impregnated With* $Ru_3(CO)_{12}$

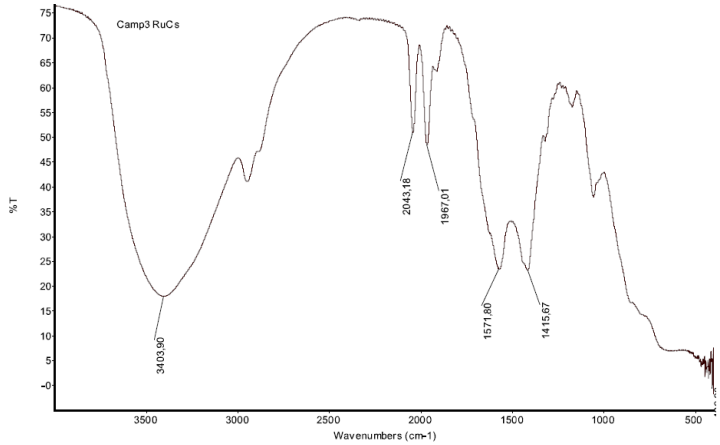

Graph 81: *CAT N8 With* $Cs_2(COO)_2$ *Added*

9.15.2) XRD ANALYSIS

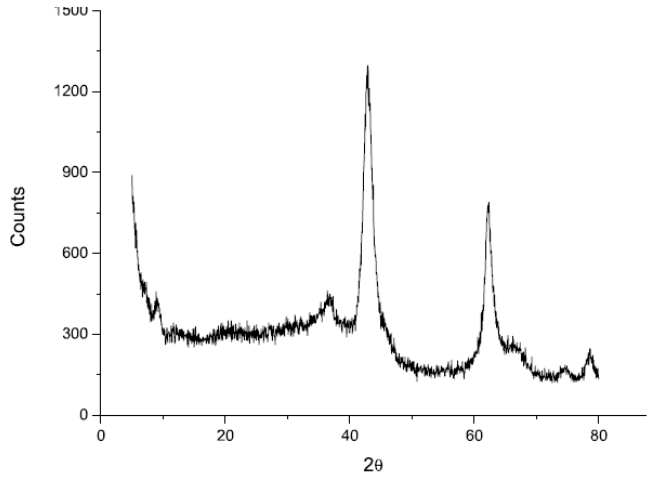

Graph 82: *XRD Trace For CAT N8*

The peaks observed at 2θ=36.955 °, 42.785 ° and 62.340 °, could be attributed to the presence of MgO while the little shoulder near 62.340 ° could be attributed to the presence of Al_2O_3. These are the unique crystalline forms identifiable.

9.15.3) SURFACE AREA MEASUREMENT

The surface area measured for the support of CAT N8 was 215 m^2/g while the catalyst which came out of the reactor gave 212 m^2/g.

9.15.4) TPR ANALYSIS

The TPR analysis which is normally used to determine the temperature of activation in the reactor, gave total reduction of the surface metals at 328 °C.

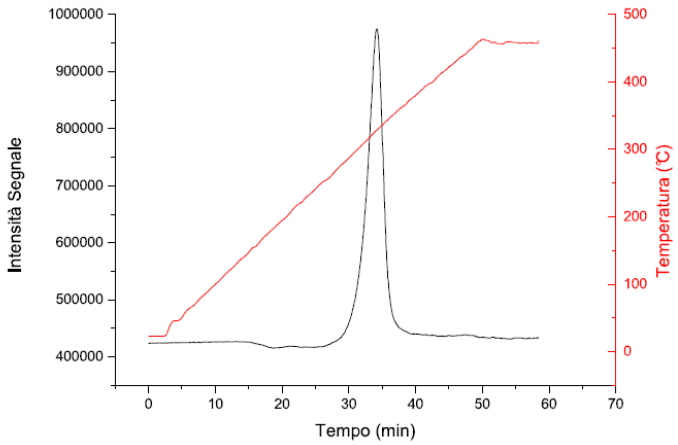

Graph 83: *TPE Analysis For CAT N8*

9.16) CHARACTERIZATION OF CAT N4

9.16.1) FT-IR SPECTROSCOPY

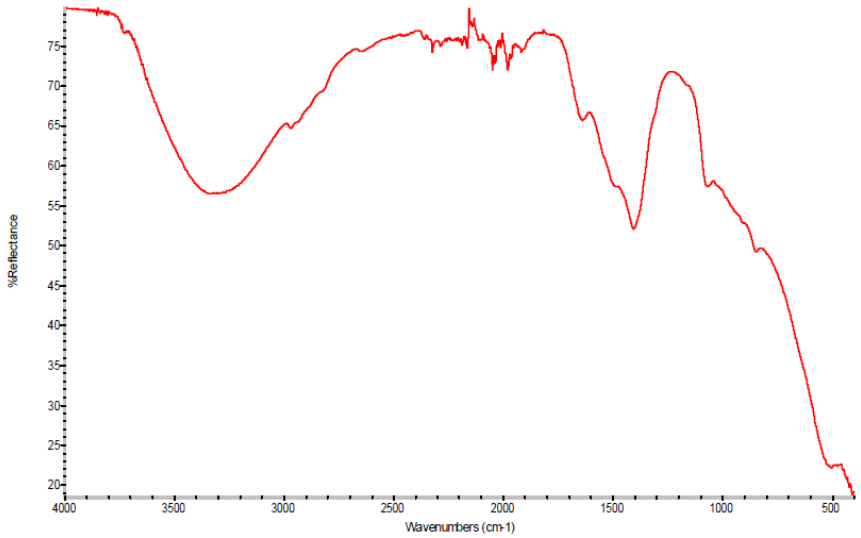

Graph 84: *FT-IR Spectrum For CAT N4*

Graph 84 shows a spectrum of CAT N4 which is a catalyst prepared by bulk sol-gel, impregnating Ru on MgO and then on Al_2O_3, and at the end impregnating the catalyst with caesium oxalate. The presence of bands around 1500 cm^{-1} might imply an incomplete

decomposition of caesium oxalate, which could be negative to the catalytic activity. Graph 85 is an enlargement of the area between 2200 and 1800 cm^{-1}.

Graph 85: *Enlarged FT-IR For CAT N4*

In this area bands could be found like those at 2050 cm^{-1} and 1980 cm^{-1}, which could be attributed to interactions between Ru and MgO, and those at 2038 cm^{-1} and at 1978.5 cm^{-1} which could also be attributed to interactions between Ru and Al_2O_3.

9.16.2) XRD ANALYSIS

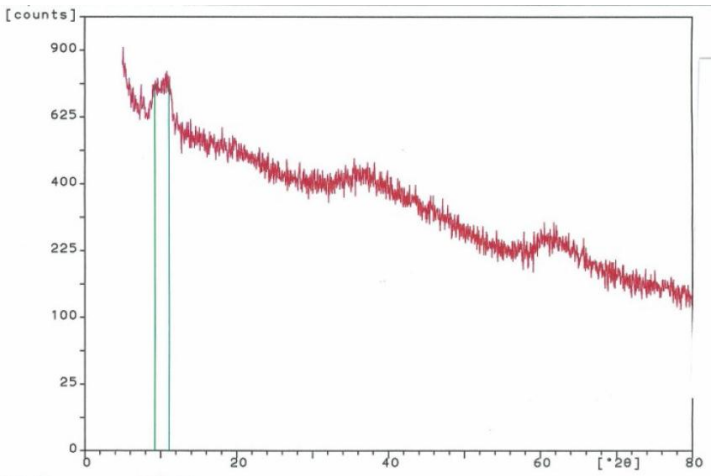

Graph 86: *XRD Trace For CAT N4*

The amorphous nature of the support completely covers the signals of the presence of any crystalline form present. This makes any trial to interpret the trace very unsure.

9.16.3) SURFACE AREA MEASUREMENT

Using as usual, the B.E.T. single point method of measuring the surface area, 264 m^2/g were obtained.

9.16.4) TPR ANANLYSIS

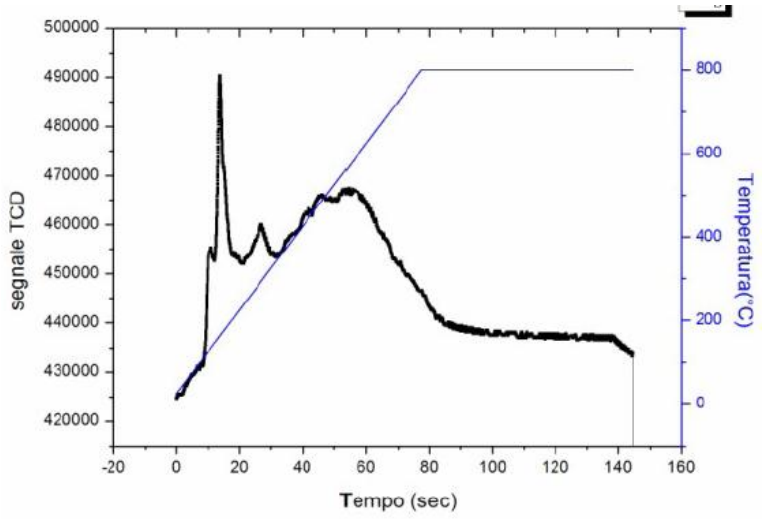

Graph 87: *TPR Trace For CAT N4*

From graph 87 it could be seen how the surface Ru is easily reduced at relatively low temperatures, even much lower than the reaction temperature (lower than 250 °C).

CHAPTER TEN

10) CONCLUSIVE DISSERTATION ON CHARACTERIZATION AND SELECTIVITY TEST RESULTS

10.1) COMPARISON OF TPR ANALYSES

The following diagrams which show the TPR traces for CAT 1 (Co on silica gel), CAT 16 (Co on alumina gel) and CAT 17 (Co/Ru on alumina gel), are intended to illustrate the differences brought about by the preparation methods, as compared to CAT 18 (Co on alumina gel) and CAT 12 (Fe/Co/Ru on alumina gel). They are later on, compared to CAT 20 (Co on silica gel) and to CAT 21 (Co with SiO_2 on alumina gel) also.

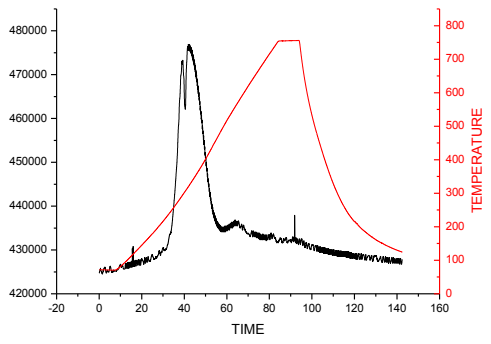

CAT 1

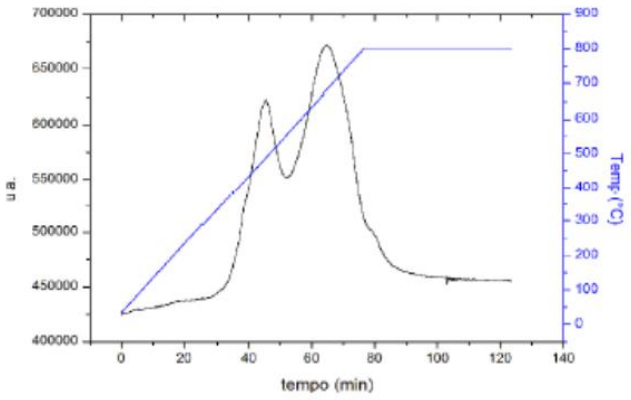

CAT 16

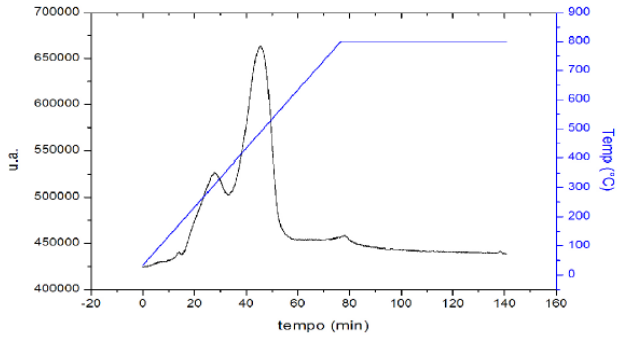

CAT 17

These samples are prepared by impregnation to incipient wetness. The most interesting characteristic worth noting is how a great quantity of the metal deposited on the surface is being reduced at temperatures lower than 600 °C. Another interesting characteristic is how in CAT 17, where Ru is used as a promoter, there's an ulterior lowering of the reduction temperature. This promoter effect of Ru is not always so definite because in the case of CAT 11 (see graph 67 on page 152) and CAT 12 (see graph 73 on page 157), a lowering of the reduction temperature is noticed for the lower temperatures and those of the higher reduction temperatures are increased. A tendency noticed in the case of CAT 18 and CAT 19 too, not forgetting the most clamorous case in CAT 3 (see graph 41 on page 133) and CAT 4 (see graph 46 on page 136). It is also worth noting that anomalous cases were noticed on samples prepared using the bulk sol-gel method, and the support is alumina gel.

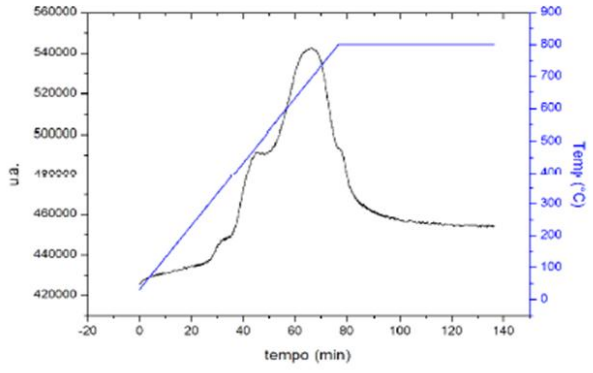

CAT 18

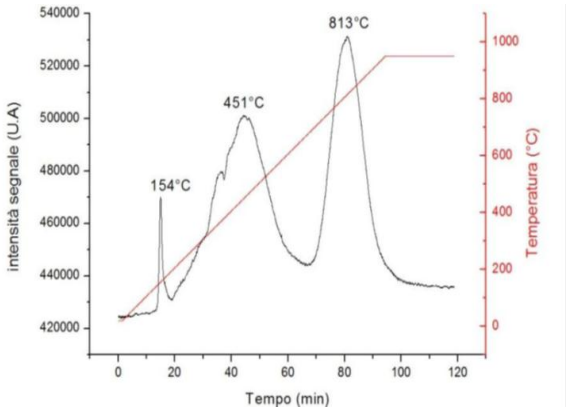

CAT 12

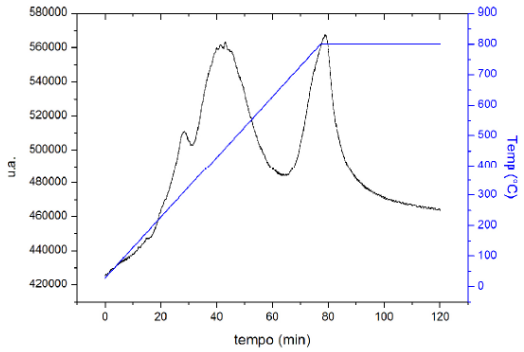

CAT19

Looking at the TPR analyses carried out for catalysts prepared using the bulk sol-gel method, it almost becomes clear why some of the catalysts prepared using this method were completely catalytically inactive. It is evident that there's a strong interaction between the support and the metal precursor. In this way it leaves very little space for the formation of surface reducible oxides. It is worth remembering that, the catalysts prepared using this method are supported on alumina. Thence, it might be reasonable to suppose that the interaction between alumina and the metal precursor is so strong that the formation of aluminates prevail. Putting this together with the fact that during gel formation, a great quantity of the metal precursor gets locked up in the bulk. This part of the metal is completely unavailable for reduction.

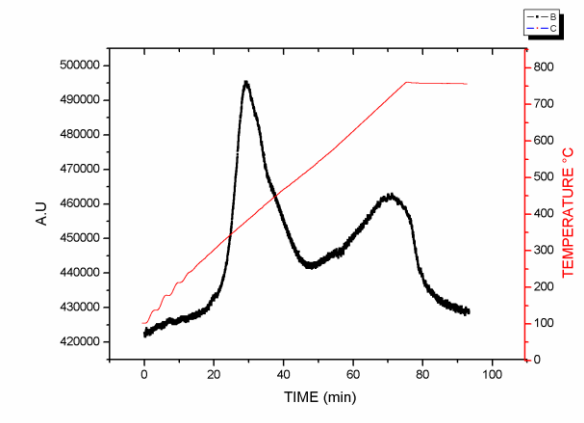

CAT 21

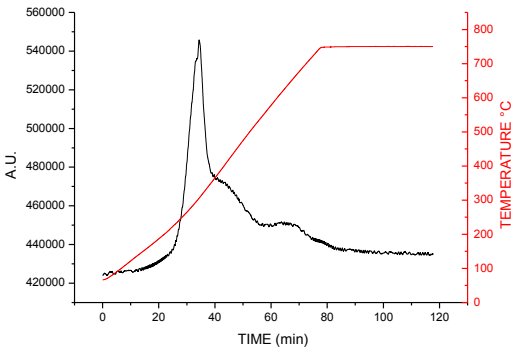

CAT 20

Taking a glance at the trace for CAT 20, it becomes obvious asking, but which is the preparation method here? Definitely interesting because this was the first attempt to prepare a catalyst using the sol-gel method and applying the anchorage to incipient wetness (grafting). Here the was a success in preparing a catalyst which had almost the total of its supported Co metal on the silica gel surface, and in an easily reducible form. This trend was not continued because of the industrial urge to work on alumina using either Fe or combinations of Fe and Co. Lately an attempt was made to anchor Co on alumina gel. In this way CAT 21 was prepared. It is simply cobalt nitrate dissolved in a mixture of TMOS and ethanol, which is then grafted on alumina. From the TPR analysis, it could be noticed the presence of superficial cobalt oxides which are easily reduced at low temperatures. Bland attempt of aluminate formation is also noticed.

10.2) COMPARISON OF TPO ANALYSES

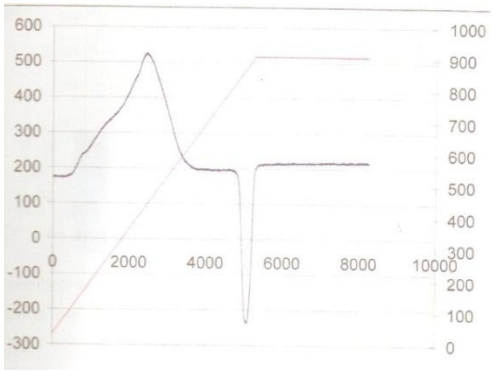

CAT 1

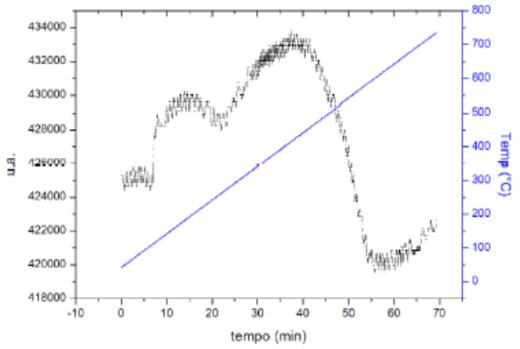

CAT 16

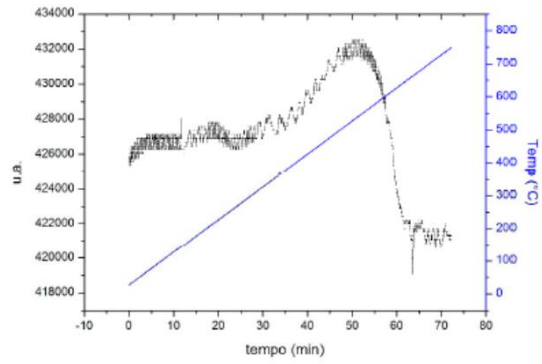

CAT 18

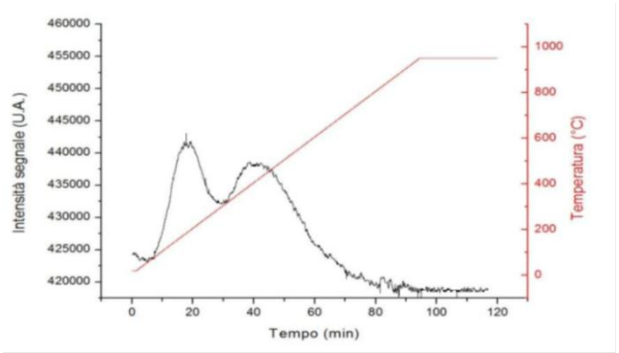

CAT 12

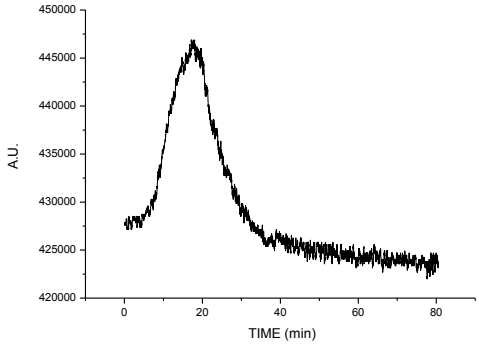

CAT 21

A glance at the TPO results for CAT 1 and CAT 16 which were prepared using the impregnation to incipient wetness method goes to confirm the great quantity of easily reducible cobalt oxide on the surface, which is completely oxidised at low temperatures i.e. below 400 °C. The same cannot be said to CAT 18. Even CAT 12 which is promoted by Ru shows a part of its reducible metals which do re-oxidise at temperatures above 400 °C. In the case of CAT 21 it could be noticed that almost all of the reducible species are re-oxidised.

10.3) COMPARISON OF H_2-TPD ANALYSIS

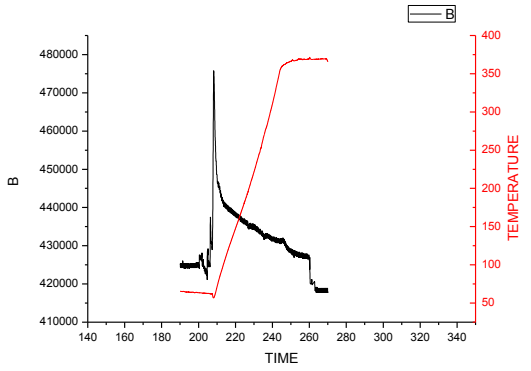

CAT 1

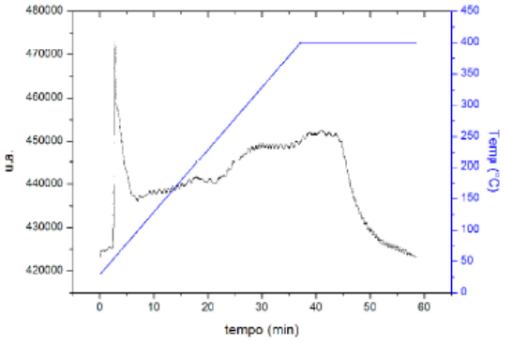

CAT 16

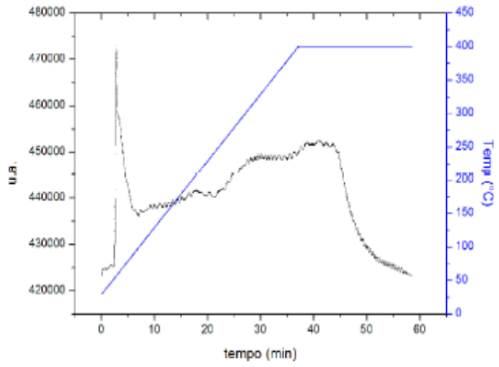

CAT 18

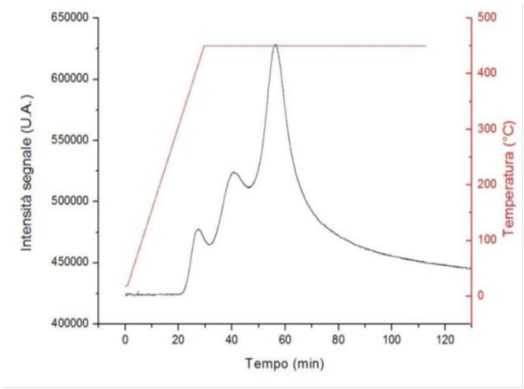

CAT 12

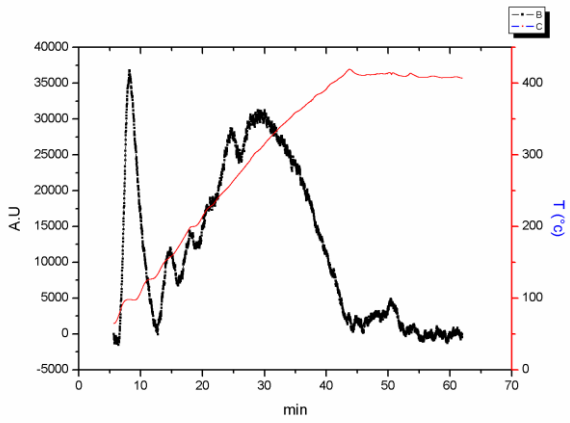

CAT 21

From the hydrogen desorption patterns, a study of the number of active sites, particle dimension and the percentage of dispersion are carried out. From the table that follows it could be observed how the number of active sites on the surface increase from 10^{19} for CAT 1 and CAT 16 to 10^{20} for CAT 17 which is using Ru as a promoter. It can also be noticed how the particle sizes and the dispersion on the surface do change. CAT 17 has smaller particles which are much more dispersed. These catalysts are prepared by impregnation to incipient wetness. The same type of reasoning could be used for CAT 18 and CAT 12, though the preparation method is different. Here the particle dimension and the metal dispersion do not follow the trend most probably because of the different types of metals involved. (For CAT 18 we have Co on alumina while for CAT 12 we have Co/Fe/Ru on alumina). In the case of anchorage to incipient wetness CAT 21, without having a very high surface area, gives the highest number of active sites (10^{21} sites/gram). This does not change in any case the dispersion pattern and the typical particle dimensions of the sol-gel methods.

The catalysts used for comparison like CAT 15 and CAT 13 and 14 also gave a good number of superficial sites (10^{19} sites/g in the case of CAT 15, 10^{20} sites/g in the case of CAT 13, which could be explained as a result of the support in silica gel, and 10^{19} sites/g in the case of CAT 14). CAT 15 shows a very little percentage of reducible metal on the surface though, and this could be explained by particle aggregation and in general by morphological hindrance. CAT 13 and 14 instead, showed very brilliant reducing capacities though the sites number was normal.

SUMMARY			TPO	TPD			TPR	
CATALYST	PERCENTAGE Co/Fe/Ru	SURFACE AREA (m^2/gm)	PERCENTAGE OF SURFACE Co REDUCED	N° OF ACTIVE SITES/GRAM	PERCENTAGE OF DISPERSION	PARTICLE DIMENSION (nm)	REDUCTION TEMPERATURES (°C)	PERCENTAGE OF TOTAL Co REDUCED
IMPREGNATION TO INCIPIENT WETNESS								
CAT 1	15/-/-	242	100	8.7E+19	6	16.1	350	86
CAT 16	20/-/-	269	59	5.3E+19	4.4	22	430-680	98
CAT 17	20/-/0.1	281	45	1.2E+20	13.2	7	225-425	54

BULK SOL_GEL								
CAT 18	20/-/-	172	37	21E+19	2.7	36	420-695	65
CAT 19	20/-/0.1	102	68	1.2E+19	1	115	400-800	56
CAT 12	1/1=15/ 0.5	110	41	2.0E+20	12.6	166	154-451-813	7.6
CAT 15	9.7573.2 5/-	423	66	5.8E+19	3.7	48	189-544-840	4.5
ANCHORAGE TO INCIPIENT WETNESS								
CAT 20	15/-/-							
CAT 21	15/-/-	256	81	1.29E+21	9	11	366-733	70
ULTRA SOUND TECHNIQUE								
CAT 13	20/-/-	458	77.6	1.3E+20	8.2	12	293	65.7
CAT 14	15/-/0.5	100	99	3.9E+19	2.9	32	163-256-322	76

Table 4: *Comparison Of Some Characterization Results*

10.4) COMPARISON OF SEM IMAGES

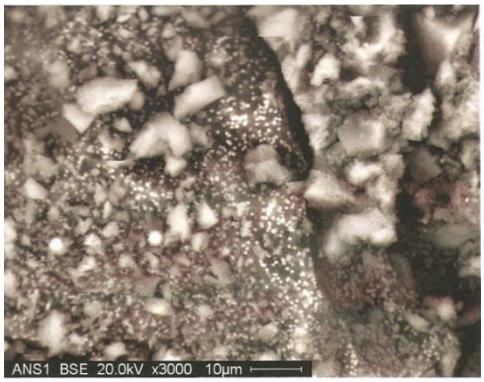

CAT 1

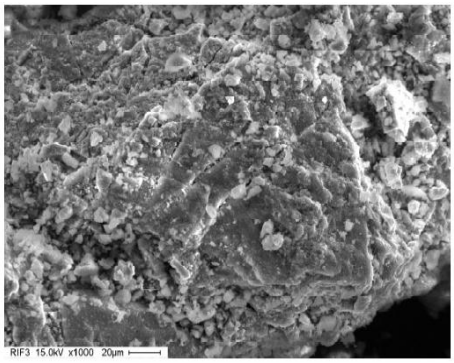

CAT 17

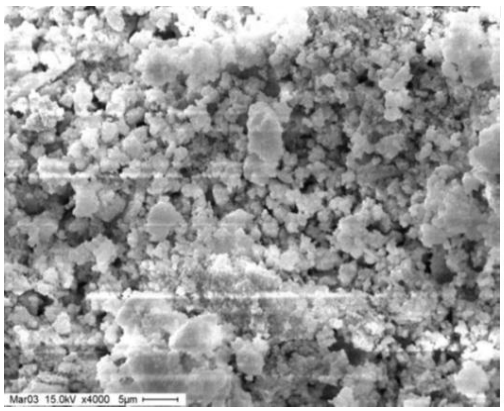

CAT 18

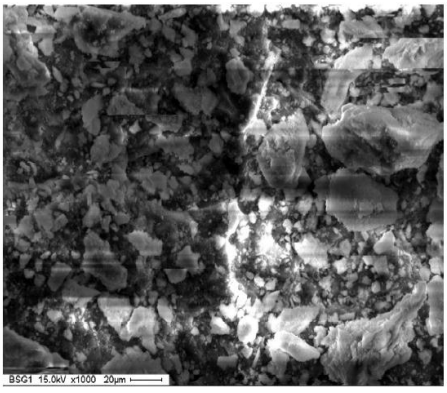

CAT 12

The SEM images show the higher particle dispersion in the case of CAT 1 and CAT 17, although as it could be seen, not very homogeneous. The same images for the bulk sol-gel methods (CAT 18 and CAT 12) have a less evident dispersion in a more homogeneous texture.

10.5) CONVERSION AND SELECTIVITY TEST RESULTS

	TEMPERATURE (°c)	CONV.%	SEL. CO_2 %	SEL. CH_4 %	SEL. C_2-C_4 %	SEL. $>C_5$ %	α
CAT 1	230	70	20	60	6	2	0.8
CAT 16	200	38	5	42	15	11	0.81
CAT 18	200	40	4	40	31	13	0.9
CAT 19	190	70	5	35	5	30	0.8
CAT 13	250	30.1	4	5	1	74	0.91
CAT 20	200	30	4	30	16	47.8	0.8
CAT21	200	63	<1	11	7	72	0.81

***Table 4**: The Results Obtained For Selectivity And Conversion Of Some Catalysts*

The two catalysts prepared by impregnation to incipient wetness clearly show a tendency towards the production of the lighter hydrocarbons, while methane is the major product. The CO_2 production is also contained. This is also clearly seen when a glance is taken on the histogram in which they are represented.

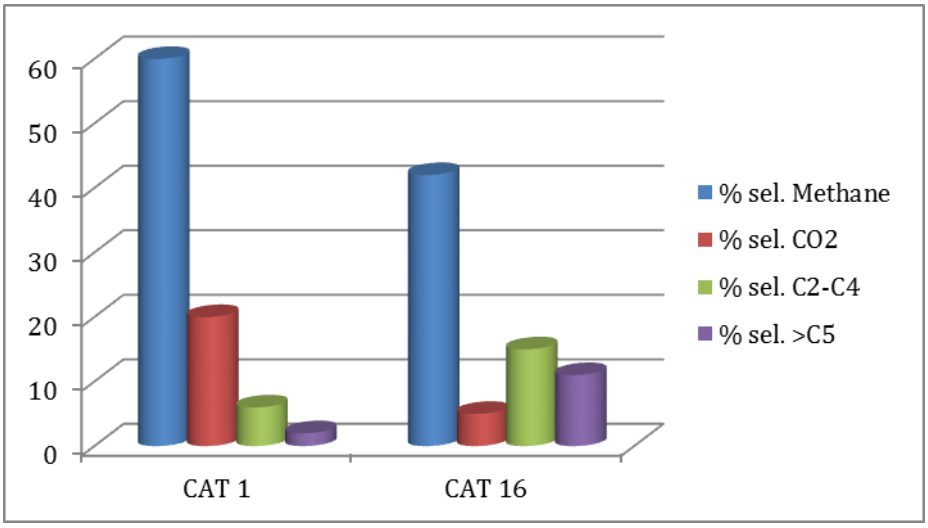

Graph 88: *Selectivity of the different Products*

As earlier mentioned, the most accepted theory which explains the chain formation of the Fisher-Tropsch synthesis is that of A.S.F. (Anderson- Schultz-Flory). This does not exclude the formation of other products. This is the reason for which Co, which is known to limit the formation of oxygenated products and to give a better control of the water/gas shift reaction is mostly studied. From graph 88, it could be noticed that the sum of the selectivities are not equal to a hundred percent. This could be justified by the lack of instruments for a complete study of the aqueous phase of the products, and a method to completely extract the waxes produced from the out coming catalyst and the inert space filling materials. The products that could be accounted for are the ones which remain in the gaseous phase, like the ramified hydrocarbons and the olefins.

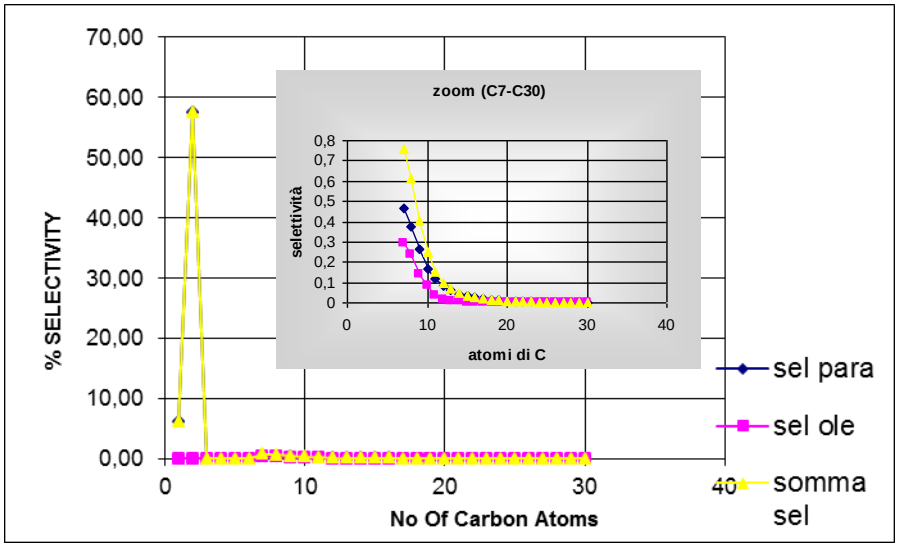

Graph 89: *Selectivity Of The Various Products CAT 1*

The bulk sol-gel catalyst (CAT 18) too has the same tendency. But CAT 19 instead, which is promoted by Ru has this tendency inverted. It produces less methane and more of the heavier hydrocarbons, and most of all at a lower temperature.

CAT 13, which is a catalyst prepared by the ultra sound technique, is a 20 % Co on silica gel. This catalyst shows a very pronounced tendency towards the production of the heavier hydrocarbons and at the same time a very low production of CO_2 and methane. The only doubt is about the temperature because of problems with the thermocouple during the tests.

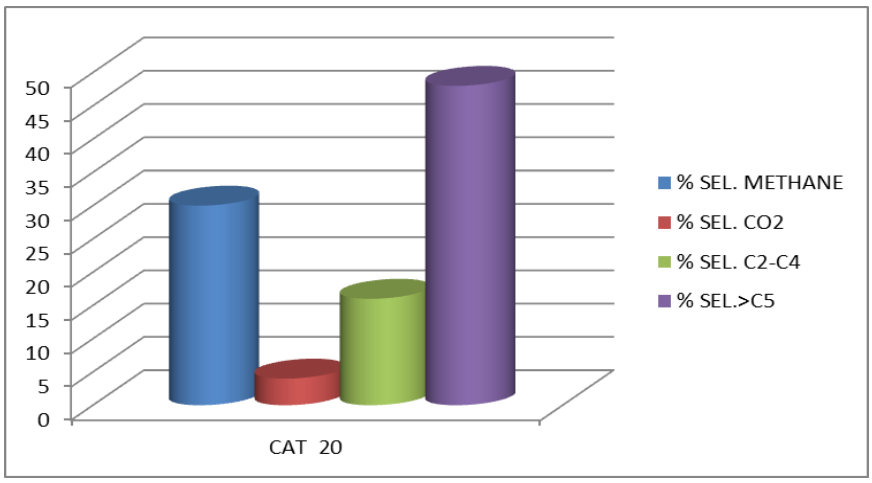

Graph 90: *Selectivity Results For CAT 20*

The two catalysts prepared by anchorage to incipient wetness, both show this tendency of producing the heavier hydrocarbons with extremely low CO_2 production and a contained production of methane. The results shown for CAT 21 on table 4 is a 24 h. data collection. The production of the higher hydrocarbons was so high that it was not possible to follow up the reaction for a longer period, because the fixed bed reactor is not an efficient method to carry on the process. At very low conversion rates the wax production is so high that the catalyst gets covered up. This tendency was noticed for all those catalysts that had the number of sites/g higher than 10^{20}. The principal suggestion is that to be able to follow up this reactions better, a slurry reactor is needed where the formed wax is easily carried out of the reactor.

10 6) PRODUCTIVTY TEST RESULTS FOR AMMONIA SYNTHESIS

If n= number of moles of N_2 in the feed, and

3n= number of moles of H_2,

y= the degree of conversion,

n_t= the total number of moles at time t,

Then from the equation:

$$N_2 + 3H_2 \rightleftharpoons 2NH_3$$

Initial molar situation	n	3n	0
Molar situation at time t	n(y-1)	3n(1-y)	2ny

Therefore n_t= 2n(2-y)

And y= moles of NH_3/2n

So the percentage of NH_3 produced is= 2ny*100/2n(2-y) = y*100/(2-y)

Calculating this value at different temperatures a curve of concentration against temperature is obtained. This curve is compared with the equilibrium curve calculated using thermodynamic data elaborations as suggested by J. Gillepsie and J. A. Beattie. The medium productivity instead is calculated as:

= number of moles of NH_3/g of catalyst*hour.

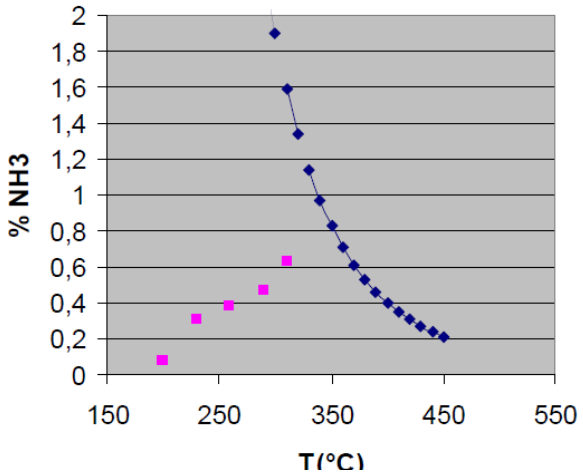

Graph 91: *% Productivity Vs Temperature Compared with equilibrium curve For CAT N4*

It could also be noticed from the next graph, how the productivity keeps increasing with the increase in temperature indicating that equilibrium productions are not yet arrived.

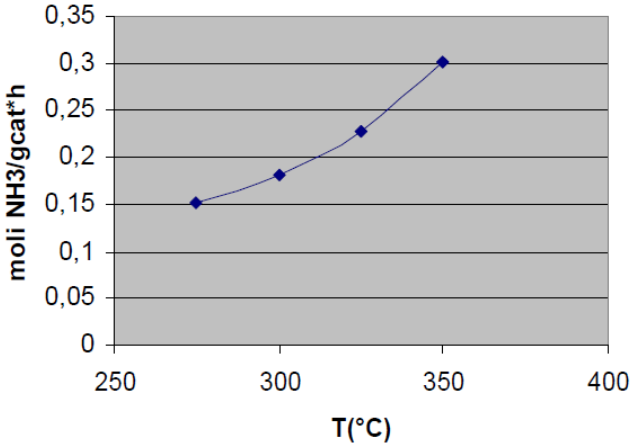

Graph 92. *The medium productivity For CAT N4*

BIBLIOGRAPHY

1) General Bibliography, Encyclopedia of Hydrocarbons,

CARRA' S., MORBIDELLI M. (1983) Chimica fisica applicata. Principi di termodinamica e cinetica chimica e loro ruolo nella teoria del reattore chimico, Milano, Hoepli.

CIMINO A., STONE F.S. (2002) Oxide solid solutions as catalysts, << Advances in Catalysis >>, 47, 141-306.

GATES B. C. et al. (1979) Chemistry of catalytic processes, New York, McGraw-Hill.

KARSTEN R., SHEFFLER M. (2003) First principles atomistic thermodynamics for oxidation catalysis, <<Physical Review Letters >>, 90, 046103-1-046103-4

LOGADO'TTIR A., NORSKOV J.K. (2003) Ammonia synthesis over a Ru(0001) surface, << Journal of Catalysis>>, 220,273-279.

SCHLOGL R. (1989) Combinatorial chemistry in heterogeneous catalysts: a new scientific approach or "the king's new clothes"?,<< Angewandte Chemie International Edition>>, 37, 2333-2336.

THOMAS J.M. (1989) Advanced catalysts: interface in the physical and biological sciences, << Angewandte Chemie international Edition>>, 28, 1079-1088.

WISE H., OUDAR J. (1990) Material concept in surface reactivity and catalysis, New York, Dover.

2) Cited Bibliography,

BERTANI V. et al. (2003) A theoretical analysis of the molecular events involved in hydrocarbons reactivity on palladium clusters, << Journal of Molecular Catalysis A. Chemical>>, 204, 771-778.

ERTL G. (1991) Dynamics of reactions at surfaces, << Advances in Catalysis>>, 45, 1-69.

FREEMAN C.M. et al. (2005) Computing the location and energetics of organic molecules in microporous adsorbents and catalysts. A hybrid approach applied to isomeric butenes in a model zeolite, << Chemical Physical Letters>>, 186, 137-142.

HONKALA K. et al. (2005) Ammonia synthesis from first principles calculations, << Science>>, 307, 555-558.

SAPOVAL B. et al. (2001) Catalytic effectiveness of irregular interfaces and rough pores: the “land surveyor approximation”,<< Chemical Engineering Science >>, 56, 5011-5023.

SOMORJAI G.A. (2004) On the move, << Nature>>, 430, 730.

THOMAS J.M. (1994) Turning points in catalysis, <<Angewandte Chemie International Edition >>, 33, 913-937.

3) Ph.D thesis of Dot. Luccarelli Carlo

4) Ph.D thesis of Dot. Di Michelli Alessandro

5) Leighton, T. G., The acoustic bubble, London: Academic, 1994.

6) Suslick, K. S., Science, 247, 1439, 1.

7) Ondrey, G.; Kim, L.; Parkinson, Chem. Eng: June, 39-45, 1996.

8) Mason, J. M., Applied Sonochemistry, Wiley-VCH, 2002.

9) Mason, T. J.; Lorimer, J. P.; Bates, D. M.; Zhao, Y.; Pugin, B., Ultrasonincs, 25, 49-55, 1987.

10) Weber, M. E:; Chon, W. Y.; Can, J., Chem. Eng., 45, 238-240, 1967.

11) Entezari, M. E.; Kruus, P.; Otson, R., Ultrason. Sonochem.,4, 49-54, 1997.

12) Contamine, F.; Faid, F.; Wilheim, A. M.; Berlan, J., Chem. Eng. Sci. 49(24B) 5865, 1994.

13) Ratorinoro, N.; Contamine, F.; Wilheim, A. M., Chem. Eng. Sci. 50(3) 554,1995.

14) Journal of molecular catalysis, J. Zwart and R. Snel.

15) Graduation thesis of Marostica A.

16) Graduation thesis of Kwamou B.

17) Graduation thesis of Martinelli S.

18) Thesis of Durante Fabio

19) T. Lopez, R. Marmolejo, M. Asomoza, S, Solis, R. Gomez, J:A: Wang, Bokhimi, O. Navarrete, M:A: Llanos, E. Lopez, Materials Letters 32 (1997) 325-334.

ACKNOWLEDGEMENTS

My greatest wish is to thank Prof. Moggi for having given to me the opportunity of getting up to this exact point in life, I also wish him the lords richest blessings till we meet again.

I very much wish to thank the “BIG TWO”, Giannina and Maryberth, for the time and patience they have dedicated to me in these years of hardship through the course. You are unsubstitutable.

I ones more wish to thank my students and ex-students; Martinelli S., Marostica A., Curtarelli L., Calzolari V., Rastelli D., Durante F., Paris E., Delindati F. and Fritella V., not forgetting my precious friends, Elisa, Monica and Robby, shouting out “ Vi voglio tanto bene”, and finally to the best, Cauzzi D, Bacchi A. and Secchi A.

May the grace of God dwell in you all forever and ever.

Acknowledgements